Proceedings of a
Topical Conference on

Nuclear Data for

Fusion Reactor Technology

Kernforschungszentrum Karlsruhe, FRG, 23rd October 1991

Fe

$d^2\sigma/d\Omega \cdot dE$ (b/sr·MeV)
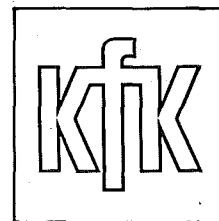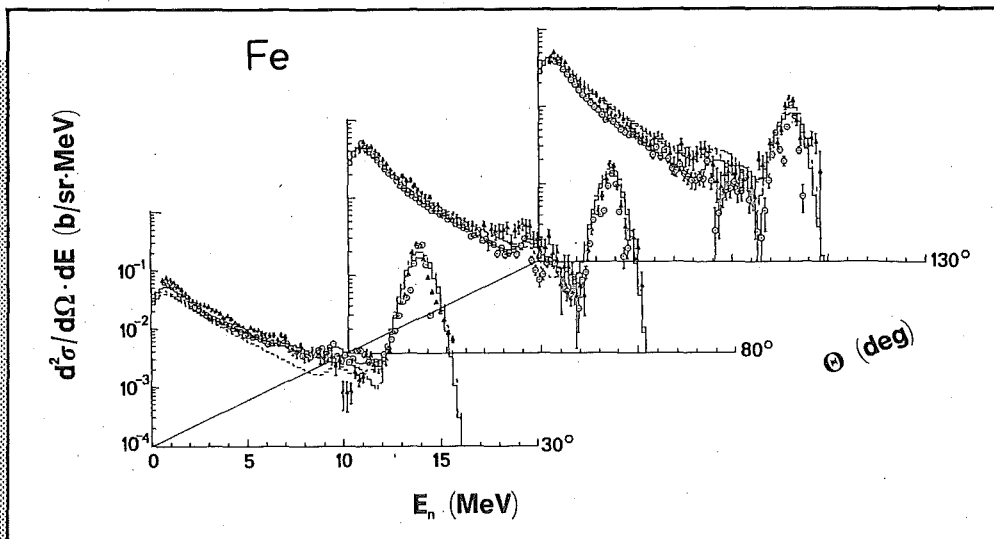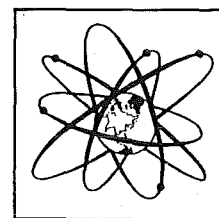
E_n (MeV)

Θ (deg)

130°

80°

30°

PROCEEDINGS OF A TOPICAL CONFERENCE ON

Nuclear Data for Fusion Reactor Technology

Kernforschungszentrum Karlsruhe, FRG, 23rd October 1991

April 1992

Edited by
S. Cierjacks
Kernforschungszentrum Karlsruhe
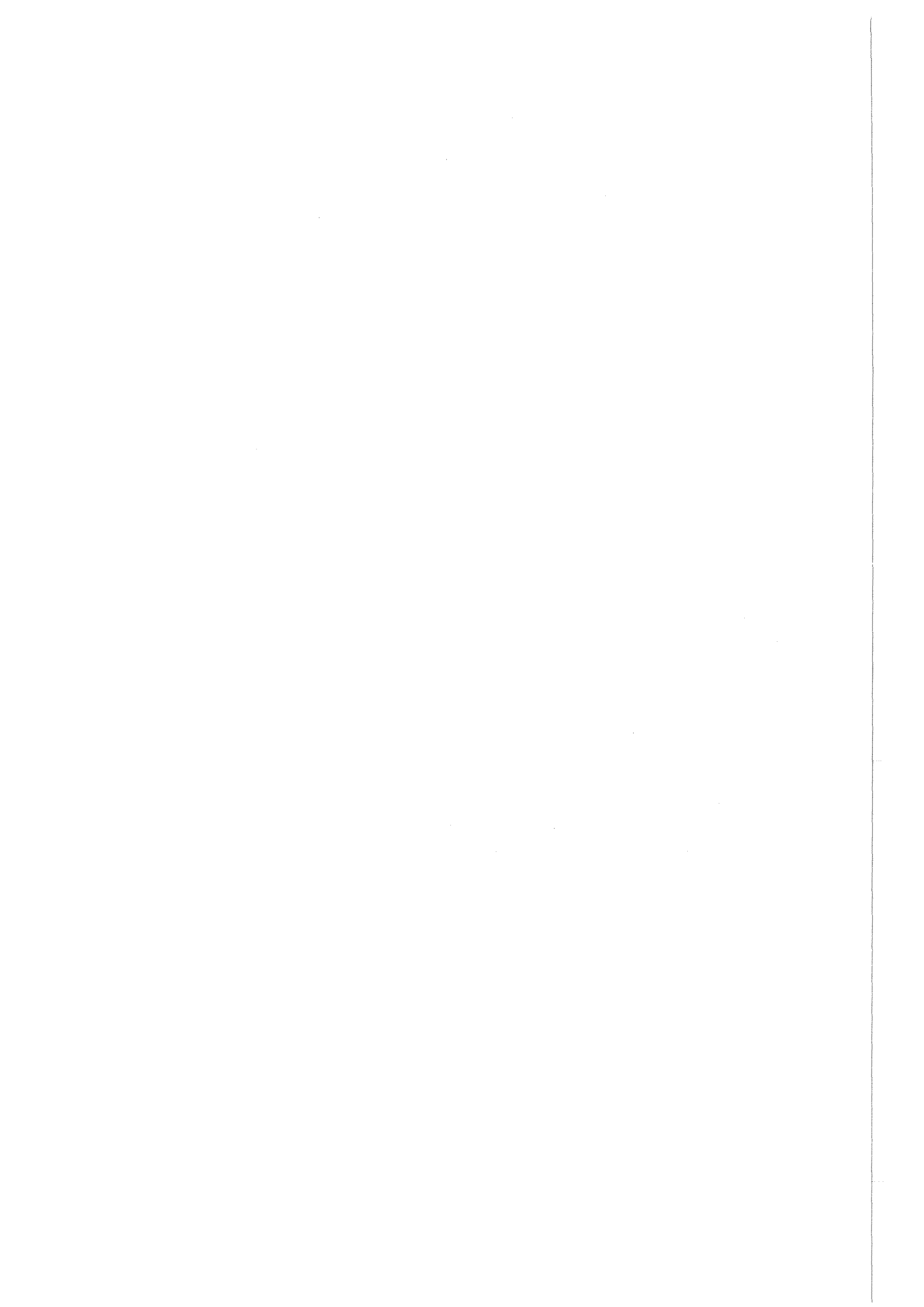Institut für Materialforschung

PREFACE

This publication contains the Proceedings of the Topical Conference on Nuclear Data for Fusion Reactor Technology held at the Kernforschungszentrum Karlsruhe in October 1991. The conference belongs to a series of special-topic conferences on nuclear data organized in the past in conjunction with regular Meetings of the Nuclear Energy Agency Nuclear Data Committee (NEANDC) in the Member States of OECD. The scientific responsibility of the conference was entrusted to the Institut für Materialforschung of KfK, and the program was established by the Local Program Committee in consultation with NEANDC Members and the OECD/NEA Secretariate. Approximately sixty scientists participated from twelve countries - Austria, Belgium, Canada, Czechoslovakia, France, Germany, Italy, Japan, Netherlands, Sweden, United Kingdom, United States of America - and from two international organizations - OECD/NEA, IAEA.

The scope of the conference extended from differential measurements and integral data testing to nuclear-model calculations, evaluations and data-file production. Both, present achievements and future developments were covered. Considerable efforts have been devoted in recent years to more refined measurements and the evaluation of existing data sets, resulting in the updating of existing fusion data files. Much emphasis was also given to further developments in evaluation methodology and production of uncertainty files. For the prediction of a large number of unknown nuclear data, nuclear theory has increasingly become an important tool. Especially statistical/precompound models are employed for this purpose. A notable advantage of these models is that they have a sound quantum-mechanical basis, but can be still formulated in a fairly transparent manner.

The conference reflected also the changing trends in nuclear data research for applications. Even for fusion technology only, nuclear data needs are much too broad to be handled on a national or regional basis. Thus, international collaboration is increasing, and major initiatives are being taken by international organizations such as OECD/NEA and IAEA.

The preparation of the Topical Conference and the production of these Proceedings required considerable voluntary effort. I am grateful to the Public Relations Office of KfK and to the Local Organizing Committee for the help extended to me.

S. Cierjacks

TABLE OF CONTENTS

SESSION I:

MEASUREMENTS AND DATA TESTING

Chairman: **S.L. Whetstone, DOE Washington**

Fast-Neutron Total and Scattering Cross Sections of ^{58}Ni and Nuclear Models *

by

A. B. Smith, P. T. Guenther, J. F. Whalen,
R. D. Lawson and S. Chiba[+]

Argonne National Laboratory

SUMMARY

An extensive experimental and theoretical study of the fast-neutron interaction with ^{58}Ni was undertaken. The neutron total cross sections of ^{58}Ni were measured from ≈ 1 to > 10 MeV using white source techniques. Differential neutron elastic-scattering cross sections were measured from ≈ 4.5 to 10 MeV at ≈ 0.5 MeV intervals with ≥ 75 differential values per distribution. Differential neutron inelastic-scattering cross sections were measured, corresponding to fourteen levels with excitations up to ≈ 4.8 MeV. The measured results, combined with lower-energy values previously obtained at this laboratory and with relevant values available in the literature, were interpreted in terms of optical-statistical, dispersive-optical and coupled-channels models using both vibrational and rotational coupling schemes. The physical implications of the experimental results and their interpretation are discussed. The considerations are being extended to collective vibrational nuclei generally, exploring the potential for utilizing electro-magnetic matrix elements, deduced from experiment or predicted by the shell model, to determine the strengths of the neutron interaction. Detailed aspects of this work are given in the Laboratory Report, ANL/NDM-120 (in press).

OBJECTIVES AND CONSIDERATIONS

It was the objective to provide comprehensive ^{58}Ni data for the design of fission and fusion energy systems by experimental and calculational means. Nickel is a primary constituent of most radiation-resistant ferrous alloys, and approximately 70% of the element consists of ^{58}Ni. In addition, the characteristics of the neutron interaction with ^{58}Ni are of fundamental interest as there are large direct-reaction components, and the isotope is a relatively simple nucleus consisting of a closed proton shell and two neutrons beyond a closed neutron shell.

A graded interpretation was followed, starting with a simple spherical optical-model interpretation providing a basis for many applications calculations. From this the effect of the dispersion relationship was explored, and then both vibrational and rotational coupling schemes were examined. A reasonable physical understanding of the neutron interaction was sought. Finally, some more fundamental aspects of the neutron interaction with collective nuclei were qualitatively examined with the objective of employing EM matrix elements and the shell model to calculate the neutron-induced processes.

MEASUREMENTS

The measurement regime extended to incident-neutron energies of > 10 MeV, and included detailed determinations of energy-averaged; i) total cross sections, ii) elastic-scattering cross sections, and iii) inelastic-scattering cross sections. The measurements were made in energy detail and with attention to accuracy so as to provide a quantitative data base consistency with the concepts of energy-averaged nuclear models. Detailed resonance behavior was intentionally energy averaged.

Mono-energetic and white source techniques were used to determine the total cross sections. The results are consistent with one another and with an equivalent energy average of the high-resolution total cross sections of Harvey [Har86], as illustrated in Fig. 1. This consistency implies no self-shielding distortions of the results.

Neutron elastic-scattering cross sections were determined with detailed energy and angle definition so as to provide a good energy-averaged data base for the model interpretations, as illustrated in Fig. 2. Particular attention was given to measurement accuracies and correction factors.

Cross sections for the inelastic-scattering excitation of 14 levels up to $E_x \approx 4.5$ were measured. A representative velocity spectrum obtained in the measurements is shown in Fig. 3. Most prominent of these inelastic cross sections are those due to the excitation of the first 1.454 (2^+) MeV vibrational level. At low
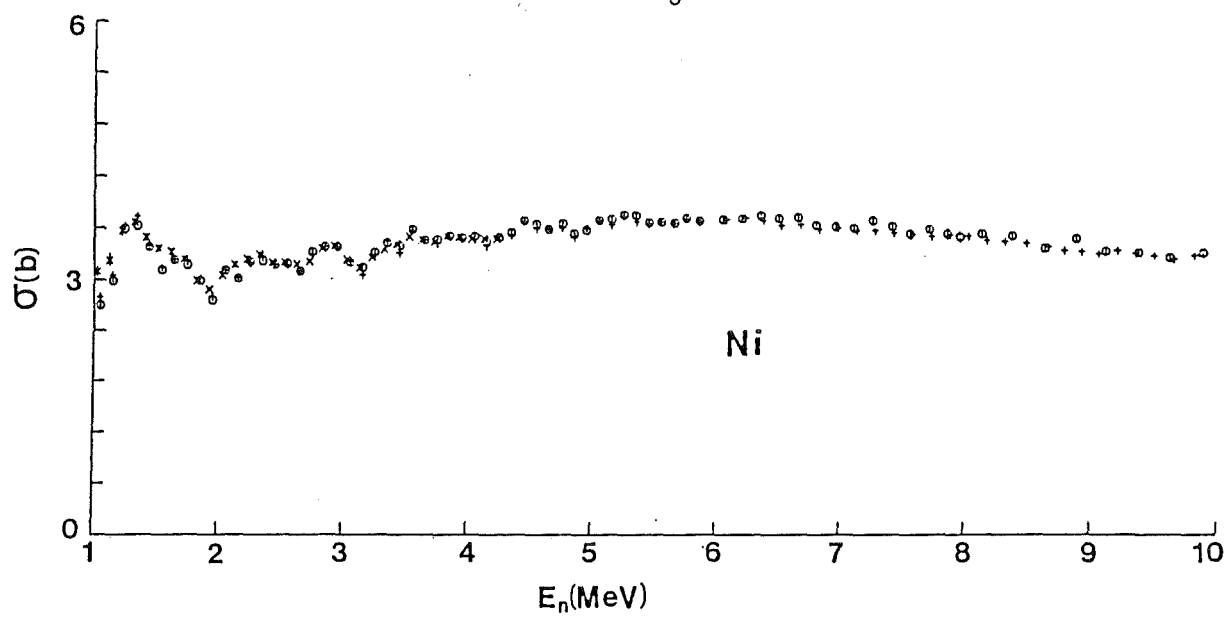
Fig. 1.   Energy-averaged σ_t of ^{58}Ni. "O" = present work,
"X" = Bud82, "+" = energy average of Har86.
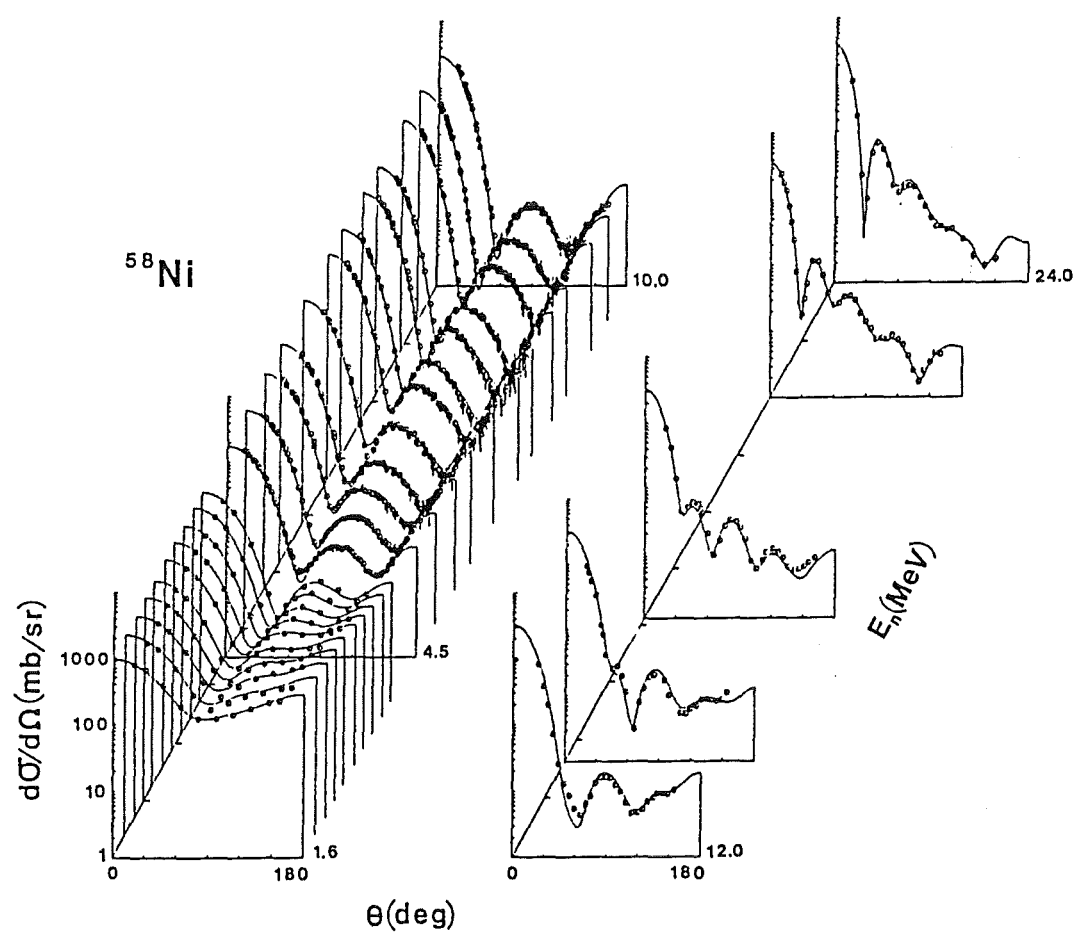
Fig. 2.   Elastic scattering cross sections.   This laboratory to 10
MeV. Higher-energy data from Gus85, Yam80, Ped88 and Ols90.
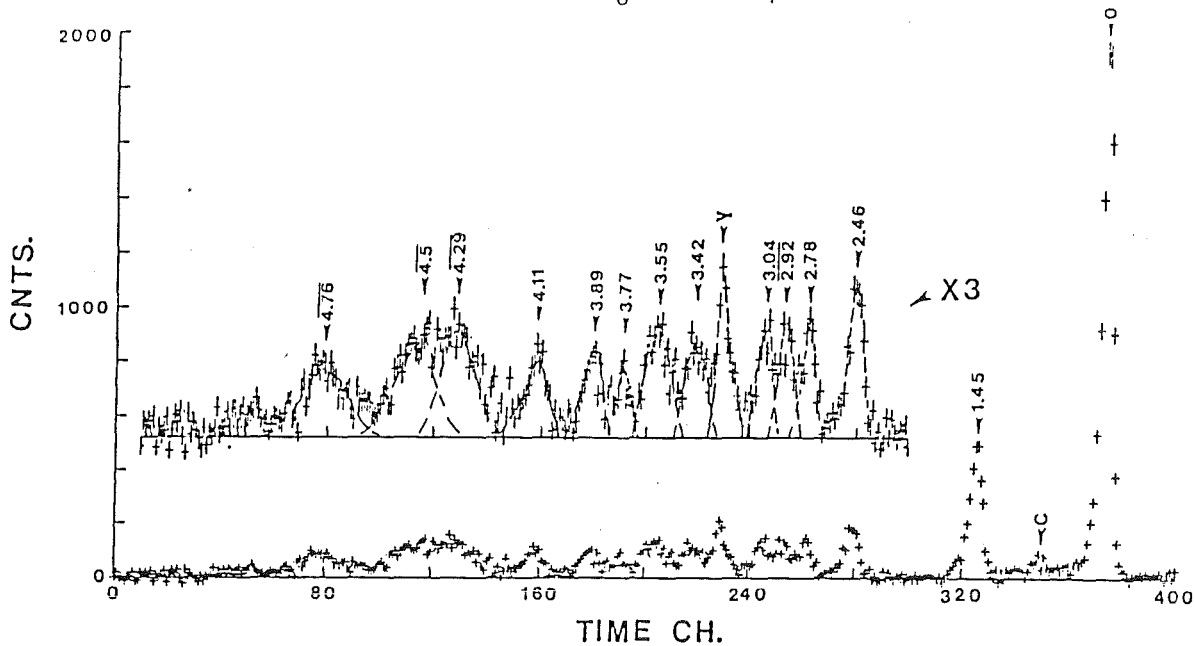
Fig. 3.   Measured velocity spectrum at 8 MeV incident energy.

energies, the latter are dominated by compound-nucleus processes, but
at higher energies the direct reaction is the governing factor with a
strong anisotropy of the scattered neutrons as illustrated in Fig. 4.
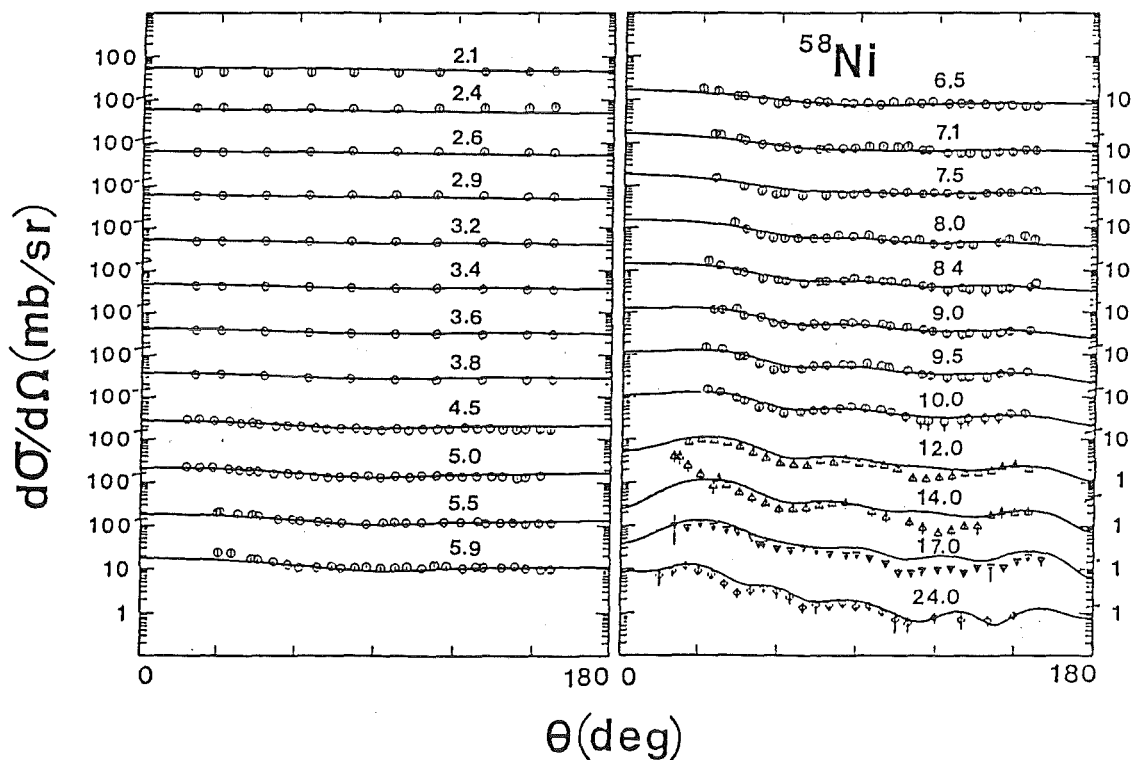
Fig. 4.   Inelastic cross sections for the 1.454 MeV level.   This
           laboratory to 10 MeV.   Higher-energy results from Gus85,
           Yam80 and Ped88.

Collectively, the measurements provide a comprehensive data base for applications, model derivation and verification, and for fundamental studies.

MODEL INTERPRETATIONS

The model interpretations followed a graded approach, extending from the simple spherical optical model to progressively more complex models. The model parameters were derived by explicit chi-square fitting of the elastic-scattering data, with concurrent subjective considerations of σ_t and σ_{inel} cross sections, and of the strength functions.

Initially, a simple spherical optical model was derived, suitable for many applications. The model geometry is energy dependent as it must be due to the dispersion relationship. The energy dependence of the real-potential strength generally follows the Hartree-Fock prediction, but there is a pronounced structure at ≈ 5 MeV, as shown in Fig. 5. The imaginary-potential strength falls with energy in a physically unattractive manner. It has been shown that such a
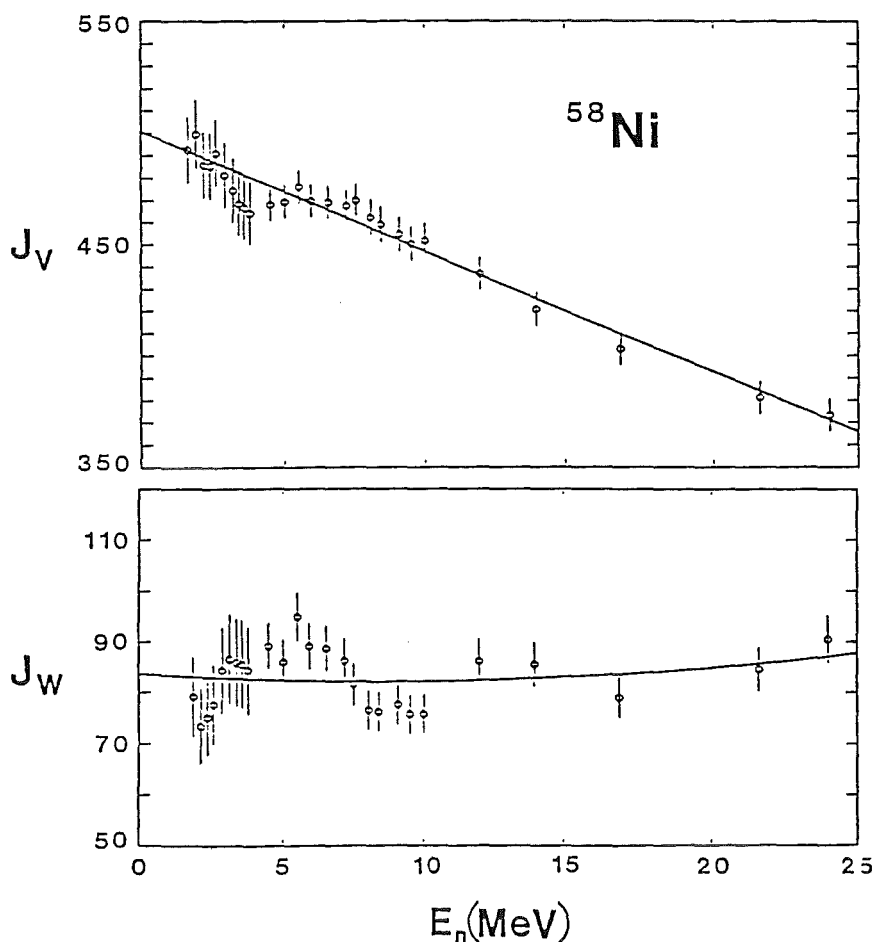
Fig. 5.   Real (J_v) and imaginary (J_w) spherical OM strengths in volume-integral-per-nucleon.

behavior is characteristic of a spherical model of a vibrational nucleus [Law87]. The simple spherical model gives a good parameterization of the observed total and elastic-scattering cross sections (see the curves of Figs. 6 and 2, respectively), and an acceptable representation of the strength functions. Further, it has the advantages of simplicity. The obvious shortcomings are; i) physically odd energy-dependencies, ii) failure to describe direct inelastic scattering, and iii) it is devoid of consideration of dispersion or collective effects.

The fundamental dispersion relationship

$$V(r,E) = V_{HF}(r,E) + \frac{P}{\pi} \int_{-\infty}^{+\infty} \frac{W(r,E')dE'}{(E-E')}$$
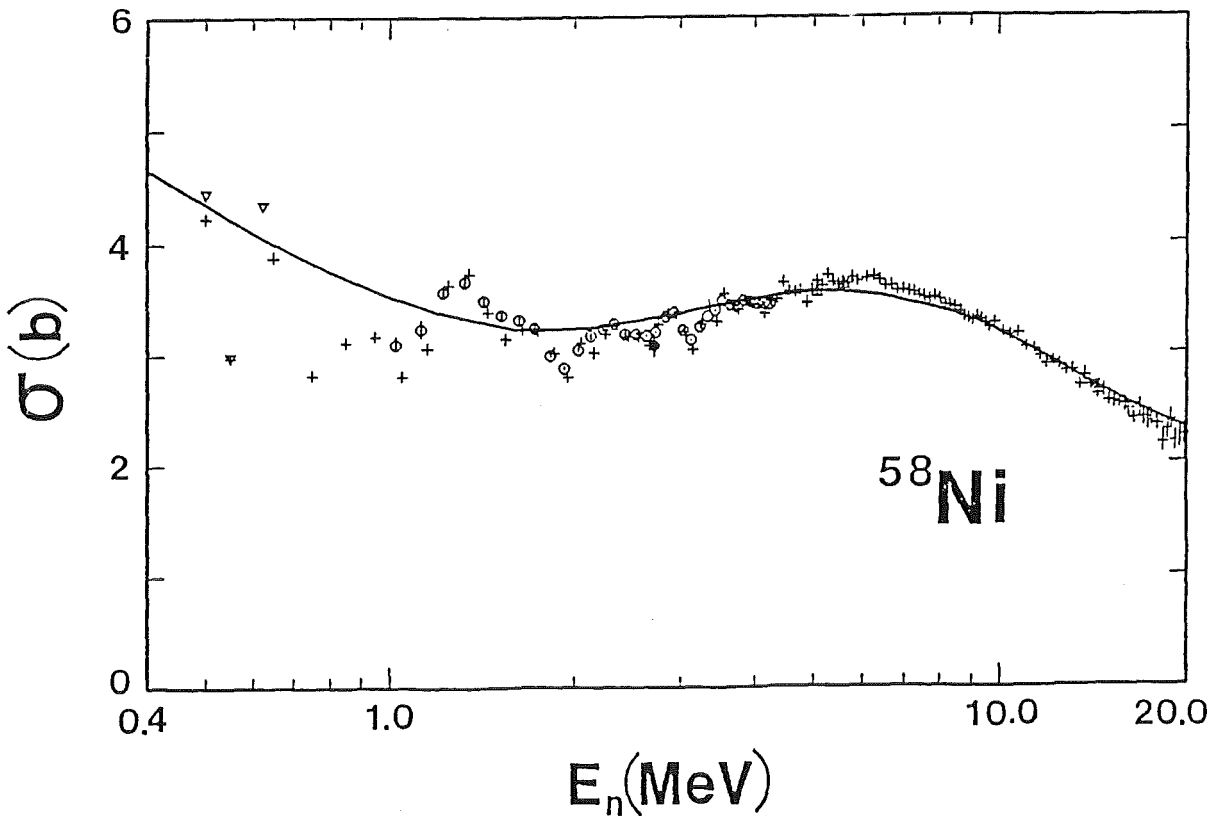
Fig. 6.   Energy-averaged σ_t of ^{58}Ni.   Symbols indicate experimental results.

couples real and imaginary potentials, and adds a surface component to the Saxon-Woods real potential [Sat83]. The Fermi surface of ^{58}Ni is at large negative energies resulting in a negative surface component of the real potential over the majority of the positive energy domain (see Fig. 7). The entire spherical interpretation was repeated using
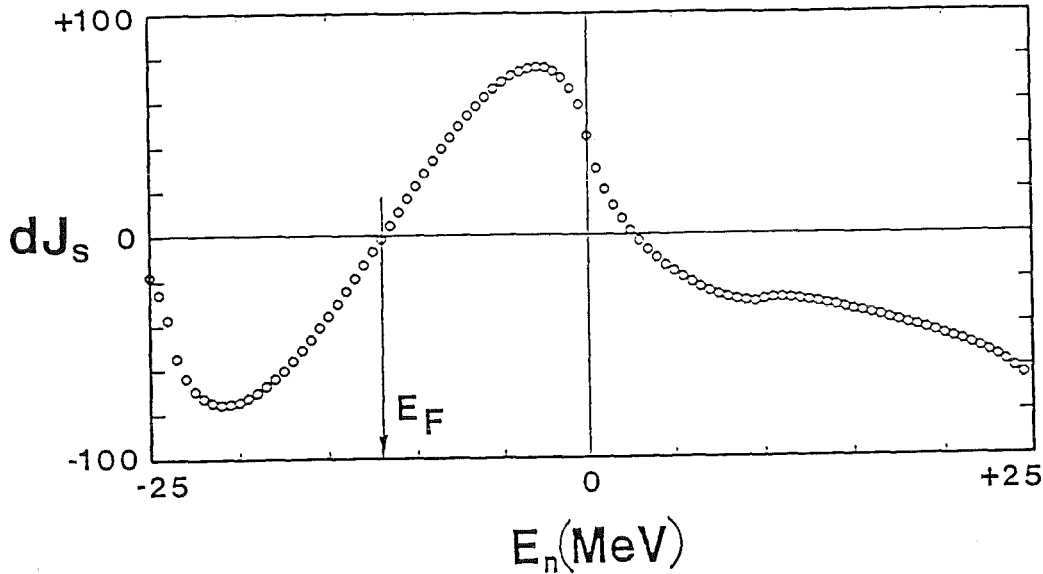
Fig. 7.   Surface component of the real-potential strength due to the dispersion relationship (dJ$_s$).

the dispersion relationship. The resulting potential gave results similar to those of the simple spherical optical model. Some of the energy dependencies of the potential geometries were alleviated (but not removed), and the energy-dependent structure of the real potential remained. In this case, the consideration of the dispersion relationship did not significantly improve on the parameterization of the simple spherical optical model outlined above.

Proceeding to more complex models, it was assumed that ^{58}Ni could be represented as a 1-phonon vibrator, coupling ground and first-excited 1.454 (2$^+$) MeV states, and β_2 was included in the variable parameters. The assumption is not exactly valid as the quadrupole moment of ^{58}Ni $\neq$ 0. With this assumption, the experimental interpretation was repeated. The model geometries remained energy dependent, but the structure in the real-potential strength, evident in the spherical models, was considerably alleviated, as shown in

Fig. 8. Moreover, the imaginary potential strength slowly increases with energy in a physically more acceptable manner. A good
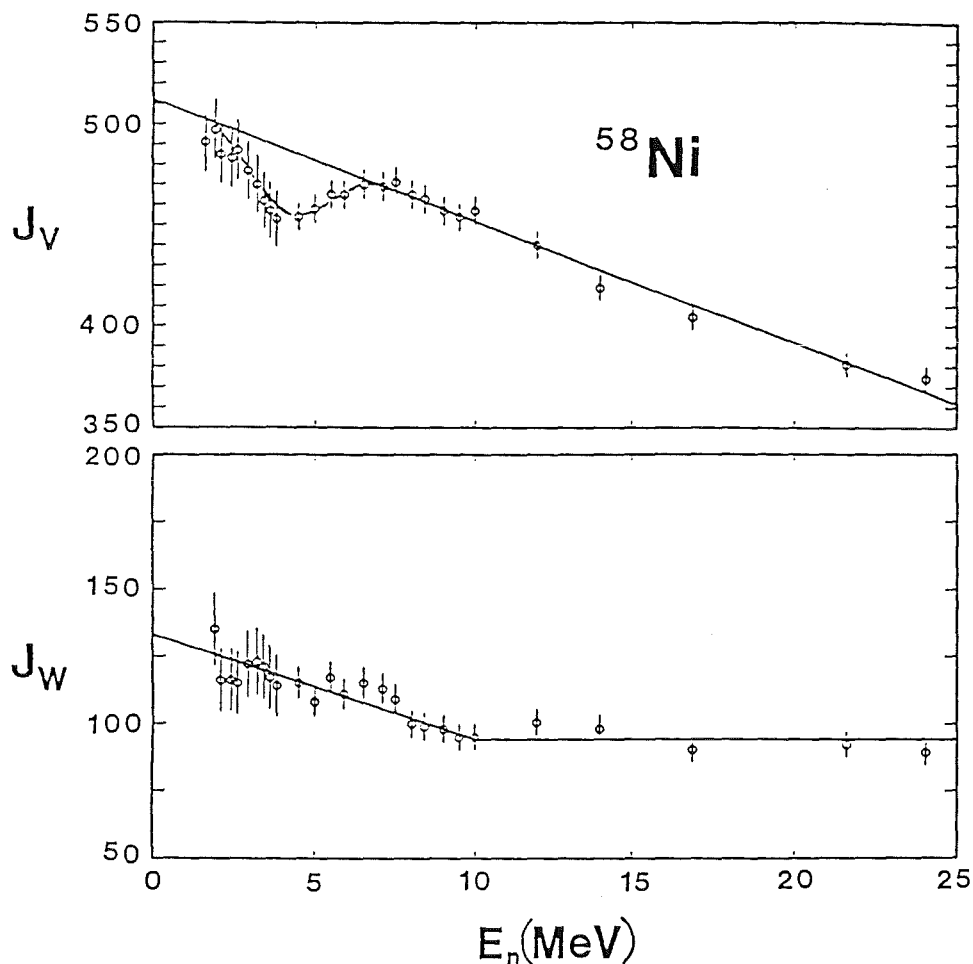
Fig. 8. Real (J_V) and imaginary (J_W) potential strengths obtained with the 1-phonon vibrational model.

description of σ_t and of the elastic scattering (Fig. 9) was retained.

In addition, the excitation of the prominent 2^+ level by inelastic scattering is very well described (see the curves of Fig. 4), and the elastic-scattering polarizations were reasonably represented. These results were obtained with $\beta_2 = 0.20 \pm 0.015$, which implies a deformation length of $\delta_{nn} = 0.8948$ at 10 MeV. This value is between the corresponding δ_{EM} of 0.849 and δ_{pp} of 0.9639, as predicted by the core-coupling model [Mad75]. However, one should remember that the deformation length, δ, is a f(R), and R is a f(E) due to the dispersion relationship, and thus the comparisons are meaningful only at specified energies.

Since the 1-phonon model leads to improved results, more complex couplings were considered. Using a 1- and 2-phonon model, results similar to those of the above 1-phonon model were obtained, with a reduction of β_2. There was a small direct-reaction component due to the inelastic-excitation of the 2-phonon states, but not an increase sufficient to greatly improve the agreement between observation and calculation. Moreover, the structure in the real-potential strength
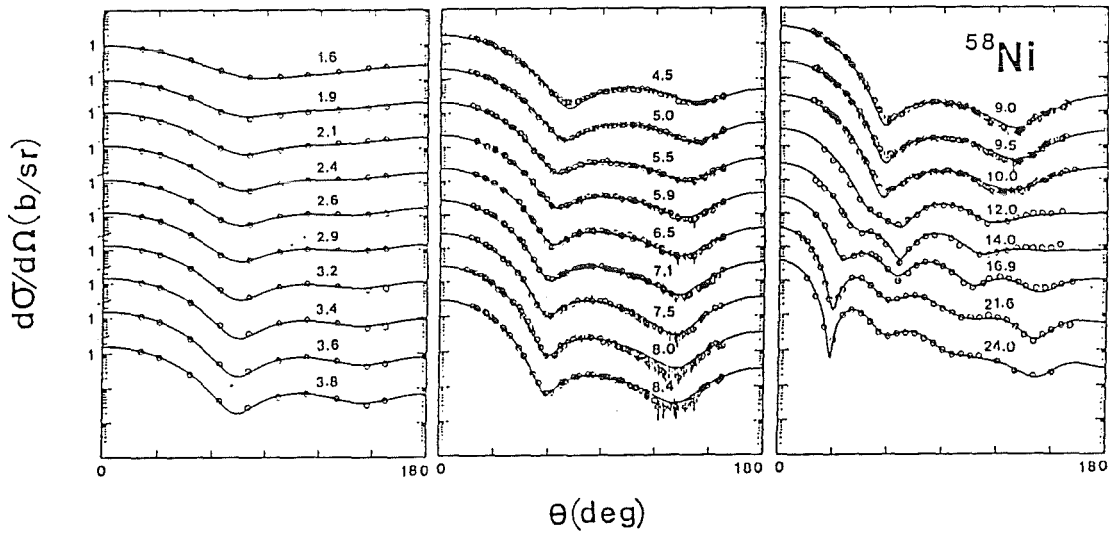
Fig. 9.   Measured (symbols) and calculated (curves) elastic scattering cross sections. Calculations used the 1-phonon model.

was not further alleviated. In order to introduce an entirely different coupling of ground and first-excited states, a simple rotational model was examined. The assumption is not particularly physically attractive, but it does grossly change the coupling scheme. The resulting rotational model did not lead to a significant improvement over the more attractive vibrational approaches.

SUMMARY COMMENTS

From this and other Argonne work, a systematic pattern is emerging. The real potential of energy-averaged models is qualitatively global with essentially a constant diffuseness. The real radius is mass and energy dependent, with the latter characteristic not entirely due to the dispersion relationship. Approximately, $r_v = r_o + r_1/A^{1/3}$, where $r_o = f(E)$ and r_1 a constant. Furthermore, the real-potential strength follows a simple dependence on isospin and r_v that is consistent with the nucleon-nucleon interaction strength. The imaginary potential is specific to each target, reflecting nuclear structure, collective effects, etc. These characteristics are mildly reflected into the real potential through the dispersion relationship. Elastic neutron scattering is not sensitive to deformation (e.g., to β_2), but inelastic scattering is. Deformation lengths are radii dependent and thus energy dependent. The measurements and associated models of this work should substantively contribute to the provision of data for the design of nuclear-energy systems. However, the collective effects in this region of structural materials are very complex, far more so than accounted for by the models. Thus, there is merit in a search for a more fundamental understanding of a very difficult problem. One approach being explored is the calculation of the neutron interaction from EM matrix elements derived from experimental measurements and/or as estimated from the shell model. This avenue has led to encouraging qualitative results, as illustrated in Fig. 10.

REFERENCES

Detailed references and numerical tables of potential parameters are given in the report ANL/NDM-120, "Fast-neutron Total and Scattering Cross Sections of ^{58}Ni and Nuclear Models", A. Smith, P. Guenther, J. Whalen and S. Chiba (1991).

Har86 J. Harvey, private communication (1986).
Bud82 C. Budtz-Jorgensen et al., Z. Phys. A306 265 (1982).
Gus85 P. Guss et al., Nucl. Phys. A438 187 (1985).
Yam80 Y. Yamanouti et al., NBS-594 (1980).
Ped88 R. Pedroni et al., Phys. Rev. C38 2052 (1988).
Ols90 N. Olsson et al., Nucl. Phys. A509 161 (1990).
Law87 R. Lawson et al., BAPS 32 32 (1987).
Sat83 G. Satchler, "Direct Nuclear Reactions" Clarendon (1983).
Mad75 V. Madsen et al., Phys. Rev. C12 1205 (1975).
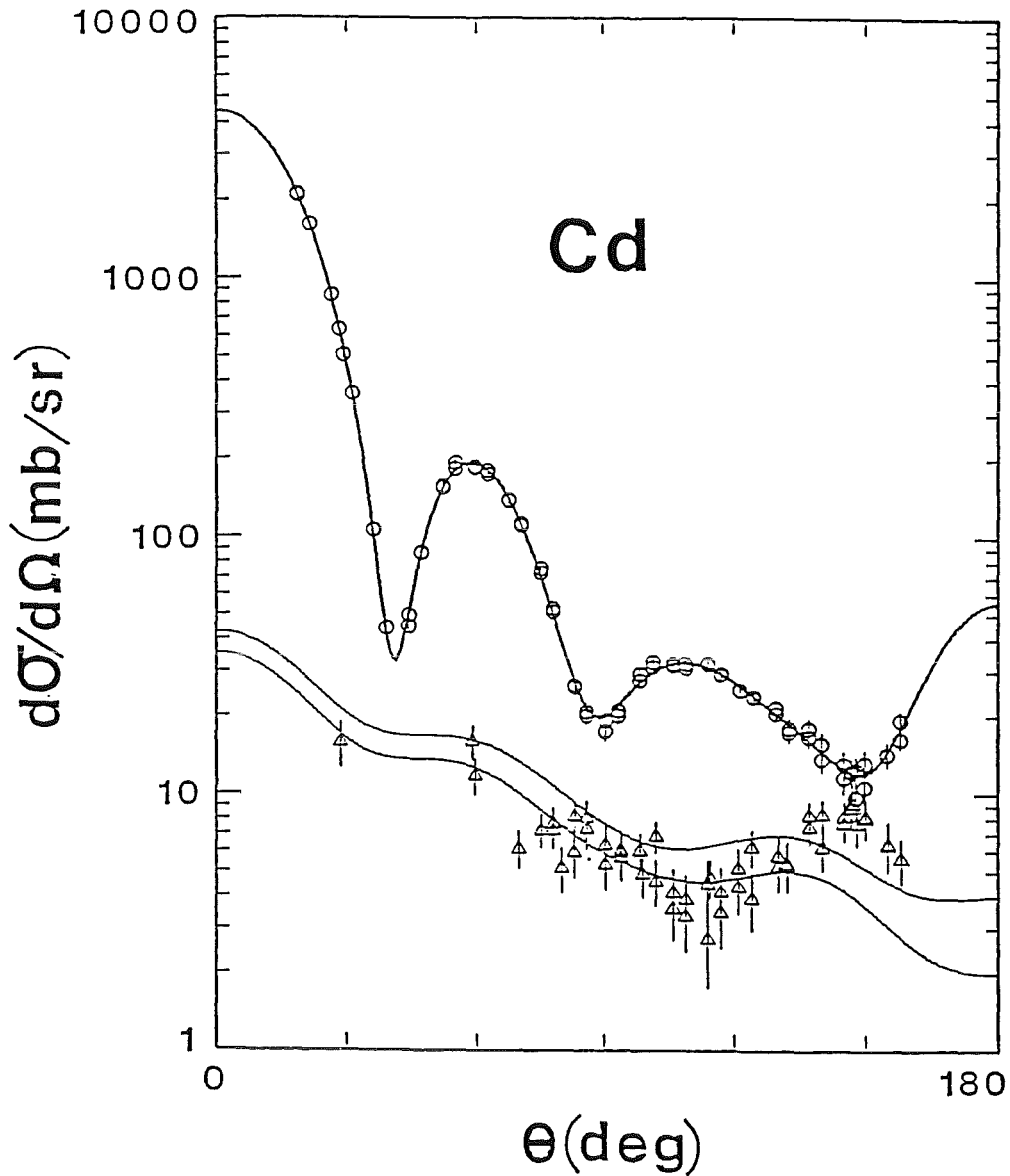
Fig. 10. Measured (symbols) and calculated (curves) scattering cross
sections of the even isotopes of cadmium. The upper
distribution is due to the elastic and inelastic scattering
from the first 2^+ level. The lower distribution is due to
the 2^+ excitation alone where the higher curve is obtained
using a 1-phonon calculation, and the lower a 3-phonon
calculation.
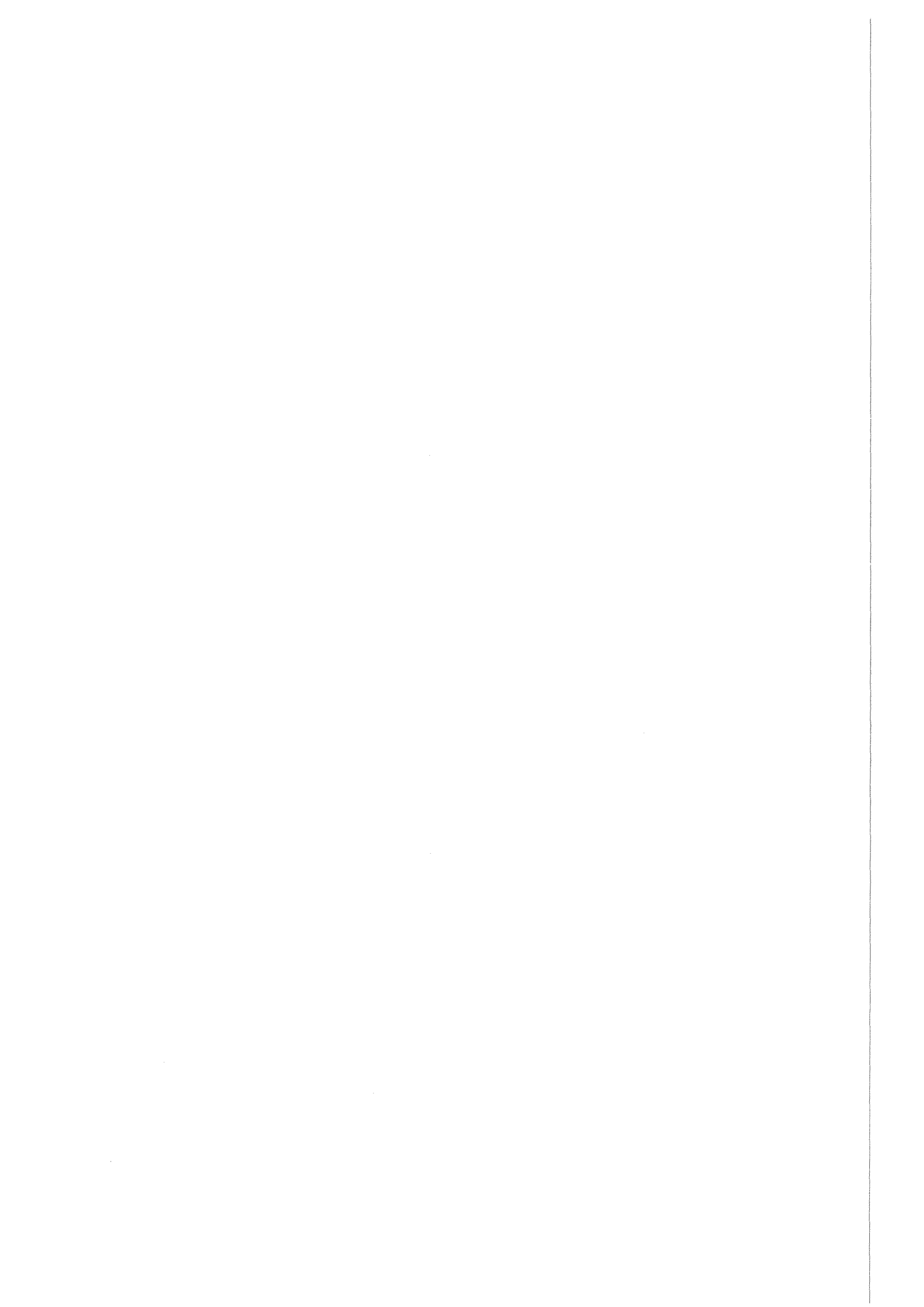
Neutron Emission Cross Sections for Neutron Transport Calculations

T. Elfruth, K. Seidel, S. Unholzer
Technical University Dresden
Insitute for Nuclear and Atomic Physics

Abstract : Differential neutron emission cross sections of V, Ta, W and U have been measured, theoretically interpreted and compared with evaluated data. Neutron fluxes of a benchmark and of a blanket mock-up arrangement obtained in transport calculations with library data show deviations from the measured flux distributions. They are understood as pre-equilibrium emission components not adequately taken into account in the evaluated library data.

1. Introduction

For calculations of the neutron flux in D-T fusion reactor components, as first wall, limiter, divertor, blanket and shield, differential neutron emission cross sections are needed for the major elements with accuracies $< 3...10$ % , for neutron incident energies E_0 up to 14 MeV [1]. The medium and heavy mass nuclei investigated in the present work are potential structure and shielding materials (^{51}V, ^{181}Ta, ^{nat}W) and are used in fusion-fast-fission hybrid-reactor projects (^{238}U). It will be shown that the evaluated library data of these nuclei deviate from measured differential neutron emission cross sections more than the accuracy needed, especially at higher emission energies. A theoretical analysis of the neutron emission reveals that pre-equilibrium emission components are not adequately included in the evaluated data. A benchmark of calculated to experimentally determined neutron leakage spectra from an uranium sphere shows similar discrepancies. They are also reflected on the time-differential neutron flux from a blanket mock-up.

2. Measured cross sections and comparison with library data

Neutron emission spectra were measured with time-of-flight spectroscopy at a pulsed D-T neutron generator. The experimental arrangement is shown in Fig. 1. The neutron flight-path was about 5 m. Neutron emission spectra from the ring samples were taken at emission angles $\vartheta = 15^o \cdots 165^o$ in steps of 15°. The neutron production was determined by counting the α-particles of the source reaction. The data corrected for differential nonlinearity of the spectrometer, dead time, uncorrelated background, source anisotropy, flux attenuation and multiple scattering in the sample were transformed from time to energy spectra. More details can be found in Ref. [2].
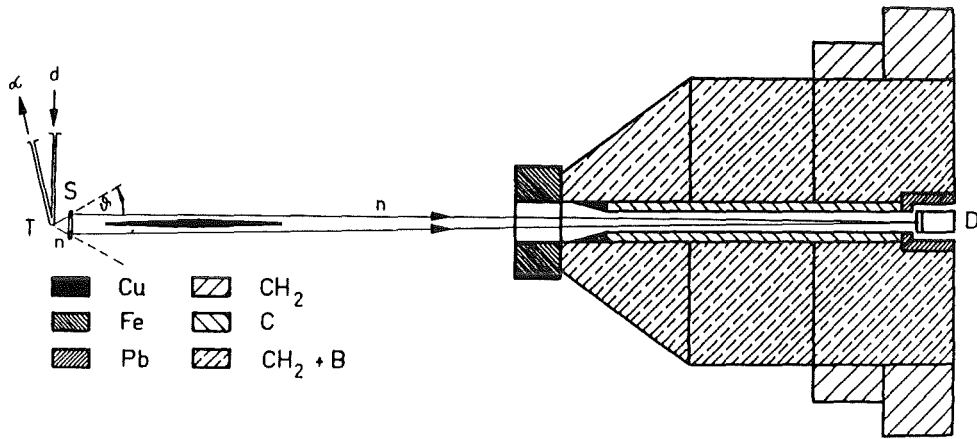
Fig. 1: Set-up for the measurement of double-differential neutron emission cross sections. T - $^3H(d,n)$ pulsed neutron source; S - sample ring; ϑ - neutron emission angle; D - neutron time-of-flight detector
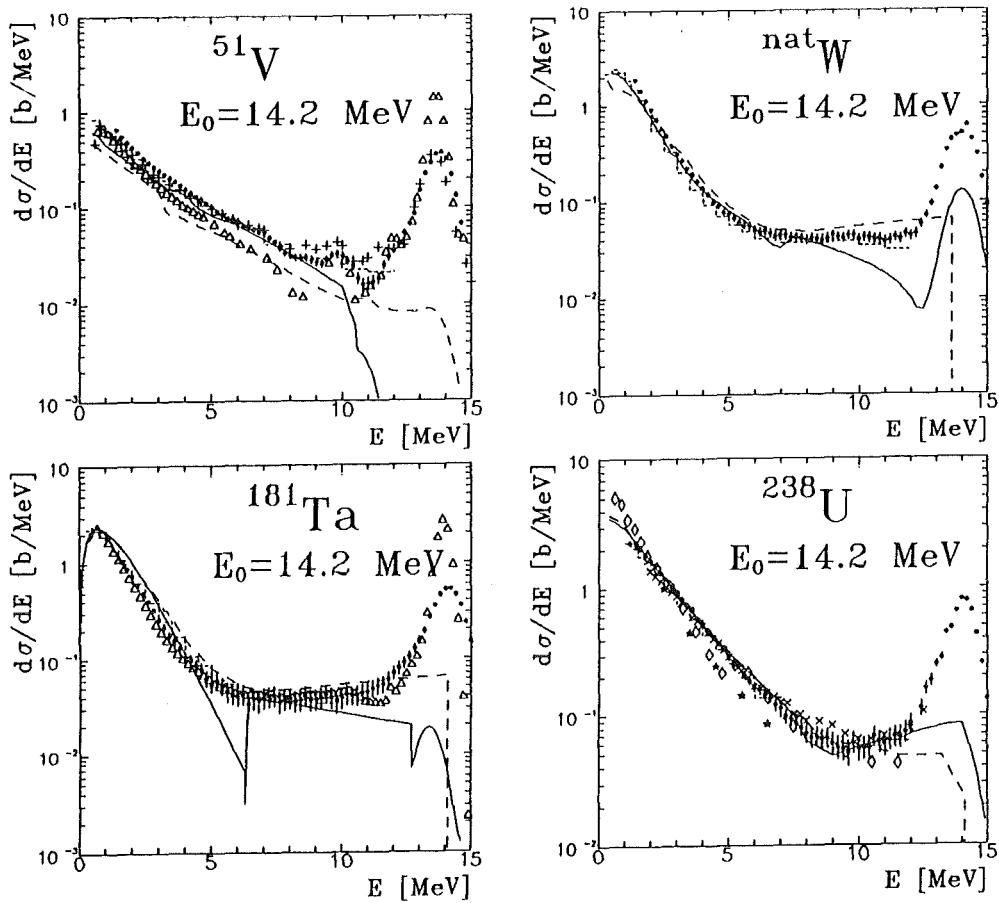
Fig. 2: Energy distributions of the neutrons emitted after 14.2 MeV neutron bombardment. Experimental data: + [3], $\triangle$ [4], $\lozenge$ [5], $*$ [6], $\times$ [7], ($\bullet$) present work; evaluated experimental data: dotted histogram for Ta and W [8], V and U present work ; library data: ENDF/B-VI (solid line), ENDL-83 (dashed line)

The angle-integrated emission cross sections are shown in Fig. 2. An example of angular distributions is presented in Fig. 3.
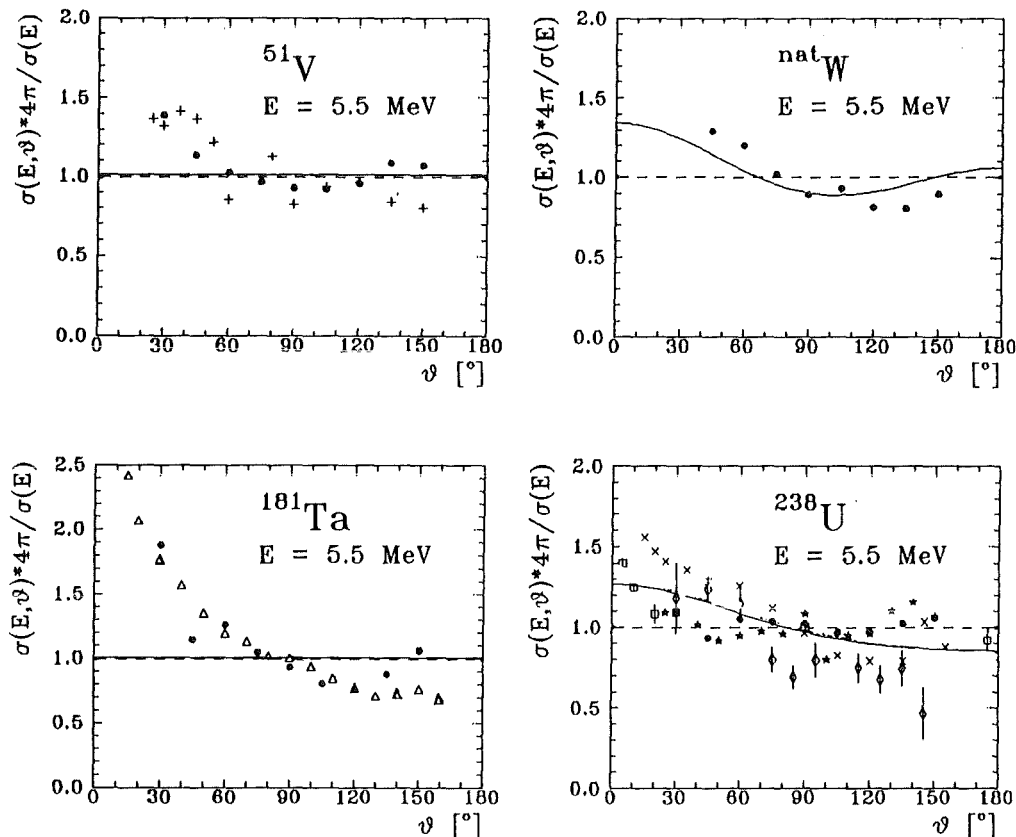
Fig. 3: Angular distributions of the neutrons emitted at E = 5.5 MeV after 14.2 MeV neutron bombarment
Experimental data: + [3], △ [4], ◇ [5], * [6], × [7], □ [10], (•) present work; library data: ENDF/B-VI (solid line), ENDL-83 (dashed line)

Significant deviations of the library data from the uncertainty-weighted evaluations of the experimental energy distributions are observed for E > 8 MeV in the case of V, Ta and W as well as at lower energies for V and Ta. The angular distributions are assumed in almost all library files to be isotropic, whereas the experimental data are forward peaked.

3. Calculation of differential cross sections with the SMD/ SMC-model

Energy-differential emission cross sections are calculated as sum of all possible emission chances (n_1, n_2, ...). As shown in Fig. 4 at each stage of the deexciting system, neutron emission competes with γ- and proton emission, and in the case of U also with fission additionally leading to fission neutrons (n_f). The n_1 are assumed to be emitted in the pre-equilibrium and in the equlibrium phase of the reaction. Pre-equilibrium neutrons arise from multistep-direct and from multistep-compound processes. Their statistical treatment
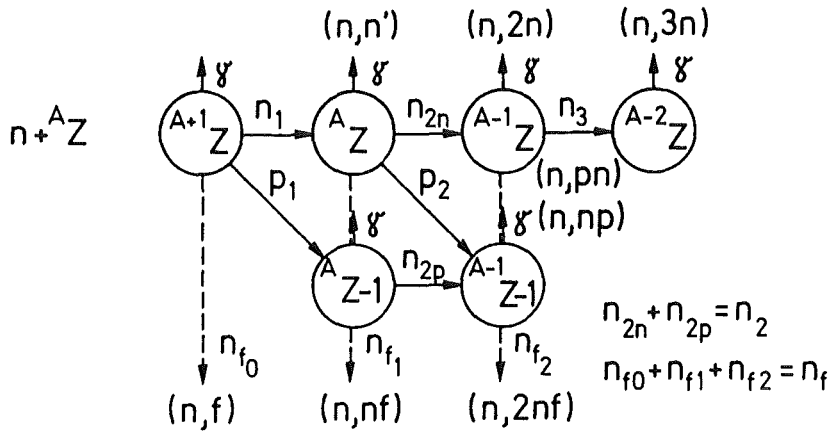
Fig. 4: Chances of neutron emission of a nucleus (mass number A, proton number Z) bombarded with 14 MeV neutrons

with the code EXIFON [9] includes as one- and two-step direct processes (SMD) both single-particle and collective excitations (2^+ and 3^- phonons). The SMC-neutron emission is calculated by solving the master equations from 5-exciton states up to the equilibrium of excited particles and holes. The n_2 and n_3 are emitted from equilibrated systems. The n_f are evaporated from the accelerated fragments. As input parameters in all cases a surface-delta interaction of $V_0 = 19.4$ MeV, $r_0 = 1.4$ fm, the single-particle level density $= A/13$ MeV^{-1} and phonon data from mass-number dependent systematics are used. Total neutron emission spectra obtained from these calculations for V, Ta and W at $E_0 = 14.2$ MeV, for U at $E_0 = 6 \cdots 14.2$ MeV are compared in Fig. 5 with experimental data. Additionally the emission of neutrons from U in coincidence with fission events at $E_0 = 6 \cdots 14.2$ MeV is shown in this figure too. Angular distributions calculated with the assumption, that the SMD-component is forward peaked and can be parametrized with the Kalbach-Mann-formula, are compared in Ref [11] with experimental data. The agreement of all calculated spectra and angular distributions with the experimental data is sufficient. Summarizing the results of the comparisons one can conclude that the model used describes the main emission components adequately.

4. Neutron leakage spectrum from a spherical assembly as benchmark

Evaluated nuclear data and transport codes are checked by comparing experimental to calculated values determined for geometrically simple and homogeneous arrangements. Fig. 6 shows a set-up with a metallic uranium sphere (depleted in ^{235}U to 0.4 %, 6 cm shell thickness). Neutron leakage spectra were measured by time-of-flight and proton-recoil spectroscopy at detector position D, and fission and activation rates were determined at the surface of the sphere [12]. The neutron leakage spectrum is shown in Fig. 7. Differences to the spectra calculated with the Monte Carlo code MCNP [13] and data of the libraries ENDF/B-IV and ENDL-85 are observed in the high- and medium-energy range. They are caused by differences in the data. Especially pre-equilibrium emission components are not adequately or not physically parametrized taken into account.
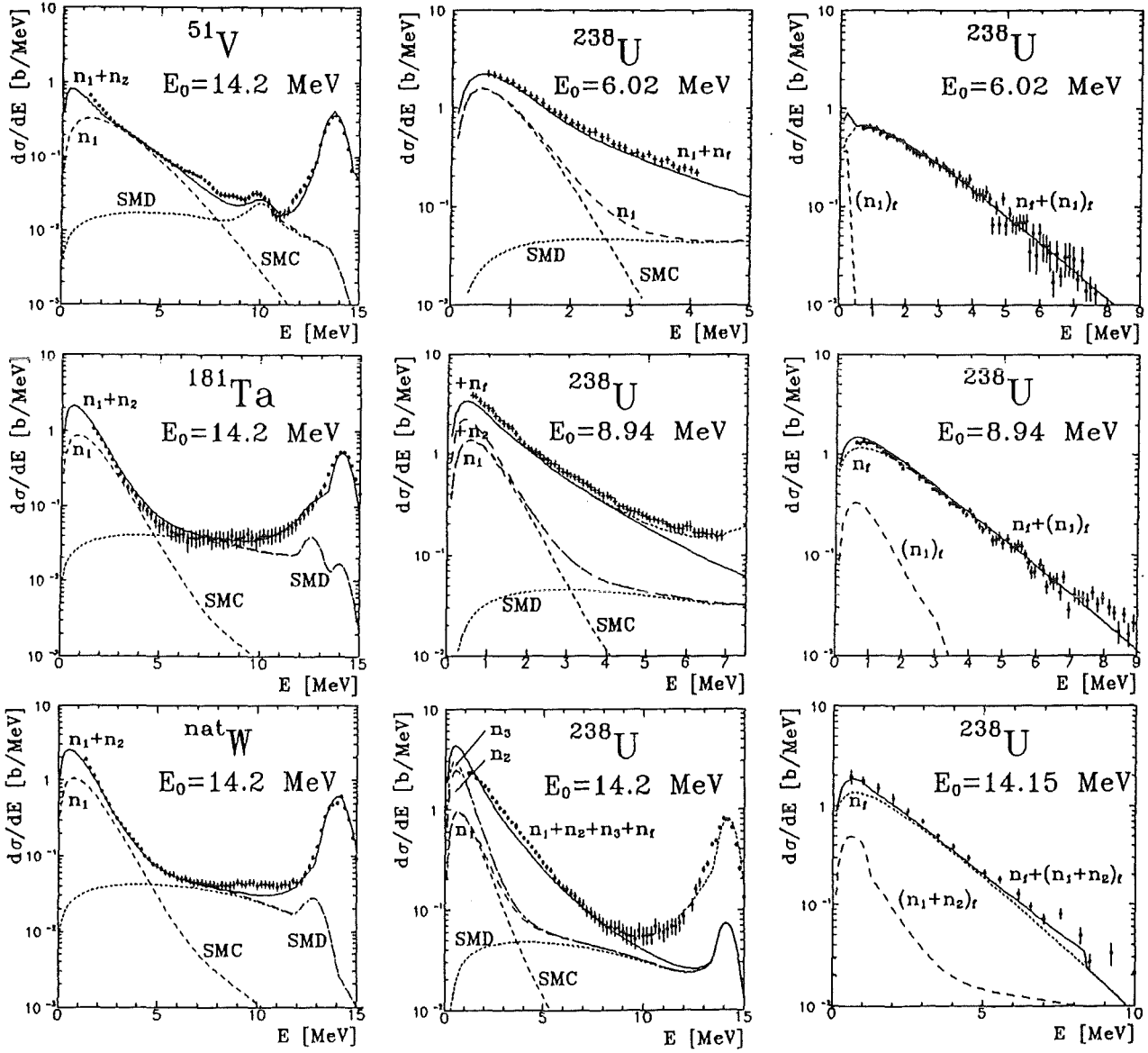
Fig. 5: Calculated neutron emission cross sections compared with experimental data. Designation of the components see Fig. 4.

left: total emission, exp. data of the present work (•); middle: total emission; exp. data of Ref [10] (+) and of the present work (•) ; right: emission in coincidence with fission; exp. data of Ref [10]
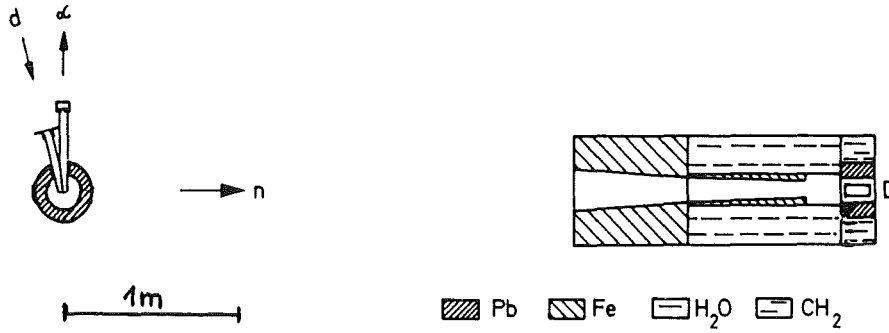
Fig. 6: Set-up for the measurement of the neutron leakage spectrum in a ^{238}U-benchmark. ^{3}H(d,n) - pulsed neutron source; n - leaking neutrons; D - neutron time-of-flight detector
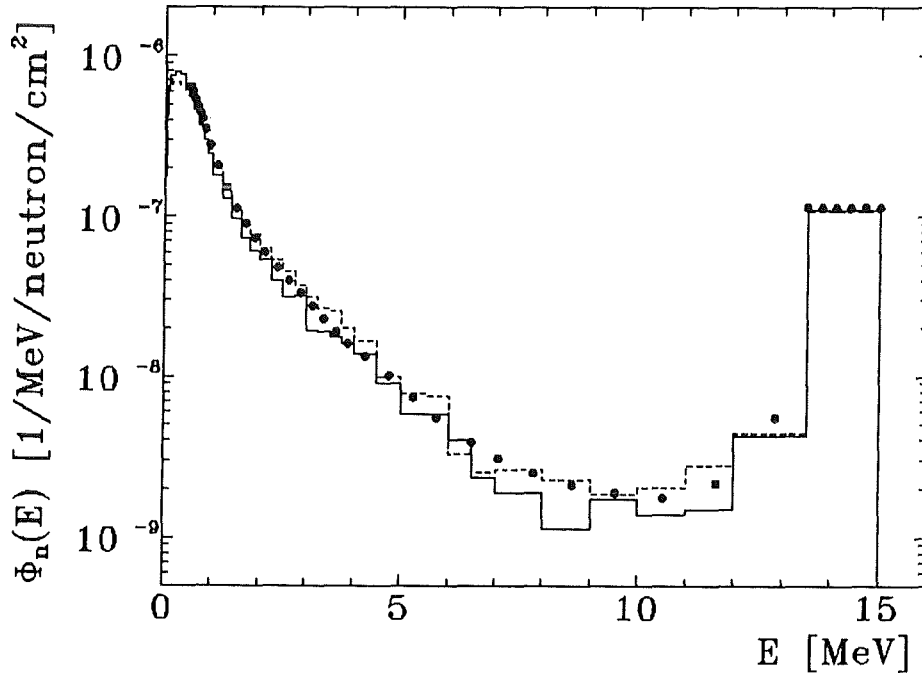
Fig. 7: Neutron leakage spectrum from a uranium sphere.
Experiment: (●); MCNP-calculations: ENDF/B-IV - solid line, ENDL-85 - dashed line

5. Neutron flux from a blanket mock-up

A blanket mock-up consisting of iron, uranium, LiAl, polyethylene and steel slabs was investigated by determing tritium production rates, ^{238}U-fission rates, ^{239}Pu-breeding rates and time- and energy-differential neutron fluxes [14]. At detector position D in Fig. 8 and using slabs I and II only, the time-differential neutron flux in Fig. 9 was measured with time-of-flight spectroscopy. Compared to the calculated distributions differences around t ≈ 70 ns and t ≈ 100 ns are observed, which are caused by data differences at energies where pre-equilibrium emissions are dominating.
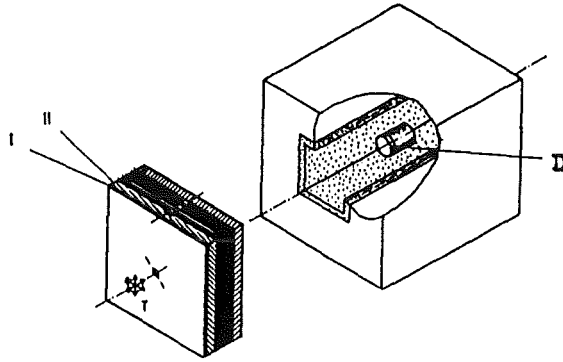
Fig. 8: Blanket mock-up and arrangement for neutron spectra measurement.
T - ^{3}H(d,n) pulsed neutron source; I - iron slab (100 × 100 × 2cm ^{3}); II - uranium slab (100 × 100 × 10 cm^3); D - neutron time-of-flight detector
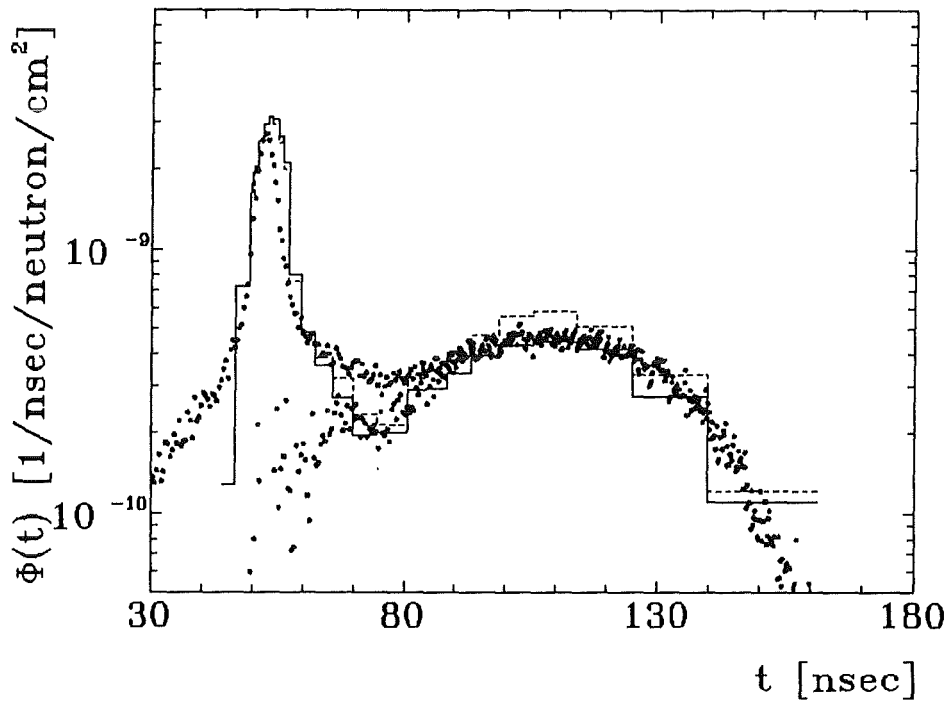
Fig. 9: Time-differential neutron flux from the blanket mock-up.
Experiment with and without peak separation: • ; MCNP-calculations: ENDF/B-IV - solid line, ENDL-85 - dashed line

6. Conclusions

The differential neutron flux from a benchmark and from a mock-up calculated with evaluated library data deviates from the measured distributions in some ranges. The origin of the differences is found in the library data, where pre-equilibrium emission components are not

taken into account with the accuracy needed. Reaction models like the SMD/SMC-model describe, even with global parameters, the experimental neutron emission cross sections with sufficient quality and can be used to improve the library data. This conclusion should be valid in principle not only for the nuclei investigated in the present paper, but for all medium and heavy mass nuclei (with exception of magic nuclei, where shell corrected parameter have to be used [15]).

References

[1] Nuclear Data for Fusion Reactor Technology, in Proc. Adv. Group Meeting of the IAEA, Gaussig 1986, IAEA-TECDOC-487, IAEA, Vienna, 1988

[2] H. Al Obiesi et al., INDC(GDR)-058/L, IAEA, Vienna, 1990

[3] M. Baba et al., JAERI-01-88-065, p. 365, Tokai, 1988

[4] A. Takahashi et al., OKTAVIAN-Report A-87-03, Osaka Univ. 1987 and INDC(JAP)-118/L, IAEA, Vienna, 1989

[5] J.L. Kammerdiener, Thesis, UCRL-51232, Livermore, 1972

[6] J. Voignier et al., CEA-3503 (1968) and EXFOR 21094.004 (1980)

[7] S. Guanren, in Proc. Adv. Group Meeting on Nuclear Theory for Application, Bejing, 1987

[8] A. Pavlik and H. Vonach, Physics Data **13 − 4** (1988)

[9] H. Kalka, INDC(GDR)-059/L, IAEA, Vienna, 1990

[10] V. Kornilov et al., in Proc. Conf. on Neutron Physics, 1980, Kiev, Vol. 3, p. 104, Moskva, 1980
D. J. Degtjarev et al., Jadernaja Fizika **34**(1981)299

[11] H. Al Obiesi et al., in Proc. Int. Conf. on Nuclear Data for Science and Technology, 13 - 17 May 1991, Juelich, in press

[12] T. Elfruth et al., Kerntechnik **55**(1990)156

[13] J. F. Briesmeister, LA-7396-M, Rev. 2, 1986

[14] J. Brose et al., in Proc. Int. Conf. on Nuclear Data for Science and Technology, 13 - 17 May 1991, Juelich, in press

[15] T. Elfruth et al., in Proc. Int. Symp. on Nucl. Physics, Gaussig, 1989, ZfK-733(1991), p. 58

Measurement of Neutron Activation Cross Sections for ^{99}Tc(n,p)^{99}Mo, ^{99}Tc(n,α)^{96}Nb and ^{99}^{99}Tc(n,n)^{99m} Reactions at 13.5 and 14.8 MeV

Y. Ikeda, C. Konno and E. T. Cheng*

Department of Reactor Engineering
Japan Atomic Energy Research Institute
Tokai-mura, Ibaraki-ken 319-11 Japan

* TSI research,
225 Stevens Avenue, Suit 110,
Solana Beach, CA 92075 USA

Abstract: The activation cross sections for the ^{99}Tc(n,p)^{99}Mo at 13.5 and 14.8 MeV have been measured using a D-T neutron source at FNS of JAERI to provide the comprehensive data base for a feasibility study of the high specific ^{99}Mo radioactivity production in the medical application. Basing on the present data, an overestimation of ^{99}Mo using REAC-2 data library was suggested. Along with ^{99}Tc(n,p)^{99}Mo, cross sections of ^{99}Tc(n,α)^{96}Nb, ^{99}Tc(n,n'α)^{95}Nb and ^{99}Tc(n,n')^{99m}Tc have been measured.

Introduction

The ^{99}Tc(n,p)^{99}Mo reaction produces ^{99}Mo radioisotope with very high specific activity ratio, which is more preferable to activities obtained from fission products or ^{98}Mo(n,γ)^{99}Mo reaction in a reactor. An idea to utilize intense neutron source for material irradiation test, e. g. FMIF[1], IFMIF, ESNIT and Fusion Reactor[2], has been investigated to produce the high specific 99Mo for medical diagnostics of liver and brain cancer. A preliminary study based on 40 mb for ^{99}Tc(n,p)^{99}Mo taken from REAC-2 [3] gave a result that an annual revenue of about $12M could be generated to finance the operation cost of FMIF.[1]

Objectives of the present study are to measure activation cross section for ^{99}Tc(n,p)^{99}Mo around 14 MeV energy region to give accurate estimation of ^{99}Mo radioactivity production utilizing FMIF (Fusion Material Irradiation Facility), and to provide basic data for better understanding

reactions with radioactive target of ^{99}Tc; ^{99}Tc(n,α)^{96}Nb, ^{99}Tc(n,n'α)^{95}Nb and ^{99}Tc(n,n')^{99m}Tc.

Experiments

Samples of 99Tc were prepared from solution of 185 MBq ^{99}Tc (21.46 MBq/ml). [LOT#57 of TCS1 (delivered by Amersham, U.K.)] Amount of 17.3 μl corresponding to 10.03 μCi was pipetted from the original liquid solution and was deposited on a thin plastic plate. After drying the solution, the sample was sealed with another thin plastic plate. The size of the sample deposition was 3 mm in diameter. Each sample contained 3.5963 x 10^{18} of 99Tc nuclei.

Irradiation experiment was performed at Fusion Neutronics Source (FNS) at JAERI. The 14 MeV Neutrons were produced via ^{3}T(d,n)^{4}He reaction. Incident deuterium energy and current were 350 keV and 2 mA, respectively. Source strength was about 3 x 10^{11}/sec. Two identical samples were positioned at 10 mm distance from the source and at 0° and 135° angles with respect to incident d$^+$ beam direction. These angles corresponded to 14.8 and 13.5 MeV neutron energies. The irradiation configuration is shown in Fig. 1 Irradiation time was about 6 hours.

The reaction of ^{93}Nb(n,2n)^{92m}Nb was used for the D-T neutron flux monitor. The cross section of 455 ± 7 mb around 14 MeV was assumed for this reaction. Two thin Nb foils were attached on the front and rear surface of the ^{99}Tc samples.

Source neutron spectra were calculated by the MORSE-DD code with JENDL-3 nuclear data. In the calculation, fine structure of the neutron target system was modeled. The spectra corresponding to the two angles are shown in Fig. 2. Low energy neutron flux contributions to the reaction rates were calculated by using the neutron spectra.

After irradiation, gamma-rays spectrum of radioactive sample were measured with a 117 % Ge detector (EG&G ORTEC). Activation rates for the reactions of interest were deduced from γ-ray counts by performing necessary corrections. The decay data used in the data processing are shown in Table 1.

Cross sections were obtained from the activation reaction-rate ratio to the monitor reaction. Table 2 summarizes the experimental errors considered.

Results and Discussion

The results are tabulated in Table 3 along with data in the literature.

^{99}Tc(n,p)^{99}Mo

The cross section of 14.0 ± 0.9 mb is in good agreement with data of 15.1 ± 2.3 by Qaim [4]. The value is supported by a comprehensive systematics for the (n,p) reaction cross section based on

data measured at FNS as shown in Fig. 3, which give a range of this cross section at 14.9 MeV from 13 to 25 mb. (See Fig. 3) From this result, the cross section of REAC-2, 52.7 mb, seems overestimated by a factor of 4. This may lead to reduce the estimation for amount of ^{99}Mo production.

^{99}Tc(n,α)^{96}Nb

The present results gave generally good agreements with data measured by Qaim[4]. Also, the systematics of REAC-ECN-3 [8] gave reasonable agreement with the present data.

^{99}Tc(n,n'α)^{95}Nb

The activity of ^{95}Nb with hale-life of 35 d was detected. However, the γ-ray counting statistics were so poor that the uncertainties of data were larger than those of the other reaction cross sections. This poor statistics was mainly due to the small number of the target nuclei of 99Tc. Even though, the present data gave a general agreement with data of Qaim[5].

^{99}Tc(n,n')^{99m}Tc

The ^{99m}Tc is the daughter of ^{99}Mo deexciting with half-life of 6 h to the ground state of ^{99}Tc. Since the ^{99}Mo is simultaneously produce, the correction for the contribution from the decay of ^{99}Mo to ^{99m}Tc was essential in this case. The present data were comparable to the data previously reported [5, 6].

Summary

An overestimation by a factor of 4 in the amount of ^{99}Mo production by FMIF is suggested as long as the present cross section is valid. However, the idea of ^{99}Mo production using ^{99}Tc(n,p)^{99}Mo is still very attractive in terms high specific activity ratio in comparison with the other methods; chemical separation from the fission products and ^{98}Mo(n,γ)^{99}Mo reaction. Thus, the feasibility study of the idea should be forwarded based on the more precise nuclear data.

Acknowledgements

Reference

[1]   E.T.Cheng, R.E. Schenter, Y. Ikeda, Nuclear Data for the Production of Radio isotope in Fusion Material Irradiation Facility, ANS Transaction,Vol. 63 (1991) 169.

[2]   B. A. Engholm, E. T. Cheng, K. R. Schultz, "Radioisotope Production   in Fusion Reactors, " Fusion Technology ; Vol. 10 (1986) 1290.

[3] F. M. Mann, "REAC2: Status of Codes and Libraries," Fusion Thechnol., Vol. 15 (1989) 449.

[4] S.M.Qaim, J.Inorg. Nucl. Chem., Vol. 35 (1973) 3699.

[5] N.W.Golchert, D.G.Gardrer, J.Sedlet, Nucl. Phys. 73 (1965) 349.

[6] G.Goldstein, J.Inorg. Nucl. Chem., Vol. 28 (1966) 676.

[7] V.S.Shirley, Edition, "Table of Radioactive Isotopes," A Wiley- Interscience Publication (1986).

[8] H. Gruppelaar, H. A. J. Van Der Kamp, J. Kopecky, D. Nierop, "The REAC-ECN-3 Data Library with Neutron Activation and Transmutation Cross-Sections for Use in Fusion Reactor Technology," ECN-207 (1988).

Table 1 Reactions investigated and associated decay data

Reaction	Half-Life	γ-ray energy (keV)	γ-ray branching (%)
^{99}Tc (n, p)^{99}Mo	2.7477 ± 0.0002 d	739.51	12.14 ± 0.22
^{99}Tc (n, α)^{96}Nb	23.35 ± 0.05 h	568.86	56.8 ± 1.5
^{99}Tc (n, n'α)^{95}Nb	34.97 ± 0.03 d	765.80	99.79 ± 0.10
^{99}Tc (n, n')^{99m}Tc	6.006 ± 0.002 h	140.47	87.2 ± 0.5

Decay data were taken from Ref-[7].

Table 2   Experimental Error

Radioactivity	99Mo	96Nb	95Nb	99mTc
Statistics	2-8	2-3	80	0.1 - 0.2
Efficiency	2.0	2.0	2.0	2.5
Numbor of 99Tc	2.0	2.0	2.0	2.0
Decay Constant	< 0.1	0.2	0.1	< 0.1
γ-ray branching	1.8	2.7	0.1	0.6
Sum-Peak correction	0.2	0.2	0.1	-
γ-ray self-absoption	0.1	0.2	0.2	0.5
Low-energy neutron	0.2	0.2	0.2	1.0

Flux Monitor :   93Nb (n, 2n)92mNb

Cross section	1.5	[455 $\pm$ 7mb]
Reaction Rate	3.0	

Total	6 - 9	6 - 7	- 80	5 - 6

Table 3   Results

Reaction	Cross Section (mb)		References	
	13.5 MeV	14.8 MeV		
^{99}Tc(n, p) ^{99}Mo	10.7 ± 1.0	14.0 ± 0.9	15.1±2.28	-a)
			6.97±1.11	-b)
			- 5	-c)
^{99}Tc(n,α) ^{96}Nb	4.5 ± 0.3	5.6 ± 0.4	7.12±1.0	-a)
			2.02±0.22	-b)
			7.5±0.2	-c)
^{99}Tc(n, n'α) ^{95}Nb	-	2.0 ± 1.6	1.28±0.2	-a)
			< 1.0	-b)
^{99}Tc(n, n') ^{99m}Tc	104 ± 6	76 ± 4	107±13	-a)
			41.3±6.6	-b)
			77±4	-c)

a) Reference [4]
b) Reference [5]
c) Reference [6]
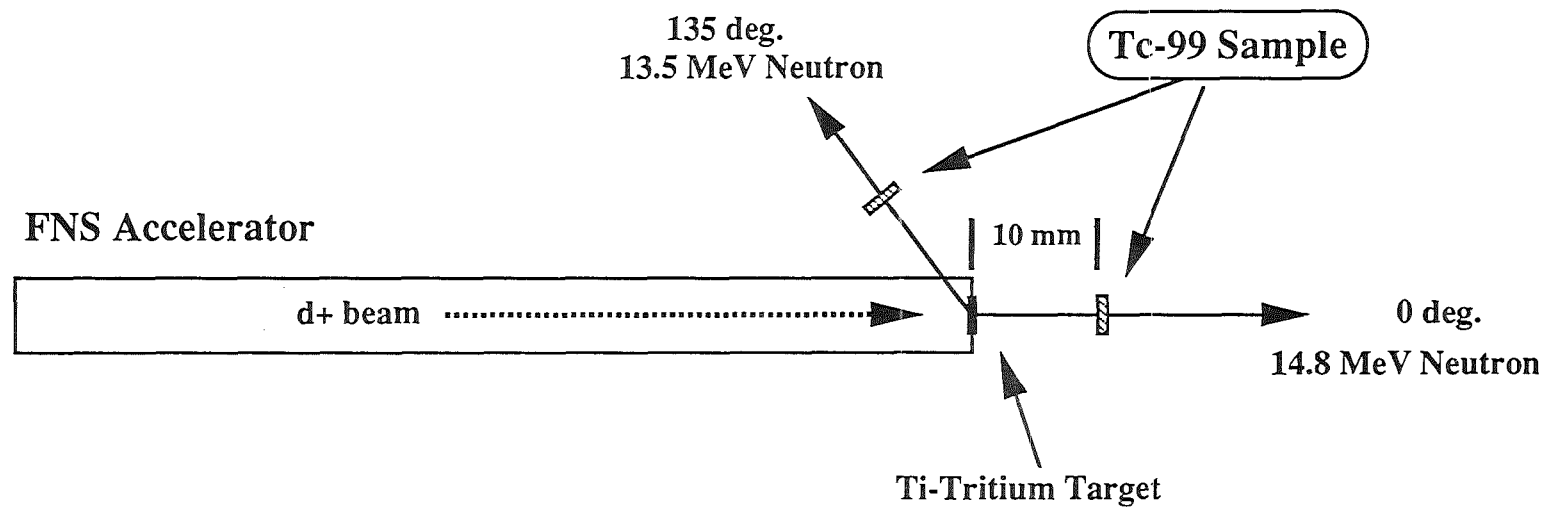
Fig. 1 Irradiation Configuration
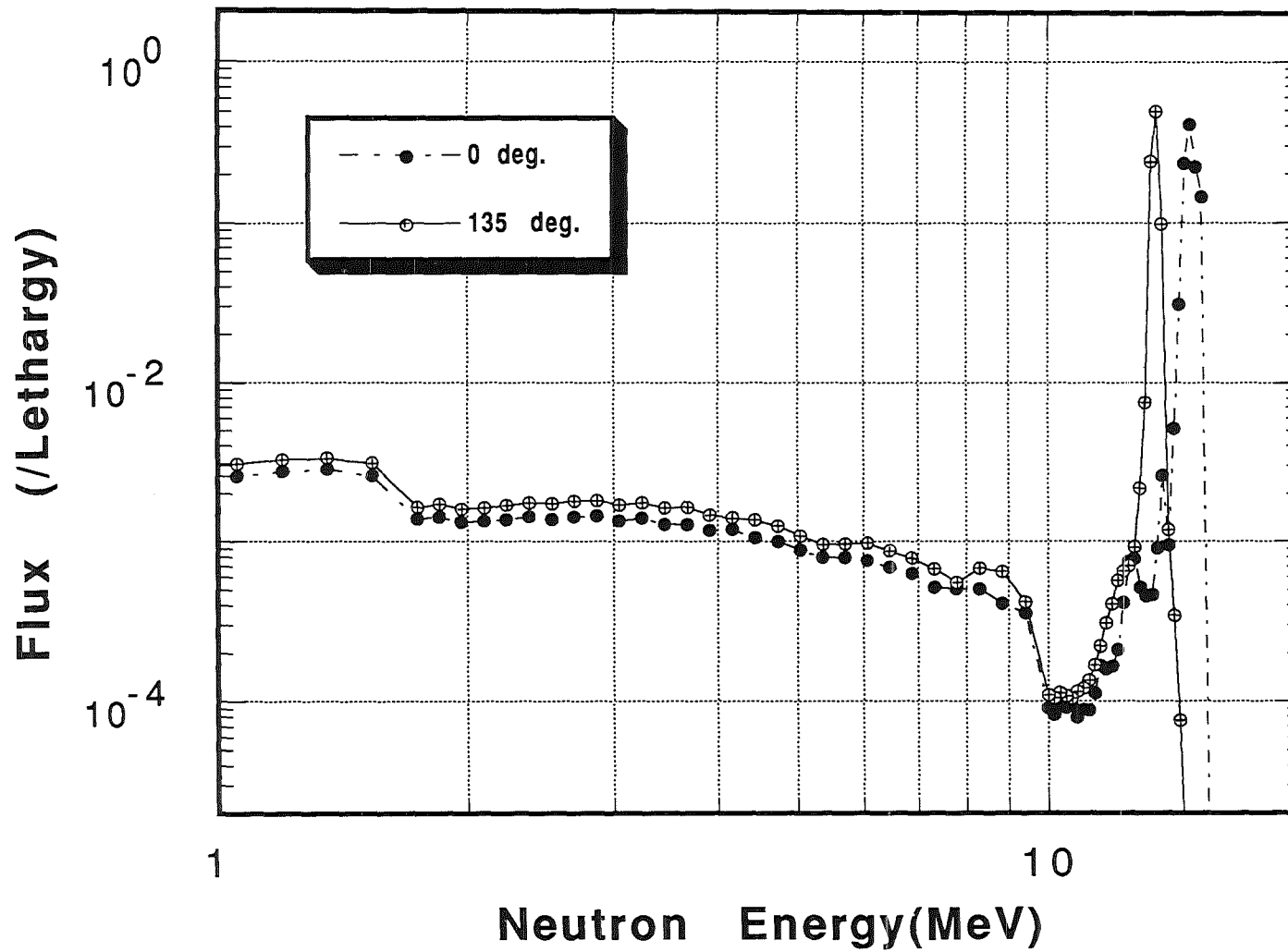
Fig. 2 Source neutron spectra at angles of 0 and 135 deg. calculated by MORSE-DD.
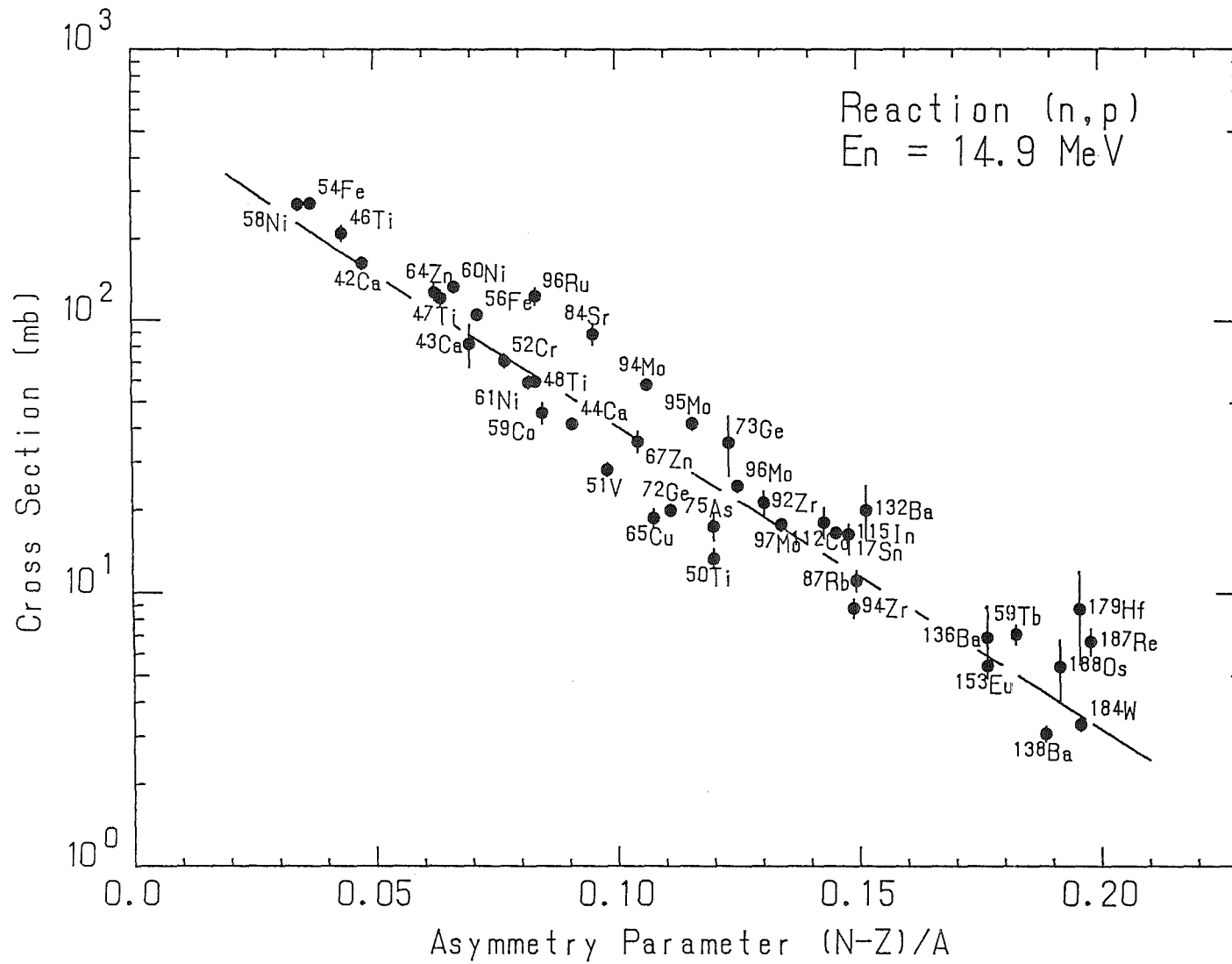
Fig. 3 Systematic trend of (n,p) reaction cross section with respect to asymmetry parameter, (N-Z)/A.

Recent Activation Cross Section Measurements at Jülich in the Neutron Energy Range of 5 to 12 MeV

S.M. Qaim

Institut für Chemie 1 (Nuklearchemie), Forschungszentrum Jülich GmbH,
5170 Jülich, Federal Republic of Germany

A programme of activation cross section measurements has been underway at Jülich for a long time. In recent years the efforts have concentrated mainly in the neutron energy range of 5 to 12 MeV. Quasi-monoenergetic neutrons in this range are produced via the $^2H(d,n)^3He$ reaction using a D_2 gas target at the variable energy Compact Cyclotron CV 28 [cf. 1]. The deuteron energy is generally varied between 3 and 10 MeV. The neutron flux density is determined via the monitor reactions [cf. 2] $^{56}Fe(n,p)^{56}Mn$ and $^{27}Al(n,\alpha)^{24}Na$, and the radioactivity of the products via diverse methods like X-ray spectroscopy, γ-ray spectroscopy, low-level β^- counting, etc. Extensive use is made of radiochemical methods of separation, especially in the study of low-yield products and β^- ray emitters. The background neutron corrections are done via gas out/gas in results [cf. 1] and dd breakup data [3,4].

There are two motivations for our investigations:
1) Fundamental studies on nuclear reactions
2) Nuclear data for fusion reactor technology (FRT)

Fundamental studies with 5-10 MeV neutrons have been performed on (n,t) reactions on some light mass nuclei like ^{10}B and ^{14}N [cf. 5] where resonance type structures were observed. A few selected (n,d) and (n,n'p) processes were also investigated [cf. 6]. For the lightest isotope of an element (e.g. ^{92}Mo), the (n,d) contribution was found to be negligible; the contribution of the (n,n'p) process, however, is strong. In recent years the emphasis has been mainly on investigations of isomeric cross section ratios [cf. 7-9]. The activation technique is ideally suited for this work. The results for $^{90}Zr(n,p)^{90m,g}Y$ - a typical case - are shown in Fig. 1 [9]. At low energies only a small fraction of the transitions occurs to the high spin (7$^+$) state; around 14 MeV, however, the

contribution increases to about 25%. Statistical model calculations involving precompound effects describe the isomeric cross section ratio well up to $E_n \approx$ 10 MeV; at higher energies some deviations occur. It was found [cf. 7,8] that the calculated isomeric cross section ratio is rather stongly dependent on the input level scheme of the product nucleus. Further experimental and theoretical studies on several reaction products, formed via various nuclear routes in the energy range extending up to 12 MeV, are underway in cooperation with the TU Dresden, University of Debrecen and University of Vienna.
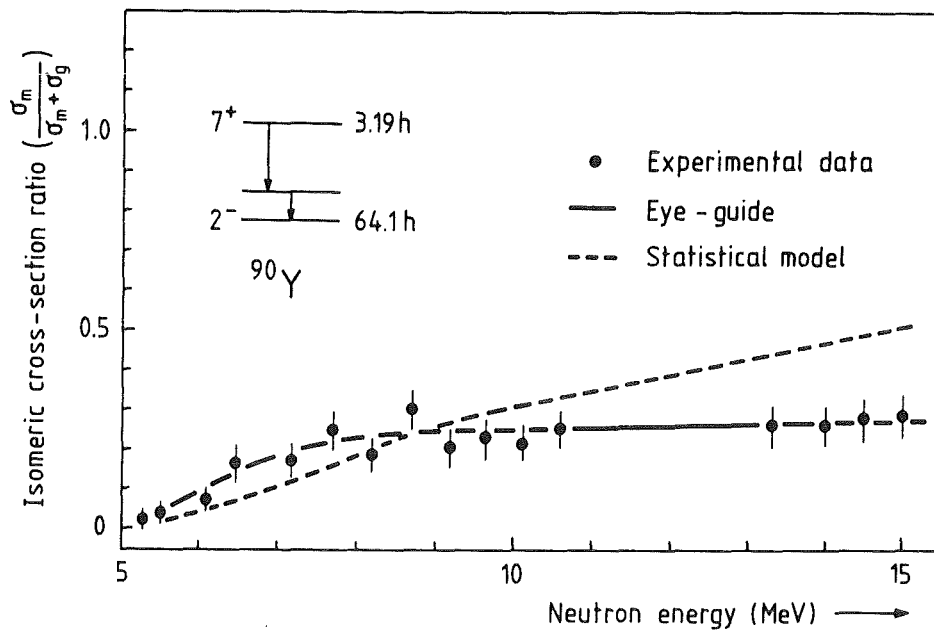
Fig. 1: Isomeric cross section ratio for the isomeric pair [90m,g]Y
(formed via (n,p) reaction on [90]Zr) plotted as a function of incident neutron energy [9].

Nuclear data measurements relevant to FRT generally deal with

-   Activation and transmutation products
-   Tritium breeding
-   Gas production

The activation of reactor components (and impurities) leading to long-lived products is presently one of the major concerns in design studies. Recently we performed measurements (in cooperation with University of Debrecen) on [151]Eu(n,2n)[150m]Eu ($T_{1/2} = 35.8$ y) and [159]Tb(n,2n)[158]Tb ($T_{1/2} = 180$ y) reactions

from threshold to 10.7 MeV. The transition from the low energy data to 14 MeV data was found to be smooth.

Regarding data relevant to tritium breeding we measured the $^7Li(n,n't)^4He$ cross sections over the neutron energy range of 8 to 10 MeV [10], and an existing discrepancy was removed.

Hydrogen and helium gas production cross sections are important in the context of radiation damage to first wall materials. Our recent studies include measurements on isotopes of Nb [11], Zr [9,12] and Ti [8,13]. These results for the $^{48}Ti(n,\alpha)^{45}Ca$ reaction are shown in Fig. 2. The excitation function appears to be rather smooth. Studies on the excitation functions of several other reactions like $^{63}Cu(n,p)^{63}Ni$ ($T_{1/2} = 100$ y) and $^{63}Cu(n,\alpha)^{60}Co$ ($T_{1/2} = 5.27$ y) are in progress.
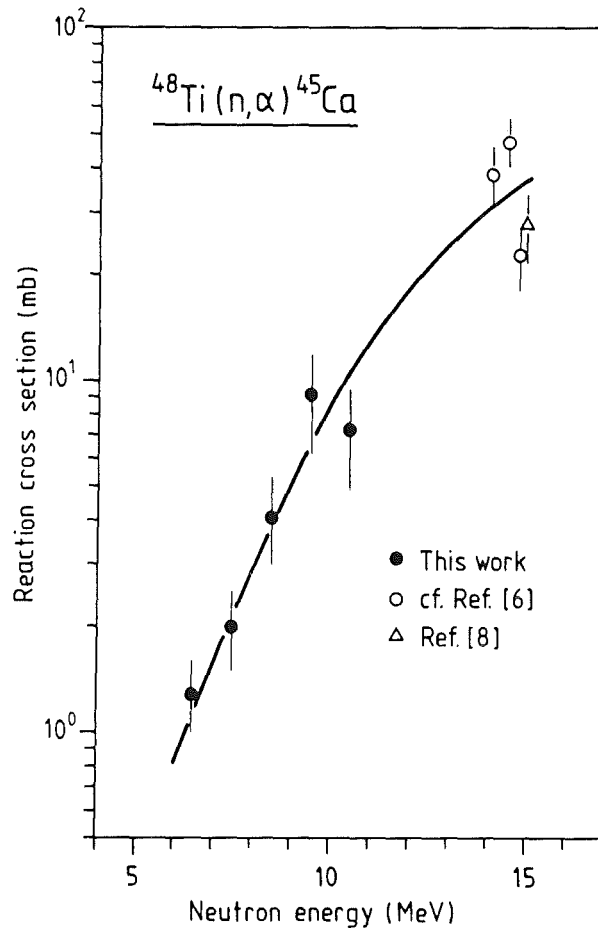
Fig. 2: Excitation function of the $^{48}Ti(n,\alpha)^{45}Ca$ reaction [13]

References

[1]   S.M. Qaim, R. Wölfle, M.M. Rahman and H. Ohlig, Nucl. Sci. Eng. 83, 143 (1984).

[2]   IRDF-International Radiation Dosimetry File (1990).

[3]   J.W. Meadows and D.L. Smith, Report ANL/NDM-53 (1980).

[4]   S. Cabral, G. Börker, H. Klein and W. Mannhart, Nucl. Sci. Eng. 106, 308 (1990).

[5]   A. Suhaimi, R. Wölfle, S.M. Qaim, P. Warwick and G. Stöcklin, Radio-chimica Acta 43, 133 (1988).

[6]   S.M. Qaim, R. Wölfle and B. Strohmaier, Phys. Rev. C40, 1993 (1989).

[7]   S.M. Qaim, A. Mushtaq and M. Uhl, Phys. Rev. C38, 645 (1988).

[8]   N.I. Molla, S.M. Qaim and M. Uhl, Phys. Rev. C42, 1540 (1990).

[9]   S.M. Qaim, M. Ibn Majah, R. Wölfle and B. Strohmaier, Phys. Rev. C42, 363 (1990).

[10]   S.M. Qaim and R. Wölfle, Nucl. Sci. Eng. 96, 52 (1987).

[11]   A. Mannan and S.M. Qaim, Phys. Rev. C38, 630 (1988).

[12]   M. Ibn Majah and S.M. Qaim, Nucl. Sci. Eng. 104, 271 (1990).

[13]   S.M. Qaim, N.I. Molla, R. Wölfle and G. Stöcklin, Proc. Int. Conf. on Nuclear Data for Science and Technology, May 1991, Jülich, Germany, in press.

Integral Data Testing of Critical Activation Cross Sections for Fusion Materials Development at the Karlsruhe Isochronous Cyclotron

S. Kelzenberg, S. Cierjacks, P. Obložinský[1] and J. Kaneko[2]

Kernforschungszentrum Karlsruhe, Association KfK-Euratom

Institut für Materialforschung

Postfach 3640, 7500 Karlsruhe

Federal Republic of Germany

Abstract

A new irradiation facility allowing for integral data testing of critical activation cross sections has been set up at the Karlsruhe Isochronous Cyclotron. Its main purpose is data testing in support of present programs for fusion materials development. For neutron production the irradiation facility presently involves a thick natural copper target bombarded by a 50-MeV, 30-μA cw deuteron beam. Test samples are placed directly to the back of the neutron-producing target, so that they can be irradiated in a high-energy, high-intensity neutron flux of $\sim 3 * 10^{12} \, n * cm^{-2} * s^{-1}$. Activation products are measured with a calibrated Ge(Li) detector system, employing computer-aided, on-line data analysis. As one of the first results obtained with the new facility the integral radioactivity produced by the two-step sequential reaction $^{19}F\,(n,\alpha)\,* \; \rightarrow \; ^{19}F\,(\alpha,n)\,^{22}Na$ is presented. The measured value is compared with contemporary activity calculations. Calculated and measured radioactivities for this sequential reaction are found to agree within a factor of 2.8. Planned improvements of the existing facility are briefly outlined.

1. Introduction

For fusion materials development a large variety of nuclear reaction data is needed. Since the majority of the required data is not available from experimental results, existing activation cross section libraries are largely based on data obtained from nuclear model calculations, often employing simple, semi-empirical prescriptions (e.g. THRESH [1]). This implies that usually large uncertainties in the calculated radioactivities and the related surface γ-dose rates, decay heats and biological hazards are introduced. Uncertainties introduced in one-step activation reactions are further enhanced, when important

---

[1] On leave from the Institute of Physics, SAS, 842 28 Bratislava, Czechoslovakia

[2] On leave from the Department of Nuclear Engineering, Tokyo University, Japan

radioactivities are produced by neutron-induced reaction chains or multistep nuclear reactions. While the first aspect has been considered sufficiently in the past [2], the latter effect has been investigated only recently [3, 4]. This applies for the so-called "sequential (x,n) reactions" (SxRs) in which light charged particles, produced in a first-step A(n,x)* reaction, create in a second-step $\bar{A}$(x,n)C process new reaction products, not primarily generated by single and multistep neutron interactions. For these reactions it has been shown that they often have large effects on the integral element activations and/or their related radiological quantities.

It is the intent of this paper to demonstrate that the irradiation facility can fullfil various needs for activation data testing. Through the measurement of the sequential reaction $^{19}F\,(n,\alpha)* \rightarrow {}^{19}F\,(\alpha,n)\,{}^{22}Na$ it is also demonstrated that the neutron flux is sufficient for the investigation of important reaction chains and two-step sequential reactions. The actual result presented in the paper is, to our knowledge, the first direct experimental proof for the occurence of a sequential (x,n) reaction in a fusion-like neutron spectrum.

2. Experimental Details and Results

2.1 General Features of the Existing Test Facility

The new irradiation facility for integral data testing has been set up at the Karlsruhe Isochronous Cyclotron (KIZ). Neutron production is performed inside the vacuum chamber using the separated beam of the main extraction channel. A schematic drawing of the target-sample arrangement is shown in Fig. 1.

For neutron production a 1 cm thick natural copper target is bombarded by a 50-MeV, 30-μA cw deuteron beam. At the neutron-producing target the beam size in the extraction channel is elliptical with 4 mm extension along the vertical and 2 mm along the horizontal main axes, respectively. The maximum range of 50-MeV deuterons in the copper target is 2.4 mm, so that no primary and secondary charged particles can escape through the upstream surface of the neutron-producing target. The irradiation samples are fixed on the back plane of the copper target, having a standard cross section of 1*1 cm^2 (quadratic). In this geometry an effective integral neutron flux of $\sim 3*10^{12}\ n*cm^{-2}*s^{-1}$ is achieved in the activation samples. The corresponding neutron flux spectrum is shown in Fig. 2.

In general this spectrum is composed of three contributions: (1) Neutron evaporation from fully equilibrated compound nuclei, (2) Neutron emission from deuteron break-up reactions and (3) neutron emission from all relevant preequilibrium states. In the "ef-
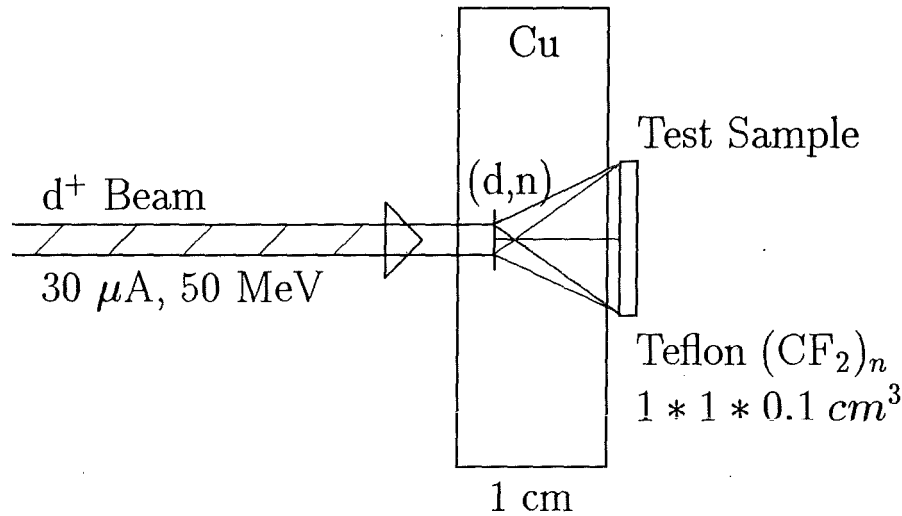
Fig. 1: Schematic drawing of the present experimental set up at the Karlsruhe Isochronous Cyclotron (KIZ)

fective" spectrum of Fig. 2 the effects of primary target extensions and source-sample angles ared included differentially. The central part of the spectrum extending from 11 to 35 MeV representing deuteron break-up in copper was derived from time-of-flight data taken by Schweimer [5]. The other two portions of the spectrum are extrapolations of the experimental data by means of statistical/preequilibrium model calculations performed with the code ALICE [6, 7]. While extrapolating the experimental data of Schweimer from break up model assumption, the calculated absolute equilibrium (evaporation) and preequilibrium contributions, adjusted for geometry effects, were added to give smooth, continuous spectra in the turn-over points close to 9 and 40 MeV.

2.2 Experimental Data Testing for $^{19}F(n, \alpha) * \rightarrow {}^{19}F(\alpha, n) {}^{22}Na$

Even though first demonstrations of the importance of sequential (x,n) reactions used well established, measured nuclear data, it was desirable to have a direct experimental proof that such reactions occur with the predicted strength in fusion-like energy spectra. The most extreme case for the influence of SxRs on integral surface γ-dase rates for a simple element was, so far, found for fluorine [8]. In this case, inclusion of the sequential $^{19}F(\alpha, n)^{20}Na$ reaction was calculated to alter the dose rate in large portions of the cooling time between 10^{-3} to 10^2 yr by 11 orders of magnitude. The result of our previous calculation is shown in Fig. 3.
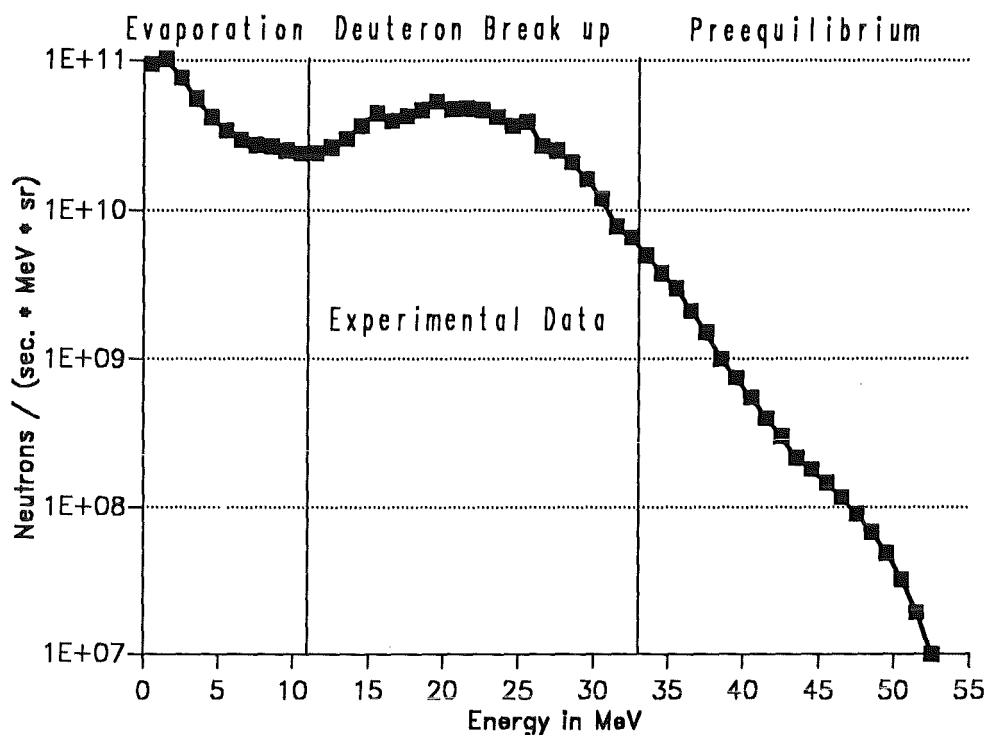
Fig. 2: "Effective" neutron flux spectrum in the irradiated test sample. For flux contributions and compositions see text.

This figure shows the calculated results including and excluding SxRs, while leaving all other calculational conditions unchanged. Thus the difference of the two curves is a direct measure of the contribution introduced by the special SxR. The corresponding inventory calculations have been performed with the European reference code, FISPACT [9, 10]. Inventory calculation for sequential (x,n) reactions, in addition, required the utilization of our new algorithm and the KfK Code PCROSS [11] with its three new input libraries KFKSPEC, KFKXN and KFKSTOP [12].

For the experimental investigation of the critical sequential (x,n) reaction on ^{19}F a $1*1$ cm^2, 1 mm thick teflon $((CF_2)_n)$ sample was employed. Verification measurements were performed in two different runs employing d-beam currents of 17 and 30 μA, respectively. In both runs the samples were irradiated for ~40 hrs. The induced radioactivities were determined by utilizing a calibrated Ge(Li) detector test stand. This device identifies individual radionuclides by specific γ-lines, γ-ray multiplicities and half lifes. Energy and efficiency calibrations were performed with an IAEA set of standard γ-sources. Fig. 4 shows the γ-spectrum measured 144 hr after the irradiation.

In the γ-spectrum there is a clear signal for ^{22}Na with its specific 1274.5 MeV γ-line with a half life of 2.6 yr. It clearly results from the sequential reaction $^{19}F (n, \alpha) * \rightarrow$
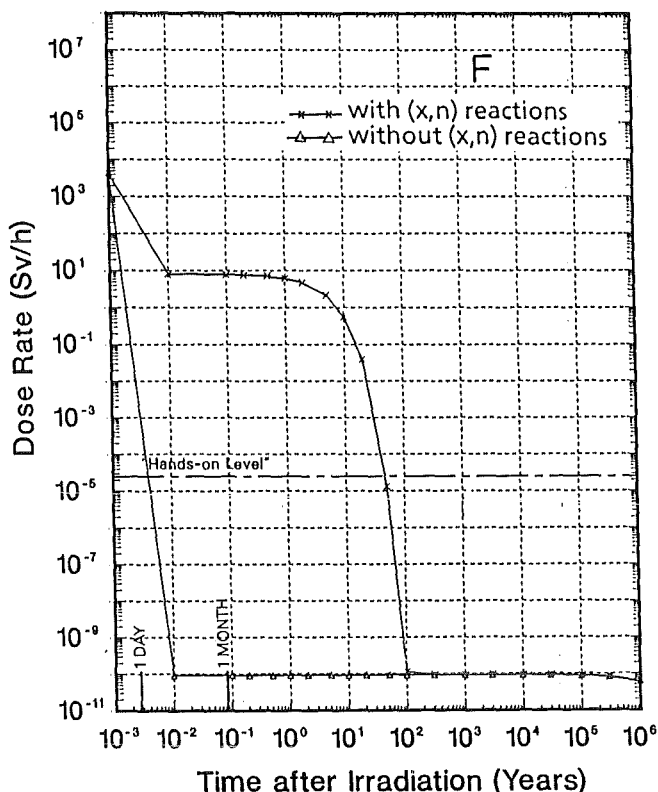
Fig. 3: Calculated surface γ-dose rate versus time after irradiation for F [8]. The results refer to neutron irradiation in the first wall of a DEMO fusion reactor. A first wall 14-MeV neutron load of 12.5 MWyr/m^2 was assumed.

$^{19}F\,(\alpha, n)\,^{22}Na$, to be verified as one of the major goals of the experiments. The total γ-ray spectrum also exhibits a lot of other γ-lines which are not further discussed here. One additional result to be mentioned is the production of ^7Be through the reaction $^{12}C(n, 2n\alpha)^7Be$ with a Q-value of -26.3 MeV. From the two independent runs with 17 and 30 μA, respectively, we finalized data analyses for Run 1 (17 μA). The result was the following total inventory at the end of neutron irradiation:

Inventory: $4.7 \pm 0.9 * 10^9$ atoms/sample mass

In the experiment there is a statistical error of 2% for the counting rates under the peak, and a 10 % uncertainty for the γ-ray efficiency of the detector. The estimated errors in neutron spectrum data are typically 15 %.

3. Comparison with Inventory Calculations

For this special case with an extended primary neutron spectrum, extrapolations of the nuclear data to energies of 50 MeV were necessary. For extended charged particle spectra and energy dependent (x,n) cross sections, statistical/preequilibrium model
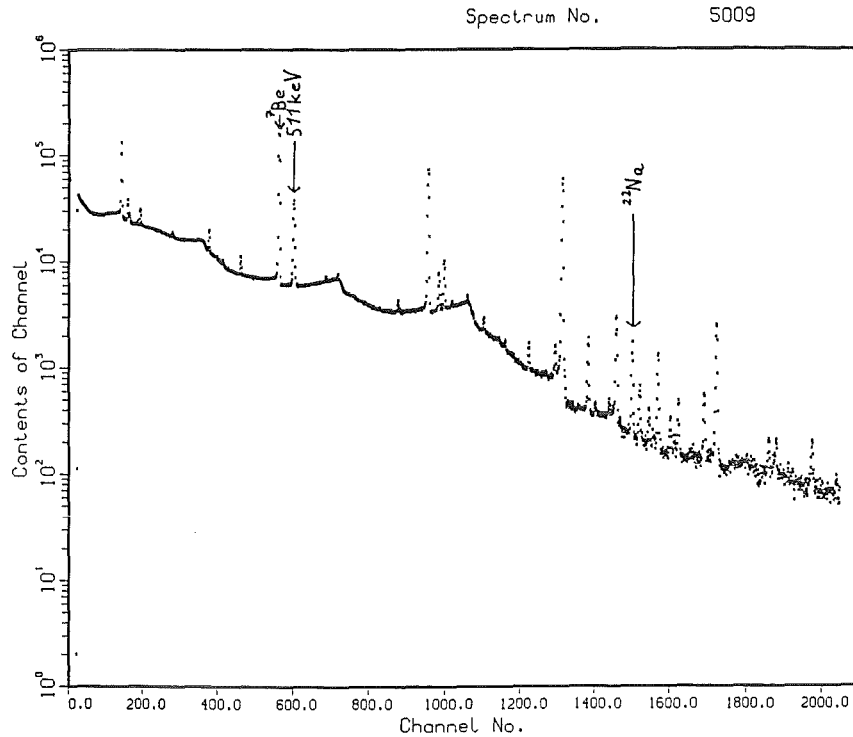
Fig. 4: γ-ray spectrum from the irradiated teflon sample after 144 hr of decay time. For details see text.

calculations were performed with the code ALICE. Differential ranges for all primary produced α-particles have been calculated with the well established code PRAL, based on Ziegler's formalism [13], and extended in the Institute of Materials Research (IMF) of KfK [14]. The results of the inventory calculations are compared in Table 1 with the measured integral values.

Type of Results	Inventory at T=0 $(10^9 \ ^{22}Na$-atoms/sample mass)
Experiment	4.7 ± 0.9
Calculation	13.0
Ratio R=Calc/Exp	2.76

Table 1. Comparison of the results from experiment and inventory calculations.

It can be seen that the calculated value is ∼2.7 times higher than the experiment. As described in Section 2.2 the total experimental uncertainty is small (∼18 %). It is however, difficult to estimate present uncertainties in model calculations. There is however, a clear indication from "blind intercomparison exercises" [15], that modern statistical/preequilibrium models are expected to calculate unknown cross sections with an

accuracy within at least a factor of 2. Since the studied process is a two-step reaction in which the individual uncertainties are multiplicative, the ratio factor of the measured to the calculated inventory is a reasonable result well within present expectations.

4. Planned Improvements of the Data Testing Facility

In order to fullfil all important requirements for activation data testing, we plan the following four major improvements of the existing facility in the near future:

1. Replacement of the Cu by a Be neutron-producing target. This will give at least a factor of 4 in neutron flux at the activation sample position.

2. A remeasurement of the primary neutron spectra by time-of-flight over the extended energy range from 1-50 MeV. This is expected to reduce the present spectrum uncertainties from ~15 % to ~5 %.

3. Addition of a Si(Li) solid-state detector for measurement of weak X-rays from ~3 keV upwards. Many of the important long-lived radioisotopes decay by electron capture i.e. by weak X-ray emission only.

4. Arrangement for a deuteron-energy reduction by suitably placed absorbers, providing a deuteron energy between 35 and 50 MeV. In some cases, such a reduction may be important to increase the sensitvity of benchmark data testing in the most interesting neutron energy region from 0-15 MeV by softening the sampling neutron spectrum.

5. Conclusions

This paper describes the general features of a new facility for integral data testing of critical activation cross sections, recently set up at the Karlsruhe Isochronous Cyclotron. Feasibility and overall specifications of the device are illustrated by a measurement of the integral ^{22}Na radioactvity produced in the two-step $^{19}F(n,\alpha) * \rightarrow \,^{19}F(\alpha,n)\,^{22}Na$ process. This result is, to our knowledge, the first experimental evidence for a sequential (x,n) reaction in a fusion-like neutron spectrum. Further improvements of the data testing facility, presently in progress, are described. With the future improvements it is expected that the facility can fullfil most of the major needs for fusion data testing.

Acknowledgements

The authors would like to thank Prof. K. Ehrlich and Prof. K.-H. Zum Gahr for stimulating discussions and their ongoing support of this work.

This work has been performed in the framework of the Nuclear Fusion Project of the Kernforschungszentrum Karlsruhe and is supported by the European Fusion Technology Program.

References

[1] S. Pearlstein; J. Nucl. Energy **27** (1973) p. 91; and S. Pearlstein; Program THRESH-2 (Dec.1975); available from NEA Data Bank, Saclay, France.

[2] R. A. Sowerby, B. H. Patrick and D. A. J. Endacott; The Data Library UKACT1 and the Inventory Code FISPACT; Proc. Int. Conf. on Nuclear Data for Science and Technology, Mito, Japan, 1988, p. 1061-1064.

[3] S. Cierjacks and Y. Hino; The Importance of Sequential Charged Particle Reactions on Element Activation of Fusion Reactor Materials; J. Nucl. Mater. **170** (1990) p. 134-139.

[4] S. Cierjacks and Y. Hino; The Role of Sequential (x,n) Reactions on Element Activation of Fusion Reactor Materials and Related Nuclear Data Needs; in Proc. of a NEANDC Specialists Meeting on Nuclear Activation Cross Sections for Fission and Fusion Energy Applications, Argonne Nat. Laborarotry, USA, 1989, NEANDC-259U, p. 19-28.

[5] G. W. Schweimer; Fast Neutron Production with 54 MeV Deuterons; Nucl. Phys. **A100** (1967) p. 537-544.

[6] M.Blann; Code ALICE/85/300; Report UCID-20169, LLNL Livermore 1984.

[7] M. Blann (LLNL Livermore); Code ALICE, Version 1990, private communication, January 1991.

[8] S. Cierjacks, Y. Hino, P. Obložinský and S. Kelzenberg; Investigation of Element Activation by Sequential (x,n) Reactions; in Progr. Report on Nuclear Data Research in the Fed. Rep. of Germany for the Period April 1, 1990 to March 31, 1991, p. 16-17, NEANDC(E)-322-U, Vol. V, INDC(Ger)-36/LN+Special, July 1991.

[9] R. A. Forrest, D. A. J. Endacott; FISPACT-User Manual; AERE-M3654 Harwell, March 1988.

[10] R. A. Forrest, D. A. J. Endacott, A. Kursheed; FISPACT-Program Manual; AERE-M3655 Harwell, April 1988.

[11] S. Ravndal, P. Obložinský, S. Kelzenberg and S. Cierjacks; User Manual for the KfK Code PCROSS; Report, KfK 4873, August 1991; and P. Obložinský, S. Cierjacks, S. Ravndal and S. Kelzenberg; this conference p. 83.

[12] S. Cierjacks, P. Obložinský and B. Rzehorz: Nuclear Data Libraries for the Treatment of Sequential (x,n) Reactions in Fusion Materials Activation Calculations; Report, KfK 4867, July 1991; and P. Obložinský, S. Cierjacks, S. Kelzenberg and B. Rzehorz; this conference p. 71.

[13] J. F. Ziegler, J. P. Biersack and U. Littmark; The Stopping and Range of Ions in Solids (Pergamon Press, New York, 1985).

[14] A. Möslang; Schädigungs- und Reichweitenberechnungen für Bestrahlungen an den KfK-Zyklotrons; Primärbericht KfK 03.02.02P94B, Karlsruhe, 1990.

[15] NEA/OECD Project Group on "Blind Intercomparison" of Nuclear Model Calculations; First Results from Group Meeting on May 26, 1991, Jülich, private communication.
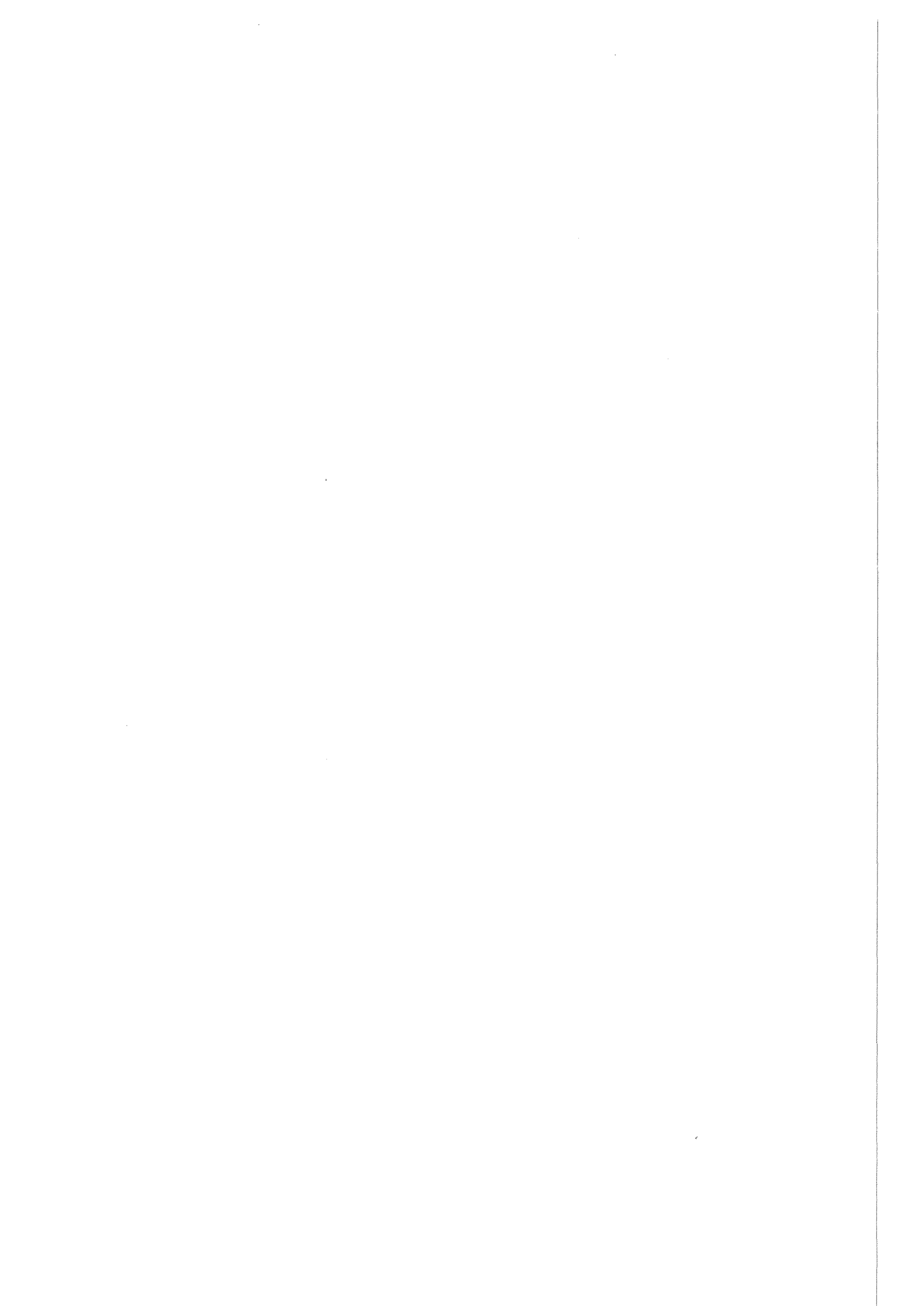
Sensitivity and Uncertainty Analysis
of the NET Magnet Neutronic Design Parameters
to Uncertainties in Cross Section Data

by
T. Parish and A. Santamarina
(presented by E. Fort)
DRN/DER/SPRC
Centre d'Etudes Nucléaires de Cadarache
13108 Saint Paul Lez Durance, France

Key Items from Fort's Presentation

An extensive nuclear data uncertainity sensitivity analysis, for super-conducting coil shielding parameters, was performed on a realistic, large toka-mak design supplied by the NET team. Calculations were carried out directly on the VITAMIN-J group structure (175 neutron groups), with the French SN Modular BISTRO Package. The EFF MATXS-87 library was used.

This study aimed to be "exhaustive" in the following sense:

- All the materials were accounted for and the sensitivity profiles were computed for each layer.

- All the nuclides with a significant concentration in the blanket/shield were investigated (Fe, Cr, Ni, Mn, Mo, H, O, ^{10}B, ^{11}B, Cu, C and Nb)

- Sensitivity profiles and uncertainty calculations were carried out for both the inboard and the outboard coil leg.

- Various coil shielding parameters (responses) were considered: Fast fluence, dpa in Cu stabilizer, nuclear heating.

Sensitivity profiles were investigated as functions of the neutron reaction type (Table 1), of the location of the nuclide in the shield, and for every nuclide of the shield/blanket.

Table 1: Integrated sensitivities of the fast fluence at the inboard coil to individual neutron reaction cross-sections

Reaction	Material				
	Fe	Cr	Ni	H	O
n, elastic	2.065	.812	.578	2.660	.518
n, inelastic (continuum)	2.065 (1.346)	.606 (.048)	.358 (.238)	.000 (.000)	.082 (.000)
n, 2n	.581	.128	.033	.000	.000
n, p	.264	.052	.165	.000	.011
n, γ	.024	.010	.008	.000	.000
n, α	.080	.022	.039	.000	.030
n, d	.031	.008	.000	.000	.004
Sum of all reactions	5.650	1.638	1.181	2.660	.645

Energy-integrated sensitivity coefficients, $\alpha = (\Delta R/R)/(\Delta\sigma/\sigma)$, pointed out that the main contribution to the uncertainty is due to iron with sensitivity coefficients of $\alpha = -5,6$ and $\alpha = -13$ in the inboard and outboard coils, respectively. Coil damage sensitivity to the cross-sections of water components is also significant amounting to $\alpha(H) = -2,6$ and $\alpha(O) = -0,6$ in the inboard region (Table 2).

The uncertainty analysis in the 175-group structure, based on our sensitivity profiles and the Vitamin-J cross-section covariance file, demonstrated a standard deviation, $\Delta R/R = +20\%$ on the calculation of coil fast fluence (Table 3) and $\pm 20\%$ on dpa in the copper stabilizer. The uncertainty on the local nuclear heating in the inboard winding pack due to the shield nuclide neutron cross-sections amounts to $+17\%$ (Table 4). The uncertainty associated with the coil damage in the outboard leg is 2.5 times higher and represents $+50\%$ at one standard deviation.

The SAD uncertainty due to the angular distribution of the scattered neutrons was assessed. Sensitivity coefficients to P_1, P_2 and P_3 Legendre coefficients enabled us to derive the uncertainty linked to anisotropic scattering: 12%, 3.5% and 1.2%, from Fe, Cr and Ni, respectively.

Table 2: Integrated total sensitivities of the inboard toroidal field coil response to the neutron cross-sections of the NET shield materials

Material	Inboard coil response		
	Fast fluence	Cu DPA	Nuclear heating
Fe	5.650	5.923	4.992
Cr	1.638	1.676	1.522
Ni	1.181	1.215	1.148
H	2.660	2.485	1.861
O	.645	.580	.637
Mo	.213	.214	.267
Cu	.208	.231	.785
Mn	.199	.203	.265
C	.189	.185	.097
B-10	.057	.056	.153
B-11	.138	.131	.098
Nb	.012	.013	.082
Total	12.790	12.912	11.907

Table 3: Uncertainty of the fast fluence to the inboard coil by individual reaction

Material	n,n elastic	n,n inelastic	n,2n	n,γ	n,p	total for all reactions
Fe	.0505	.1501	.0535	.0019	.0130	.167
Cr	.0480	.0467	.0141	.0014		.068
Ni	.0361	.0453	.0053	.0012	.0203	.062
H	.0246					.025
O	.0170	.0162				.023
						.194

Combining SAD uncertainties and cross-section uncertainty components, the total uncertainty on the NET coil parameters ranges between 20% for the nuclear heating and up to 25% for the damage reponses. These uncertainties (in the standard deviation) are twice the design target accuracy required by the NET team.

Table 4: Uncertainties (%) for the fast fluence, Cu dpa, and nuclear heating of the inboard coil by material

Material	Fast fluence	Cu dpa	Nuclear heating
Fe	16.7	18.4	13.7
Cr	6.8	7.2	6.3
Ni	6.2	6.5	5.5
H	2.5	2.3	1.7
O	2.3	2.2	2.3
Total (Uncorrelated)	19.4%	21.0%	16.2%

S E S S I O N II :

MODEL CALCULATIONS, EVALUATIONS AND DATA FILES

Chairman: M.G. Sowerby, AEA Harwell

Fusion Cross Sections
from Los Alamos R-Matrix Analyses

G. M. Hale

Theoretical Division, Los Alamos National Laboratory
Los Alamos, New Mexico 87545, USA

Introduction

We have been using R-matrix theory for many years at Los Alamos to describe reactions in light systems, especially those containing fusion reactions. The theory is ideally suited for describing the resonances that are usually seen in light-element reactions, and at the same time it builds in the correct energy dependence of the transition matrix elements at low energies by making explicit use of the solutions for the external (long-ranged) parts of the interaction (Coulomb and angular momentum barriers, etc.). Thus, the method gives reliable extrapolations to low energies for both neutron- and charged-particle-induced reactions.

We will present here the results of analysis that have been done, or are in progress, for reactions in the four- and five-nucleon systems, containing the fusion reactions of major interest: $T(d,n)^4He$, $^3He(d,p)^4He$, $D(d,p)T$, and $D(d,n)^3He$. These analyses contain all possible types of data (in addition to the cross sections) that have been measured for the two-body reactions of these systems, a method that we have found crucial for determining their true resonant structures, and for ensuring reliable R-matrix interpolations and extrapolations of even the cross-section data. Integrated cross sections will be presented in the form of astrophysical S-functions, as functions of center-of-mass energy, in order that their low energy behavior might be better displayed.

In addition to the R-matrix results, we will also show earlier cross-section parametrizations by Duane [1] and by Peres [2] that still are used widely within the fusion reactor community. Some severe shortcomings of these earlier data sets are revealed by comparisons with modern measurements and with the R-matrix calculations. More details about these comparisons and useful representations of the R-matrix cross sections and their associated reactivities ($<\sigma v>$) recommended for use in fusion reactor design are given in a paper by Bosch and Hale [3] that has been submitted for publication.

The Reaction $T(d,n)^4He$

The R-matrix analysis of the ^5He system that we completed several years ago gives a remarkably good description of all the reactions involving d+t and n+^{4}He. The results have been used to investigate the pole structure of the famous $J^\pi=3/2^+$ resonance [4,5] and to study nuclear effects on the low-lying states of the dtµ molecule [6].

The S-function for the reaction $T(d,n)^4He$ is shown in Figs. 1 and 2. Fig. 1 shows a selection of earlier data, along with the more recent data of Brown [7] and Jarmie [8], at center-of-mass energies below 75 keV. Some of the earlier data disagree quite strongly with the most recent measurements at energies below the peak of the resonance, and even the Arnold [9] data have a different low-energy behavior. The R-matrix calculation follows the Brown and Jarmie data quite well down to the lowest measured energies, where it disagrees with the earlier parametrization of Peres [2], and especially with that of Duane [1]. In Fig. 2, the calculations are compared with data measured up to higher energies. Good agreement is seen with Conner's measurement [10] at all but the lowest energies, where the first point is consistent with the parametrization of Duane [1].

The Reaction $^3He(d,p)^4He$

The R-matrix analysis of the reactions in the ^5Li system was done more than 10 years ago, at a time when the measurements of the $^3He(d,p)^4He$ reaction cross section near its peak, especially, were in significant disagreement. This can be seen in the S-function for the reaction, shown at low energies in Fig. 3 and at higher energies in Fig. 4. One also sees in these figures that the R-matrix calculation did not agree particularly well with the data that were included in the fit, but agrees much better with measurements of Krauss [11] and of Möller [12] that were made well after the analysis was done. This is probably a consequence of the theoretical constraints imposed by R-matrix theory on the

energy dependence of a near-threshold resonance, and of the multi-reaction, multi-observable approach used at Los Alamos for these analyses.

Neither of the other parametrizations accounts as well for the more recent measurements as does the R-matrix calculation. Duane's dotted curve shows its characteristic roll-off at low energies below the Krauss data, and Peres' dashed curve shows a displacement in the peak of the S function away from the position indicated by the recent measurements [11,12].

The d+d Reactions

The A=4 analysis is particularly interesting because it illustrates the ability to incorporate fundamental theoretical constraints in R-matrix descriptions. In this case, all possible reactions involving the channels n+T, n+^{3}He, p+T, p+^{3}He, and d+d are described using a single set of Coulomb-corrected, charge-independent R-matrix parameters [13]. The T=1 parameters were first determined by fitting p+^{3}He scattering data, checked by a prediction of the n+T total cross section, then taken essentially unchanged into an analysis of the reactions in the ^{4}He system in which only the T=0 parameters were varied (along with an overall Coulomb energy shift of the T=1 levels). Isospin constraints were used to relate the p-T and n-^{3}He widths in the T=0 levels, and a small amount of Coulomb isospin mixing was allowed in the d-d widths. Such a model accounts quite well for the experimental data in the ^{4}He system, including those indicating sizeable differences between the two branches of the d+d reaction.

Figs. 5 and 6 show the calculated S-function for the D(d,p)T reaction compared to a selection of the data, and to the parametrizations of Duane and of Peres. The R-matrix calculation follows closely the recent measurements of Brown [14] and the earlier ones of Wenzel [15]. The Duane curve again falls off sharply at low energies, as do the earlier data of Arnold [16].

Similar plots for the D(d,n)^{3}He reaction are shown in Figs. 7 and 8. The R-matrix calculation follows the recent measurements of Brown [14] and the earlier measurements of Ganeev [17] and of Preston [18]. The curves of Duane [1] and Peres [2] do not give large enough D(d,n) cross sections at the higher energies, despite the fact that they are unconstrained by a charge-independent fit, as is the R-matrix calculation.

Predictions

A novel application of the A=4 analysis has been to compare its results [13] with measurements being done for the d+d muon-catalyzed fusion (μCF) reactions. Information from the standard scattering experiments done at low energies involves mainly the S-wave transitions of the reactions. Because of the selection rules involved in muon fusion at room temperature, however, μCF experiments give information primarily about the P-wave transitions at low energies. Such measurements [19] give the surprising result that the branching ratio for the P-wave part of the d+d reactions favors the n+^{3}He branch over that for p+T by about 40%. At lower temperatures, where the molecular transitions allow increasing amounts of S-wave formation between the two deuterons, the branching ratio has recently been observed [20] to decrease toward unity.

The P-wave branching ratio calculated from the analysis is 1.43, while that for the S-waves is 0.886, giving excellent agreement with the measured room-temperature number, and also accounting qualitatively for the decrease in the branching ratio toward unity as the S-wave admixture increases at lower temperatures. The calculated absolute muon fusion rate for both branches, using information about the molecular wavefunction and transition rates from the work of Bogdanova et al. [21], is λ_f = 3.8 × 10^8 s^{-1}, compared to the measured value of (4.1 ± 0.1) × 10^8 s^{-1} [22]. Thus, the analysis successfully accounts for all the new experimental information (including the surprises) about the d+d reactions that has come from this exciting new field, confirming by individual partial waves the reliability of R-matrix extrapolations to low energies.

The R-matrix parameters for the ^{5}He system predict a resonance in the back-angle T(d,n)^{4}He differential cross section that is consistent with a new measurement by Drosg [23]. The calculated curve and his data point are shown in Fig. 9. Also, new measurements of the outgoing neutron polarization for the reaction just completed at Tübigen are in excellent agreement with the predictions of the analysis.

Conclusion

We have given examples that illustrate the reliability of fusion cross sections and other data obtained from R-matrix analyses that include many reactions and observable types over a wide range of energy. The analyses give good representations of the most recent measurements, even in a case where the analysis was done long before the recent data became available. Because it is relatively unaffected by inconsistent data, this approach enjoys clear advantages over methods that fit simple mathematical forms to the measured cross-section data, which are still being used by many evaluators.

These R-matrix calculations have also been used to predict with high accuracy the results of conventional beam-target experiments, and the sometimes surprising results of muon-catalyzed experiments that probe the fusion reactions at energies below the range of usual measurements. The latter comparisons, especially, verify that the calculations provide reasonable extrapolations of the unscreened nuclear cross sections to very low energies in every partial wave.

Acknowledgments

References

[1]   B. H. Duane, "Fusion Cross Section Theory," in *Annual Report on CTR Technology 1972*, Batelle Pacific Northwest Laboratory report BNWL-1685 (1972).

[2]   A. Peres, *J. Appl. Phys.* **50**, 5569 (1979).

[3]   H.-S. Bosch and G. M. Hale, "Improved Formulas for Fusion Cross Sections and Thermal Reactivities," submitted to *Nuclear Fusion* (1991).

[4]   G. M. Hale, R. E. Brown, and N. Jarmie, *Phys. Rev. Lett.* **59**, 763 (1987).

[5]   L. N. Bogdanova, G. M. Hale, and V. E. Markushin, *Phys. Rev. C* **44**, (October 1991).

[6]   M. C. Struensee, G. M. Hale, R. T Pack, and J. S. Cohen, *Phys. Rev. A* **37**, 340 (1988).

[7]   R. E. Brown, N. Jarmie, and G. M. Hale, *Phys. Rev. C* **35**, 1999 (1987).

[8]   N. Jarmie, R. E. Brown, and R. A. Hardekopf, *Phys. Rev C* **29**, 2031'(1984).

[9]   W. R. Arnold *et al.*,"Absolute Cross Section for the Reaction T(d,n)^{4}He from 10 to 120 keV," Los Alamos Scientific Laboratory report LA-1479 (1953).

[10]   J. P. Conner, T. W. Bonner, and J. R. Smith, *Phys. Rev.* **88**, 468 (1952).

[11]   A. Krauss *et al.*, *Nucl. Phys.* **A465**, 150 (1987).

[12]   W. Möller and F. Besenbacher, *Nucl. Inst. Meth.* **168**, 111 (1980).

[13]   G.M. Hale, in Proc. Int. Conf. on Muon Catalyzed Fusion, May 1990, Vienna, Austria (to appear as a volume of *Muon Catalyzed Fusion*, 1991)

[14]   R. E. Brown and N. Jarmie, Phys Rev. C **41**, 1391 (1990).

[15]   W. A. Wenzel and W. Whaling, *Phys. Rev.* **88**, 1149 (1952).

[16]   W. R. Arnold *et al.*, *Phys. Rev.* **93**, 483 (1954).

[17]   A. S. Ganeev *et al*, Supplement No. 5 of *Sov. J. Atomic Energy* **21** (1957).

[18]   G. Preston, P. F. D. Shaw, and S. A. Young, *Proc. Royal Soc. (London)* **A226**, 206 (1954).

[19]   D.V. Balin *et al.*, *Phys. Lett.* **141B**, 173 (1984); *JETP Lett.* **40**, 112 (1984).

[20]   D.V. Balin *et al*, in Proc. Int. Conf. on Muon Catalyzed Fusion, May 1990, Vienna, Austria (to appear as a volume of *Muon Catalyzed Fusion*, 1991).

[21]   L. N. Bogdanova, V. E. Markushin, V. S. Melezhik, and L. I. Ponomarev, *Phys. Lett.* **115B** (1982) 171; *Erratum* **167B** (1986) 485.

[22]   M. P. Faifman *et al.*, *Zh. ETP* **92**, 1173, (1987).

[23]   M. Drosg (University of Vienna), private communication (1991).
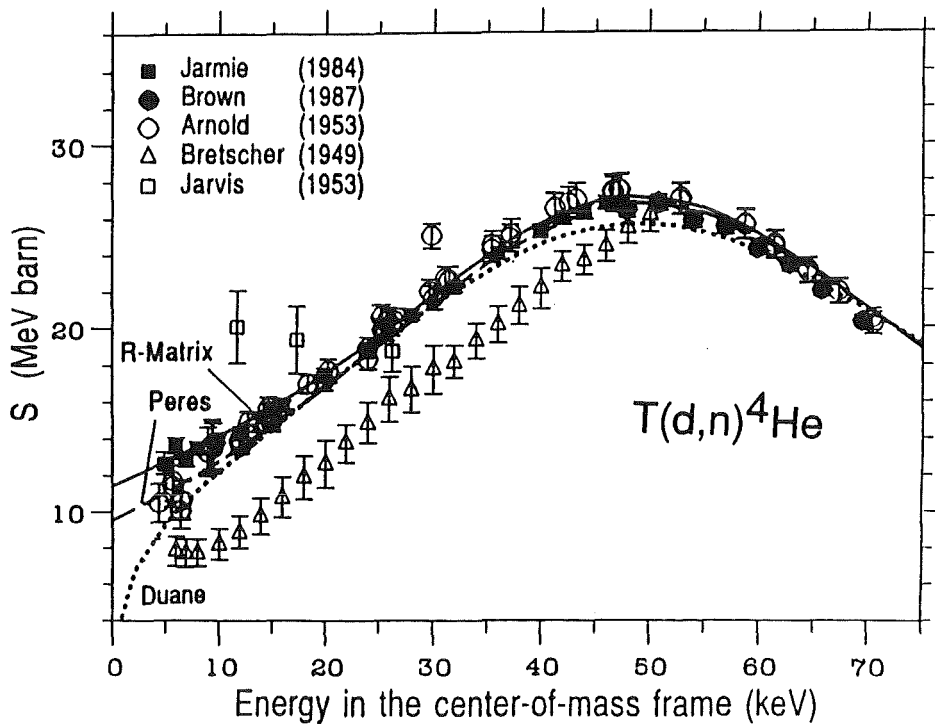
Fig. 1.   Calculated S-functions for the T(d,n)^{4}He reaction at energies below 75 keV compared with various measurements. In this, and all subsequent figures, the solid line is the LANL R-matrix calculation, the dotted line is Duane's [1] parametrization, and the dashed line is that of Peres [2].
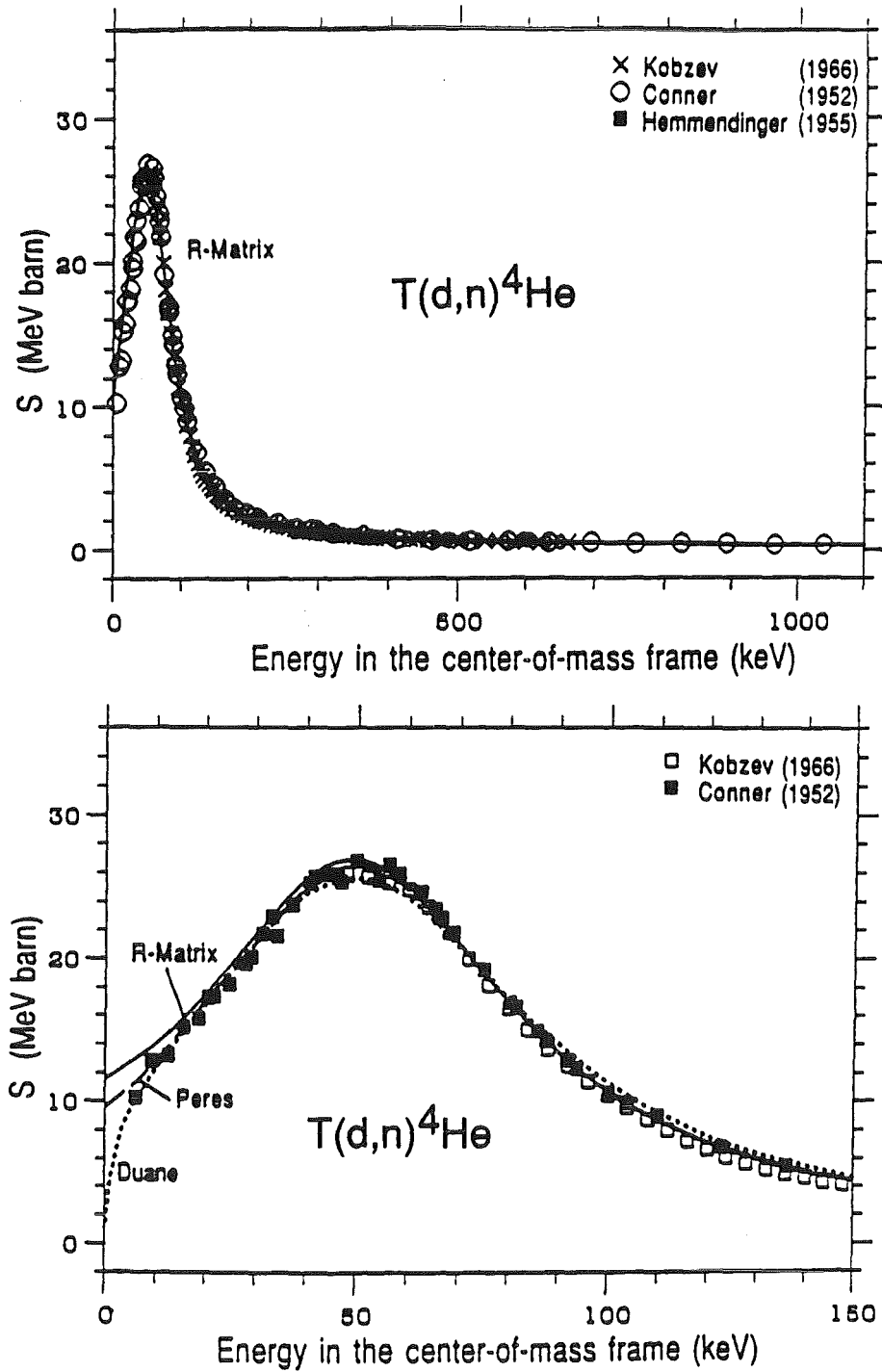
Fig. 2. Calculated S-functions for the T(d,n)^{4}He reaction at energies below 1.1 MeV compared with various measurements.
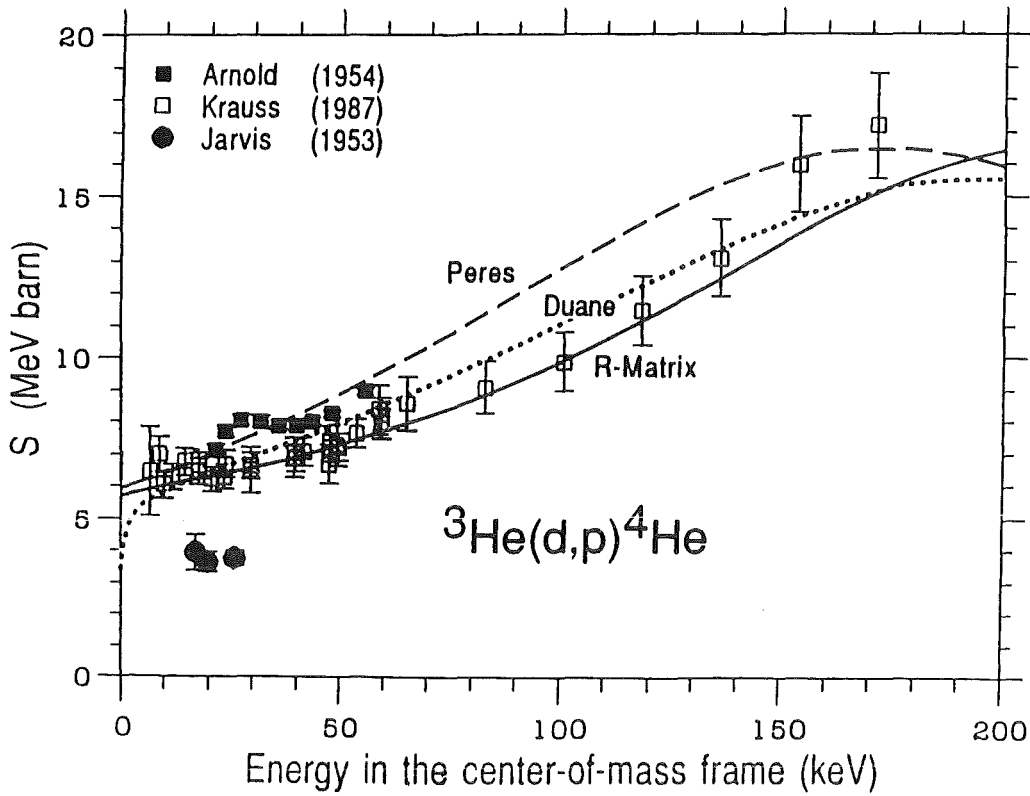
Fig. 3. Calculated S-functions for the ^{3}He(d,p)^{4}He reaction at energies below 200 keV compared with various measurements.
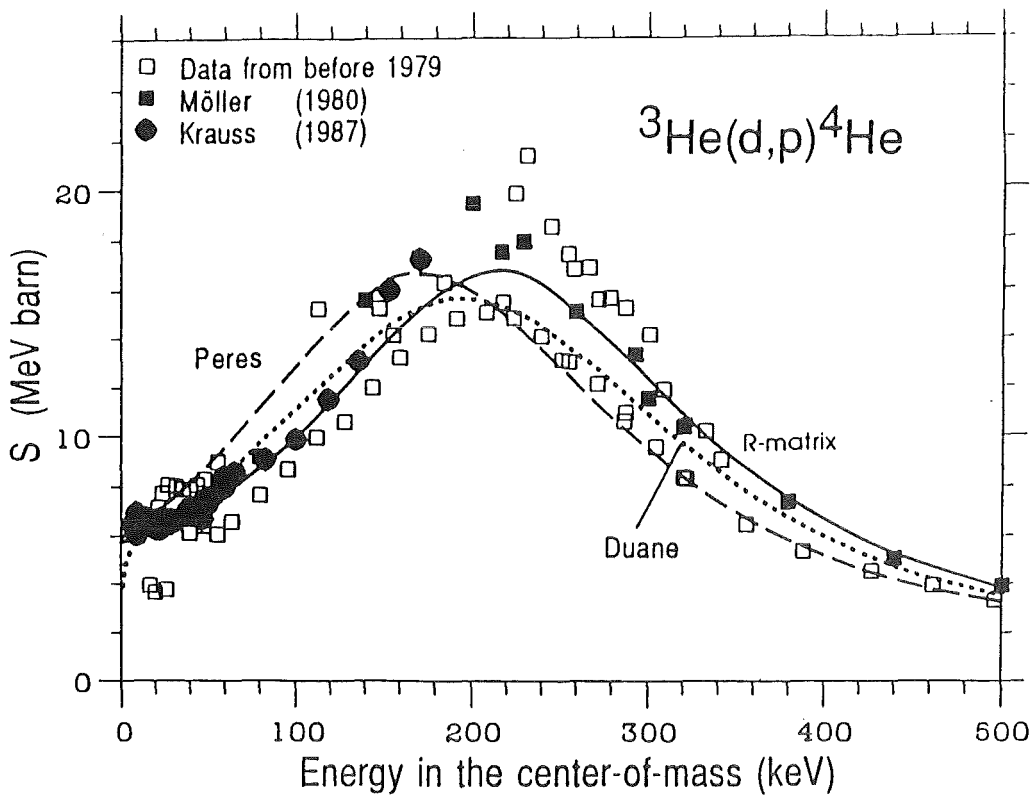
Fig. 4. Calculated S-functions for the ^{3}He(d,p)^{4}He reaction at energies below 500 keV compared with various measurements.
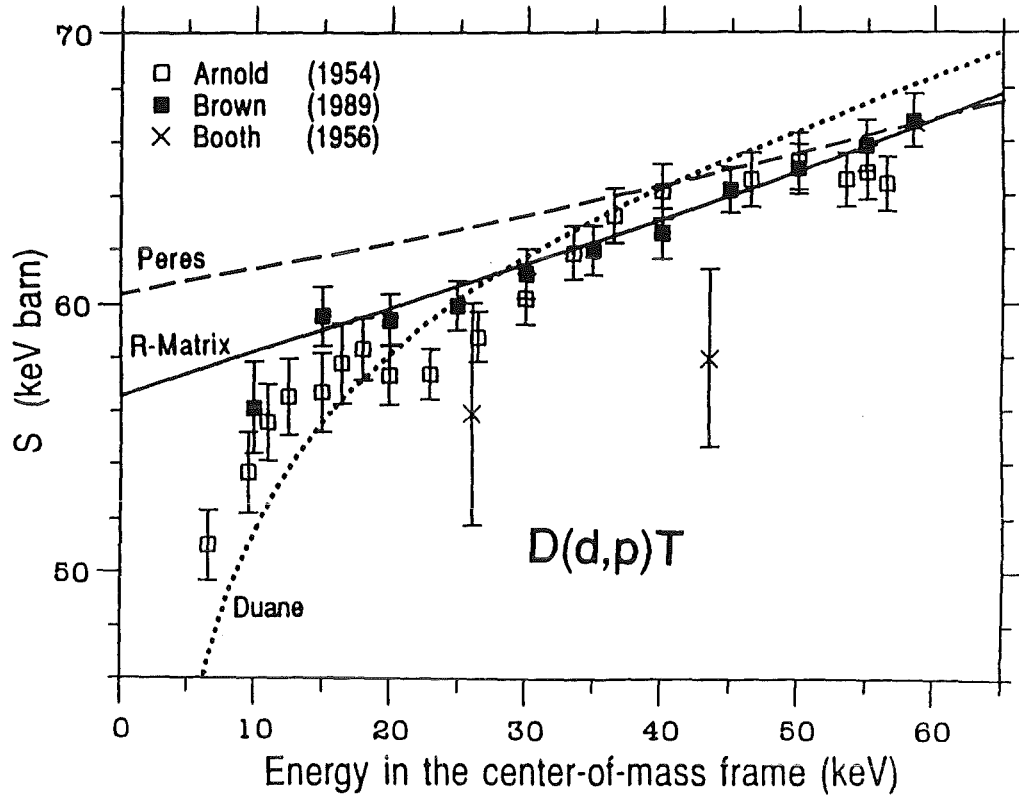
Fig. 5. Calculated S-functions for the D(d,p)T reaction at energies below 65 keV compared with various measurements.
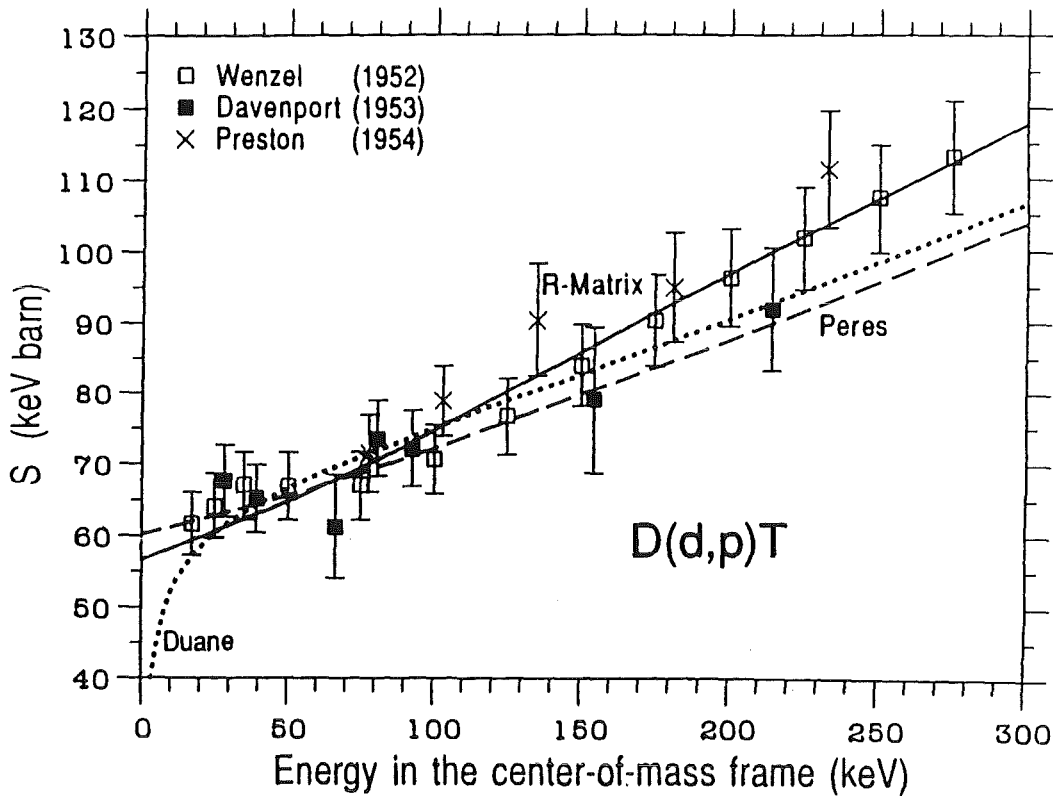
Fig. 6. Calculated S-functions for the D(d,p)T reaction at energies below 300 keV compared with various measurements.
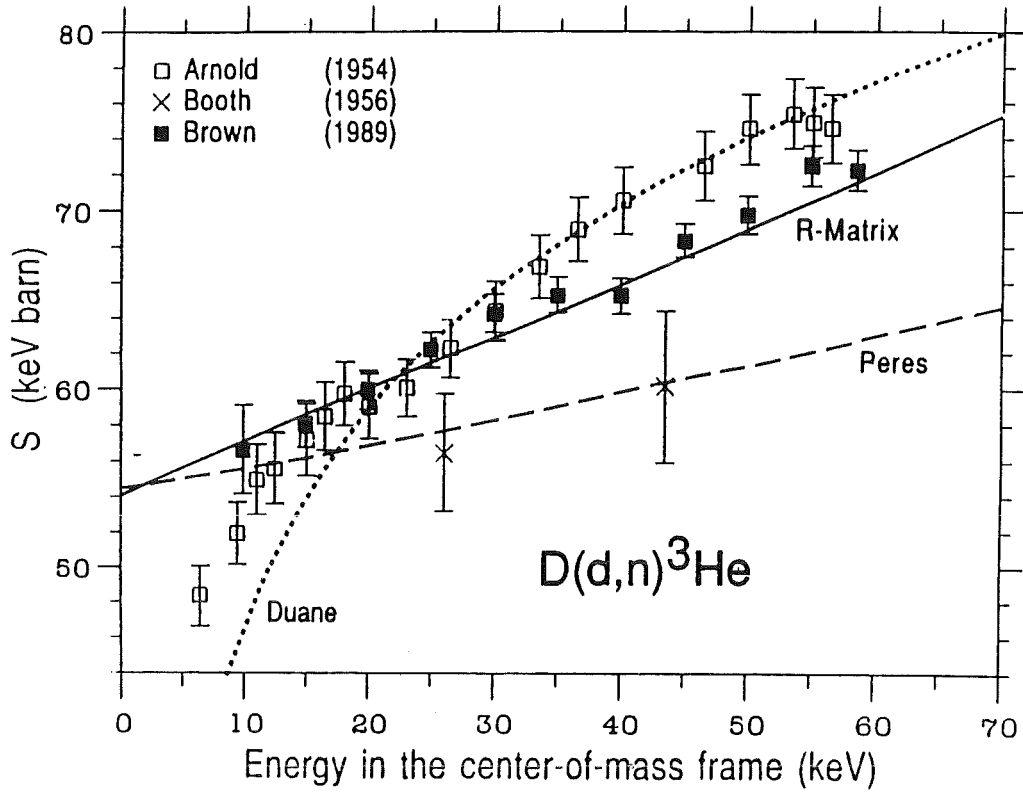
Fig. 7. Calculated S-functions for the D(d,n)^{3}He reaction at energies below 70 keV compared with various measurements.
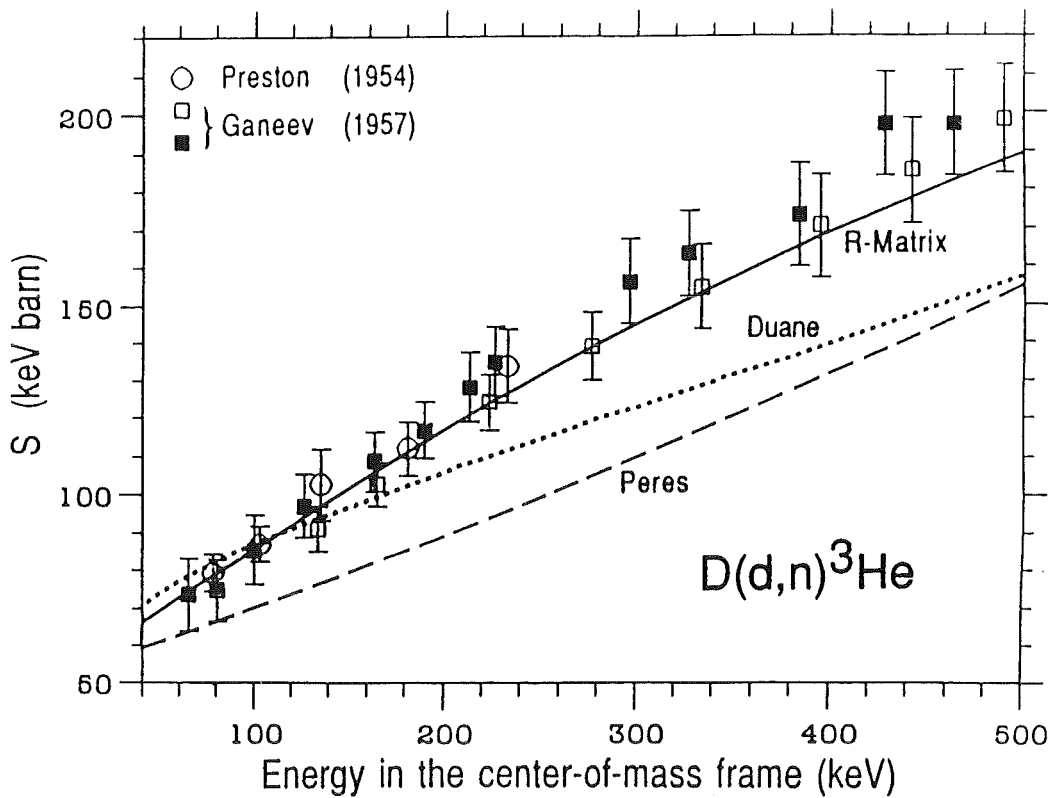
Fig. 8. Calculated S-functions for the D(d,n)^{3}He reaction at energies between 70 and 500 keV compared with various measurements.
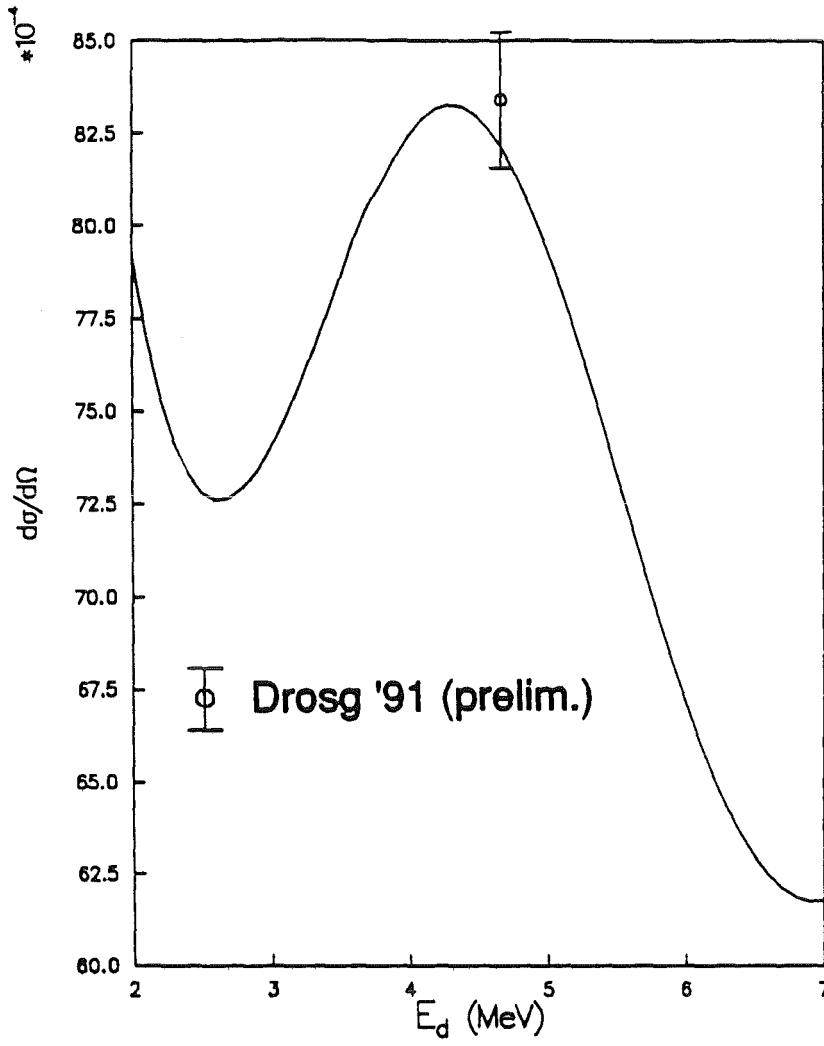
Fig. 9. Calculated center-of-mass differential cross section for the T(d,n)^{4}He reaction at 180^0 for laboratory. deuteron energies between 2 and 7 MeV The data point is from Drosg [23].

Calculations of Long-Lived Isomer Production in Neutron Reactions

M.B. Chadwick and P.G. Young

Theoretical Division, Los Alamos National Laboratory, Los Alamos, New Mexico 87545

I. INTRODUCTION

We have carried out theoretical calculations for the production of the long-lived isomers ^{93m}Nb(1/2$^-$, 16 yr), ^{121m}Sn (11/2-, 55 yr) , ^{166m}Ho (7-, 1200 yr), ^{184m}Re (8+, 165 d), ^{186m}Re (8+, 2 × 10^5 yr), ^{178m}Hf (16+, 31 yr), ^{179m}Hf (25/2-, 25 d) ^{192m}Ir (9+, 241 yr), all of which pose potential radiation activation problems in nuclear fusion reactors. We consider $(n, 2n)$, (n, n'), and (n, γ) production modes and compare our results both with expermental data (where available) and systematics. We also investigate the dependence of the isomeric cross section ratio on incident neutron energy for the isomers under consideration. The statistical Hauser-Feshbach plus preequilibrium code GNASH was used for the calculations. Where discrete state experimental information was lacking, rotational band members above the isomeric state, which can be justified theoretically but have not been experimentally resolved, were reconstructed.

The isomeric state production cross sections that we have considered were calculated at the request of the United Kingdom and United States fusion programs, which are in the process of establishing nuclear data libraries and inventory code packages to enable activation in virtually any material to be estimated. In a recent paper [1] we presented theoretical calculations of the production cross sections of hafnium isomers in 14 MeV reactions, using the GNASH [2] code. These calculations were performed prior to the release of experimental measurements [3] of the cross sections for hafnium isomer production, and agreement to within a factor of 2-3 was found. Because the cross sections under consideration were rather small and the isomer spins very large, the agreement obtained was encouraging, and suggested that our theoretical approach can be extended for use in other isomer-production calculations. We have, therefore, now determined production cross sections for long-lived isomers in Nb, Sn, Ir, Ho and Re at 14 MeV. In addition, we have determined the variation of the production cross section with incident neutron energy, since neutron energies below 14 MeV are produced in fusion reactors in inelastic collisions. As the energy variation of the hafnium isomer production was not shown in Ref.1 we summarize our previous results for hafnium and give this variation.

The systematics of neutron-induced isomeric cross section ratios at 14.5 MeV have been been studied by Kopecky and Gruppelaar [4]. They used a simplified

version of the GNASH code to determine the ratio of the cross section to the isomeric state and ground state in (n, n'), (n, p), (n, t), (n, α), and $(n, 2n)$ reactions, replacing the realistic nuclear level structure by two discrete states (the ground state and the isomeric state) plus a continuum of statistically described states. Their, approach is, therefore, considerably simpler than our calculations and so we have compared our results with the Kopecky systematics. We shall show that while such systematics are very useful, in many cases a full calculation (with a realistic description of the nuclear structure) is important in accurately determining isomer ratios. Also, Kopecky and Gruppelaar point out that their calculation is particularly sensitive to the simple model parameters that they adopt for the $(n, 2n)$ reaction. Our investigations into an analogous simple model confirm this, and indicate that for certain reactions one should be wary about using simple sytematic predictions. Finally, our calculations also include isomeric ratios for states formed in (n, γ) reactions, which are particularly resistant to simple systematics-based descriptions.

II. DESCRIPTION OF THE CALCULATIONS

A. General Description

The GNASH nuclear theory code [2] is based on the Hauser-Feshbach statistical theory with full angular momentum conservation, and with width fluctuation corrections obtained from the COMNUC code [5] using the Moldauer approach. Precquilibrium emission processes, which are important for incident energies above about 10 MeV, are calculated using the exciton model of Kalbach [6]. Transmission coefficients for neutrons and charged particles are calculated using an optical model, and gamma-ray transmission coefficients are obtained from giant dipole resonance approximations [7,8],making use of detailed balance. The level structure for each residual nucleus in a calculation is divided into discrete and continuum regions, with the former obtained from experimental complilations and the latter from phenomenological level density representations.

B. Optical Model

Both the Hauser-Feshbach theory and the exciton model require optical potentials to calculate transmission coefficients and inverse reaction cross sections. The coupled channels code ECIS [9] was used for deformed nuclei, and the code SCAT2 [10] for spherical nuclei. Potentials derived from analyses of nearby nuclei were usually modified for the present calculations. Before using an optical potential to generate transmission coefficients and reaction cross sections, the potentials were checked by comparing their predictions of elastic and total cross sections with experimental data, where available.

C. Gamma-Ray Transmission Coefficients

Transmission coefficients for gamma-ray emission were obtained using detailed balance, exploiting the inverse photoabsorption process. The Brink-Axel hypothesis is used, permitting the cross section for photoabsorption by an excited state to be equated with that of the ground state. The gamma-ray transmission coefficients were obtained from the expression

$$T^{X\ell}(\epsilon_\gamma) = 2\pi f_{X\ell}(\epsilon_\gamma)\epsilon_\gamma^{2\ell+1} , \tag{1}$$

where ϵ_γ denotes gamma-ray energy, $X\ell$ indicates the multipolarity of the gamma-ray, and $f_{X\ell}$ is the energy-dependent gamma-ray strength function. The strength functions for E1 decay were calculated either from standard Lorentzian expressions [7], given by

$$f_{E1}(\epsilon_\gamma) = K_{E1}\frac{\sigma_0\epsilon_\gamma\Gamma^2}{(\epsilon_\gamma^2 - E^2)^2 + \epsilon_\gamma^2\Gamma^2} \tag{2}$$

or from the generalized Lorentzian of Kopecky and Uhl [8]

$$f_{E1}(\epsilon_\gamma, T) = K_{E1}\left[\frac{\epsilon_\gamma\Gamma(\epsilon_\gamma)}{(\epsilon_\gamma^2 - E^2)^2 + \epsilon_\gamma^2\Gamma(\epsilon_\gamma)^2} + \frac{0.7\ \Gamma\ 4\pi^2T^2}{E^5}\right]\sigma_0\Gamma , \tag{3}$$

where

$$\Gamma(\epsilon_\gamma) = \Gamma\frac{\epsilon_\gamma^2 + 4\pi^2T^2}{E^2} \tag{4}$$

$$T = \sqrt{\frac{B_n - \epsilon_\gamma}{a}} , \tag{5}$$

and $K_{E1} = 8.68 \times 10^{-8}\text{mb}^{-1}$ MeV^{-2} (nominally) but was usually determined empirically by matching the theoretical gamma-ray strength function for s-wave neutrons to experimental values compiled by Mughabghab [11]. The quantities B_n and a are the neutron binding energy and Fermi gas level density parameter, respectively. The Lorentzian parameters of the giant-dipole resonance, E and Γ, are taken from the tables of Dietrich and Berman [12].

In addition to E1 radiation, M1 and E2 components are also included. For M1, a standard Lorentzian expression was used for the gamma-ray strength function. When the Kopecky-Uhl formulation was employed, a giant resonance formulation was also used to calculate the E2 strength function [8]; otherwise, a Weisskopf expression (f_{E2} = constant) was incorporated.

D. Nuclear Structure and Level Densities

The level density model of Gilbert and Cameron [13,14] was used in the Hauser–Feshbach calculations. At high energies the Fermi gas model is used along with a constant temperature form for lower energies. A gaussian distribution of spin states is taken to describe the angular momenta of levels at a certain excitation energy

$$\rho(E, J, \pi) = \frac{(2J + 1)}{2\sqrt{2\pi}\sigma^2} \exp\frac{-(J + \frac{1}{2})^2}{2\sigma^2}\rho(U) \tag{6}$$

where $U = E - \Delta$ (Δ is the pairing energy) and σ^2 is the spin cut–off parameter which is determined via $\sigma^2 = 0.146\sqrt{aU}A^{\frac{2}{3}}$ for the Fermi gas region. The spin cut-off factor is also determined from the spin distribution of observed low lying discrete levels and in the constant temperature region σ^2 is linearly interpolated between this value and the value of σ^2 where the Fermi gas region begins.

The production cross section of a certain isomeric state is often particularly sensitive to the discrete nuclear level structure, since the gamma cascade of discrete states into the isomeric state will enhance its production. In many cases, the isomeric state of interest is a band-head, with a rotational band built upon it, though often the rotational band members have not been experimentally resolved and lie in a high-excitation energy region. Accordingly, the energies of the rotational levels were assessed theoretically (obtaining the moment of inertia from observed rotational bands at lower excitation energies) and GNASH was modified to allow these discrete levels to be embedded within the continuum of statistically described levels. In the case of our calculation of Hf isomers [1], this procedure was particularly important; we found that over 40% of the production of the ^{178}Hf(16+) in an $(n, 2n)$ reaction came from the decay of the 14- level and the inferred discrete rotational band states above the 14- and 16+ levels. In Fig. 1 we show schematically the combination of discrete and statistical levels for the case of the ^{178}Hf nucleus.

III. RESULTS

A. The $(n, 2n)$ Isomeric Cross-Section Ratios

We have concentrated on the $(n, 2n)$ reaction mechanism for isomer production since, at 14 MeV, this is the dominant process through which most of the reaction flux goes. The following isomeric states, in addition to the hafnium states, have been considered in detail: ^{121m}Sn (11/2-, 55 yr) , ^{166m}Ho (7-, 1200 yr), ^{184m}Re (8+, 165 d), ^{186m}Re (8+, 2 × 10^5 yr), and ^{192m}Ir (9+, 241 yr). In all cases the experimentally measured discrete states have been examined and a matching point above which experimental data is missing has been determined. Rotational bands above the isomers were determined theoretically and included in the calculation, as discussed above. Optical potentials were found and checked against elastic and total scattering data, where available.

The isomer ratios can be compared with the Kopecky systematics for $(n, 2n)$ reactions. Kopecky and Gruppelaar [4] showed that a simplified version of GNASH predicted 14- MeV isomer cross-section ratios that have a "parabolic" dependence on the isomer spin, with a peak at isomer spins between 3 and 5. Their calculated isomeric ratio described the library of experimental ratios reasonably well, though they commented that for the case of the $(n, 2n)$ calculation their results were particularly sensitive to the model parameters describing the simplified nuclear structure. In Fig. 2, we show the 14-MeV isomer ratios compared with the Kopecky systematics. The differences between the line (the Kopecky prediction) and our theoretical results (triangles) can be understood as a measure of the need to perform full GNASH calculations with realistic nuclear structure and optical models. In the case of the hafnium isomers (25/2- and 16+) we have shown the experimental isomer ratio, from Patrick *et al.* In most cases the Kopecky systematics yield isomer ratios that are close to our detailed GNASH calculations. Our GNASH calculations for the isomer production cross section ratios of the 25/2- and 16+ levels in hafnium are seen to lie below the experimental numbers by about a factor of 2. The Kopecky sytematics overestimate the isomeric ratio for the 25/2- by about a factor of 4-5, and interpolating their curve to an isomer spin of 16 suggests that their systematics agree with the experimental measurement reasonably well.

The energy dependence of the isomeric ratio is of importance when assessing activation in a reactor induced by neutrons with degraded energies, after inelastic scattering processes have occurred. In Fig. 3. we show the variation of the isomer ratio with isomer spin for three different incident neutron energies: 14, 11 and 9 MeV. It is seen that, for a given incident neutron energy, the $(n, 2n)$ isomer ratio decreases with increasing isomer spin (at least for isomer spins above 4). This feature, which is also seen in experimental data and in the Kopecky calculations [4], can be simply understood in the following way. In $(n, 2n)$ reactions both outgoing neutrons generally have low energies and are dominated by s-wave transitions. However, in order to produce a high-spin isomer, the intermediate nuclear states also have to be of high spin, and since the transmission coefficients decrease with increasing l for large l, it would be expected that the isomer ratio would decrease strongly with increasing isomer spin. At lower energies the angular momentum brought in by the incident neutrons is less, so the isomer ratio falls off more rapidly with increasing isomer spin.

B. The (n, n') Isomeric Cross Section Ratios

The ground states of ^{178}Hf and ^{179}Hf are stable and are naturally occuring in hafnium, and natural niobium is monoisotopic in ^{93}Nb. Therefore we have calculated the (n, n') reactions to the isomeric states for these nuclei over the incident neutron energy range of 1 to 14 MeV. In addition, we have calculated the (n, n') reaction on ^{166}Ho to the isomeric state, the ground state of ^{166}Ho having a 1.1 day lifetime.

For the high-spin isomers [all except ^{93m}Nb (1/2-)], the isomer ratio is a strongly-

decreasing function of incident energy, and the higher isomer spins have the stronger energy dependencies. This is because the angular momentum brought in by the projectile neutron decreases with decreasing energy, and therefore results in a reduction in the high-spin isomer population. It is interesting to note that the energy dependence of the (n, n') isomer cross-section ratio is weaker than that of the $(n, 2n)$ reaction.

The Kopecky-Gruppelaar systematic calculations for the (n, n') isomeric cross section ratio again show a peak at an isomer spin $J^m = 3 - 5$, and are compared in Fig. 4 with our calculations at 14 MeV. In general, the Kopecky-Gruppelaar systematics agree fairly well with our detailed GNASH calculations (to within a factor of 2-3). One notable exception is the isomer cross section ratio for the production of the ^{179m}Hf(25/2-), for which our calculation exceeds the systematics by more than an order of magnitude (and the experimental result of Patrick et al exceeds the systematics by an even greater factor). This is probably due to the fact that Kopecky et al adopt a ground-state spin of 0.5 in their model calculation, whereas in this case the ground-state spin is 4.5. Hence they overestimate the spin change in the reaction and consequently underestimate the isomeric cross section ratio.

C. Isomeric Cross Section Ratios for (n, γ) Reactions

A limited amount of cross-section data for total (n, γ) radiative capture reactions is available at neutron energies in the MeV region, and simple systematic behavior with atomic number A has been noted for 14-MeV neutrons [16]. In the case of (n, γ) reaction to isomeric states, however, experimental data are much more limited and consist mostly of data for thermal incident neutrons. Thermal (n, γ) isomer ratios for an assortment of heavy nuclei are plotted versus the spins of the isomeric states in Fig. 5. Clearly, simple systematic behavior is much less evident for thermal neutron capture data than for 14-MeV particle-production cross sections, especially for isomeric states with spins greater than 5. This situation, coupled with the almost complete lack of experimental data at higher energies, results in a pressing need for reliable theoretical estimates of (n, γ) isomer ratios.

The GNASH code was used to calculate (n, γ) cross sections leading to isomeric states in ^{166}Ho(7-, 1200 y), ^{178}Hf(16+, 31 y; 8-, 4 s), ^{179}Hf (25/2-, 25.1 d; 1/2-, 18.7 s), ^{186}Re (8+, 2 x 10^5 y), and ^{188}Re (6-, 18.6 m). Except as noted below, the generalized Lorentzian form was utilized for the gamma-ray strength functions. The calculations were performed down to an incident energy of at least 1 keV in each case, at which energy the neutron transmission coefficients are completely dominated by s-waves, and it is possible to make a crude comparison with the thermal neutron experimental data. A selection of the isomeric ratios [relative to the total (n, γ) cross section] that results from the calculations for ^{165}Ho$(n, \gamma)^{166m}$Ho, ^{177}Hf$(n, \gamma)^{178m}$Hf, and ^{187}Re$(n, \gamma)^{188m}$Re reactions are shown in Fig. 6.

A feature of the isomer ratios of Fig. 6 is a general trend of increasing ratio with increasing neutron energy. This behavior reflects the fact that more angular

momentum is brought into the reactions as the neutron energy is increased thus increasing the population of higher spin states. For both the ^{165}Ho$(n, \gamma)^{166m}$Ho and ^{187}Re$(n, \gamma)^{188m}$Re reactions, an anomaly is seen in the calculated isomer ratios near 300 keV that interrupts this general trend of increasing isomer ratios with neutron energy. This effect is thought to result from the fact that thresholds for one or more high spin states in the target nucleus open in this energy region. The presence of these open channels to higher spin states permits neutron decays to occur more readily from higher spin states in the compound nucleus, thus reducing the high-spin population available for cascading to the isomeric state. As the incident neutron energy is further increased, more and more channels of all spins are opened, and the anomalous effect is overwhelmed by the increasing angular momentum brought into the reaction.

The agreement (or lack of agreement) between our calculated isomer ratios at lower energies and the thermal neutron measurements depends upon the extent to which the average properties (widths) embodied in our statistical model coincide with the very few channels involved in the thermal neutron measurements. Clearly, large differences between the calculations at ~ 1 keV and the thermal measurements are possible, and such are seen in the case of the ^{177}Hf$((n, \gamma)^{178m}$Hf isomer ratios ($\sim$ factor of 20 differences). In the cases of the ^{165}Ho$(n, \gamma)^{166m}$Ho and ^{187}Re$(n, \gamma)^{188m}$Re reactions, however, the differences between the calculated ratios near 1 keV and the thermal experimental values are much smaller, of the order of 30%.

To investigate the behavior of isomer ratios with neutron energy and with isomer spin, a simple parametric study was performed using the ^{187}Re$(n, \gamma)^{188m}$Re reaction as a base case. In this study various values of spin between 0 and 16 were assumed for the isomeric state in ^{188}Re at $E_x = 172$ keV, and the isomer ratio was calculated as a function of incident neutron energy for each isomer spin. The ^{187}Re$(n, \gamma)^{188m}$Re reaction was chosen because the real isomer ($J^\pi = 6^-, E_x = 172$ keV) is not fed by any of the known discrete states, so all the isomer's excitation comes from decays from the continuum. Additionally, the calculated isomeric state branching ratio for the real isomer is consistent (within 30%) at the lowest energy of the calculation (0.1 keV) with the measured ratio for thermal neutrons. The results of these calculations, performed using a standard Lorentzian, are shown in Fig. 7 for incident neutron energies of 0.001, 1, and 14 MeV. The calculated isomer ratios show strong dependence on both incident neutron energy and on isomer spin. The calculations for the higher spin states are thought to depend strongly on details of the gamma-ray strength functions as well as on the level density in the compound nucleus, since populating the isomeric states occurs almost exclusively through multiple γ-ray cascades in the compound nucleus.

While it is attractive to consider using calculations such as those illustrated in Fig. 7 to search for systematic relationships that might be useful in making simple predictions of isomer ratios, we found that the calculated results for the various cases were strongly dependent on the properties of the nuclei in question. The (n, γ) reaction is specifically excluded from the "one-step reaction" systematics identified

by Gruppelaar *et al.* [16], because the validity of those systematics was primarily established for (n, n'), (n, p), and (n, α) reactions and was doubtful for (n, γ). However, it was necessary for those authors to use the one-step reaction systematics for (n, γ) reactions in the REAC-ECN-3 library, due to the lack of other alternatives. A comparison between the one-step reaction systematics of Gruppelaar it et al. and our calculated (n, γ) isomer ratios at $E_n = 14$ MeV is given in Fig. 8. The calculated ratios are seen to differ significantly from the systematics, thus confirming the conclusion of Gruppelaar *et al.* that the one-step reaction systematics might not be valid for (n, γ) reactions. This further highlights the need for careful nuclear theory calculations for important reactions.

IV. CONCLUDING REMARKS

We present calculations of the energy dependence of isomer ratios for long-lived metastable states in ^{93}Nb, ^{121}Sn, ^{166}Ho, ^{184}Re, ^{186}Re, ^{178}Hf, ^{179}Hf, and ^{192}Ir, populated by means of (n, n'), $(n, 2n)$, and (n, γ) reactions. The calculated ratios for $(n, 2n)$ reactions generally support predictions from systematics at 14 MeV except for isomer spins above ~ 12. The agreement with systematics is not as good for (n, n') reactions as is the case for $(n, 2n)$, but the systematics obviously are good enough to still be useful in developing large activation libraries. In the case of (n, γ) reactions, the theoretical values cannot be compared directly with the thermal neutron measurements but are roughly consistent at the lower energy range of the calculations.

Because of the limited amount of experimental data available on isomer ratios, nuclear theory codes such as GNASH provide a useful complement to the data base. The calculations are particularly important for (n, γ) reactions, as experimental data are extremely limited and systematics provide little guidance, as well as for determining the energy dependence of (n, n') and $(n, 2n)$ isomer ratios, for which there is little experimental information. In general, we recommend that evaluations of important long-lived isomers be based on detailed theoretical analyses matched to the available experimental data. The use of systematics should be limited to providing data for less important reactions. In cases where systematics are used, particular care should be exercised with (n, γ) isomeric ratios, and the procedure, which is sometimes used, of setting the isomer ratio to 1/2 of the total (n, γ) cross sections should *never* be used at low energies, as it can lead to errors of many orders of magnitude.

A detailed description of the present work will be presented at the upcoming IAEA Research Coordination Meeting on "Activation Cross Sections for the Generation of Long-Lived Radionuclides of Importance in Fusion Reactor Technology," in Vienna, 11-12 November 1991.

V. REFERENCES

[1] M.B. Chadwick and P.G. Young, 'Calculations of the Production Cross Sections of High-Spin Isomeric States in Hafnium', Nucl. Sci. and Eng. **108**, 117 (1991).

[2] E.D. Arthur, 'The GNASH Preequilibrium-Statistical Model Code', Los Alamos National Laboratory report LA-UR-88-382 (1988); P.G. Young and E.D. Arthur, 'GNASH: A Preequilibrium, Statistical Nuclear-Model Code for Calculation of Cross Sections and Emission Spectra', Los Alamos Scientific Laboratory report LA-11753-MS (1990).

[3] B.H. Patrick, M.G. Sowerby, C.G. Wilkins and L.C. Russen, 'Measurements of 14-MeV Neutron Cross Sections for the Production of Isomeric States in Hafnium Isotopes,' presented at the Specialists' Mtg. Neutron Activation Cross Sections for Fission and Fusion energy Applications, Argonne, Illinois, September 13-15 1989.

[4] J. Kopecky and H.Gruppelaar, 'Systematics of Neutron-Induced Isomeric Cross Section Ratios at 14.5 MeV', ECN report ECN-200 (1987).

[5] C.L. Dunford, 'Compound Nucleus Reaction Programs COMNUC and CASCADE', AI-AEC-12931, Atomics Int. (1970).

[6] C. Kalbach,'The Griffin Model, Complex Particles and Direct Nuclear Reactions', Z. Phys. **A283**, 401 (1977).

[7] D.M. Brink, 'Some Aspects of the Interaction of Fields with Matter', D.Phil. Thesis, Oxford (1955); P. Axel, 'Electric Dipole Ground State Transition Width Strength Function', Phys. Rev. **126**, 671 (1962).

[8] J. Kopecky and M. Uhl, 'Test of Gamma-Ray Strength Functions in Nuclear Reaction Model Calculations,' Phys. Rev. C **42**, 1941 (1990).

[9] J. Raynal, 'Optical Model and Coupled-Channel Calculations in Nuclear Physics', SMR-9/8, International Atomic Energy Agency (1972).

[10] O. Bersillon, 'SCAT2 - A Spherical Optical Model Code',in Progress Report of the Nuclear Physics Division, Bruyeres-le-Chatel (1977), CEA-N-2037, p. 111 (1978).

[11] S.F. Mughabghab, 'Neutron Resonance Parameters and Thermal Cross Sections', Parts A and B, in Neutron Cross Sections, V. 1, Academic Press Inc., New York, (1981) (part A) and (1984) (part B).

[12] S.S. Dietrich and B.L. Berman, 'Atlas of Photoabsorption Cross Sections Obtained with Monoenergetic Photons', Atomic and Nuclear Data Tables, 199 (1988).

[13] A. Gilbert and A.G.W. Cameron, 'A composite Nuclear-Level density formula with Shell Corrections', Can. J. Phys. **43**, 1446 (1965).

[14] J. L. Cook, H. Ferguson, and A. R. Musgrove, Aus. J. Phys. **20**, 477 (1967).

[15] E. D. Arthur, P. G. Young, A. B. Smith, and C. A. Philis, Trans. Am. Nucl. Soc. **39**, 793 (1981).

[16] H. Gruppelaar, H. A. J. van der Kamp, J. Kopecky, and D. Nierop, 'The REAC-ECN-3 Data Library with Neutron Activation and Transmutation Cross Sections for Use in Fusion Reactor Technology,' ECN report ECN-207 (1988).
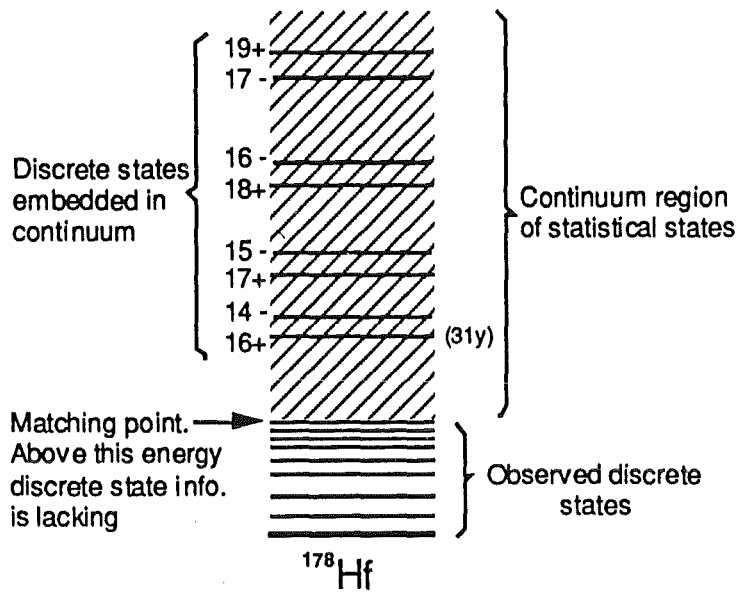
Fig. 1. A schematic representation of the combination of discrete, statistical and discrete levels embedded in the statistical continuum region used to describe the nuclear structure of ^{178}Hf.
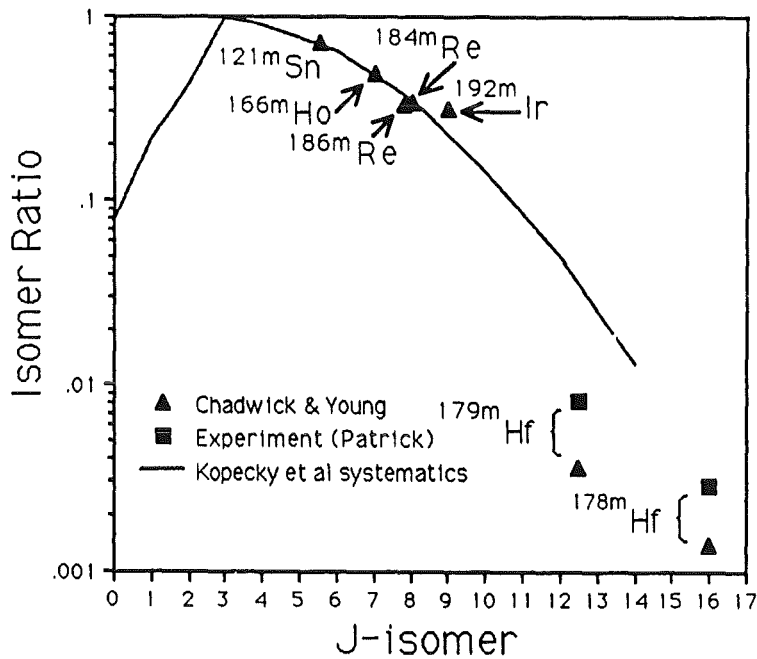
Fig. 2. The $(n, 2n)$ isomeric cross section ratio as a function of isomer spin, for 14 MeV incident neutrons. The Kopecky systematics calculation is compared with our GNASH calculations, and a comparison with data is made for the 25/2- and 16+ hafnium isomers.
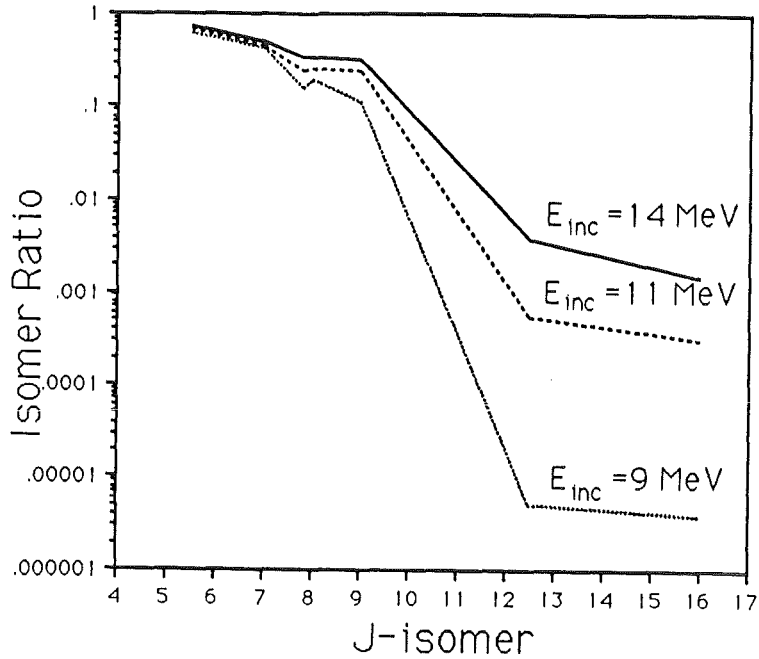
Fig. 3. The $(n, 2n)$ isomeric cross section ratio as a function of isomer spin, for three different incident neutron energies. The lines connect GNASH calculations for the same isomers that are shown in Fig. 2.
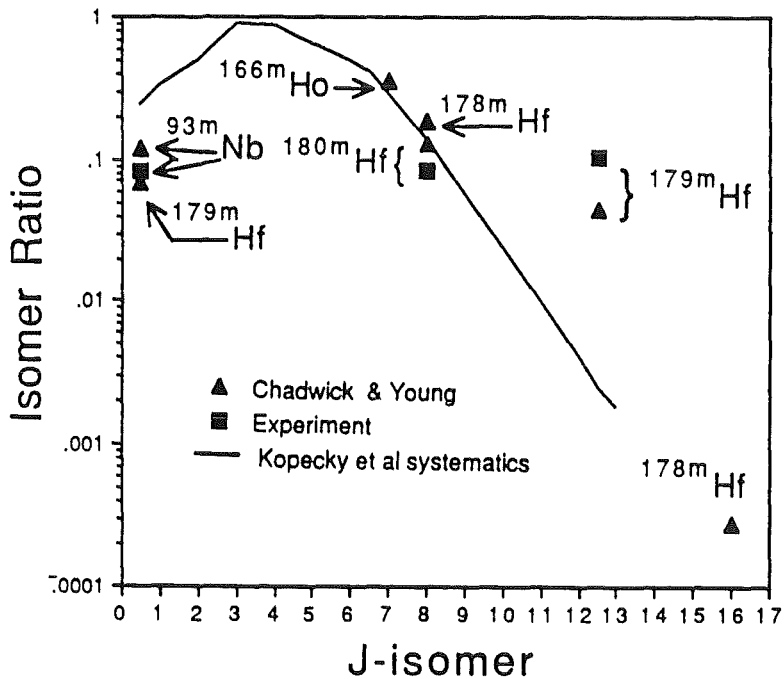
Fig. 4. The (n, n') isomeric cross-section ratio as a function of isomer spin for 14-MeV incident neutrons. The Kopecky systematics for one-step reactions are compared with GNASH calculations and with experimental data.
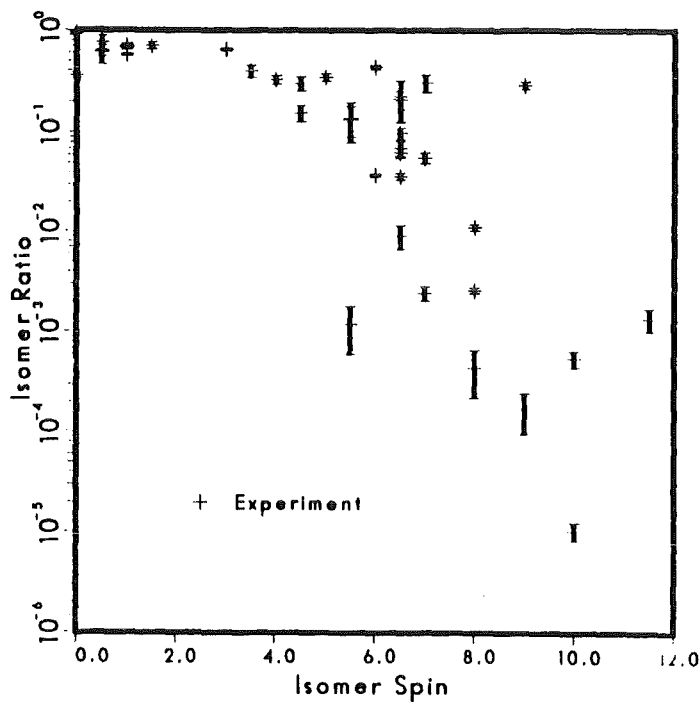
Fig. 5. Experimental isomer ratios for (n, γ) reactions with thermal neutrons, plotted as a function of spin of the isomeric states.
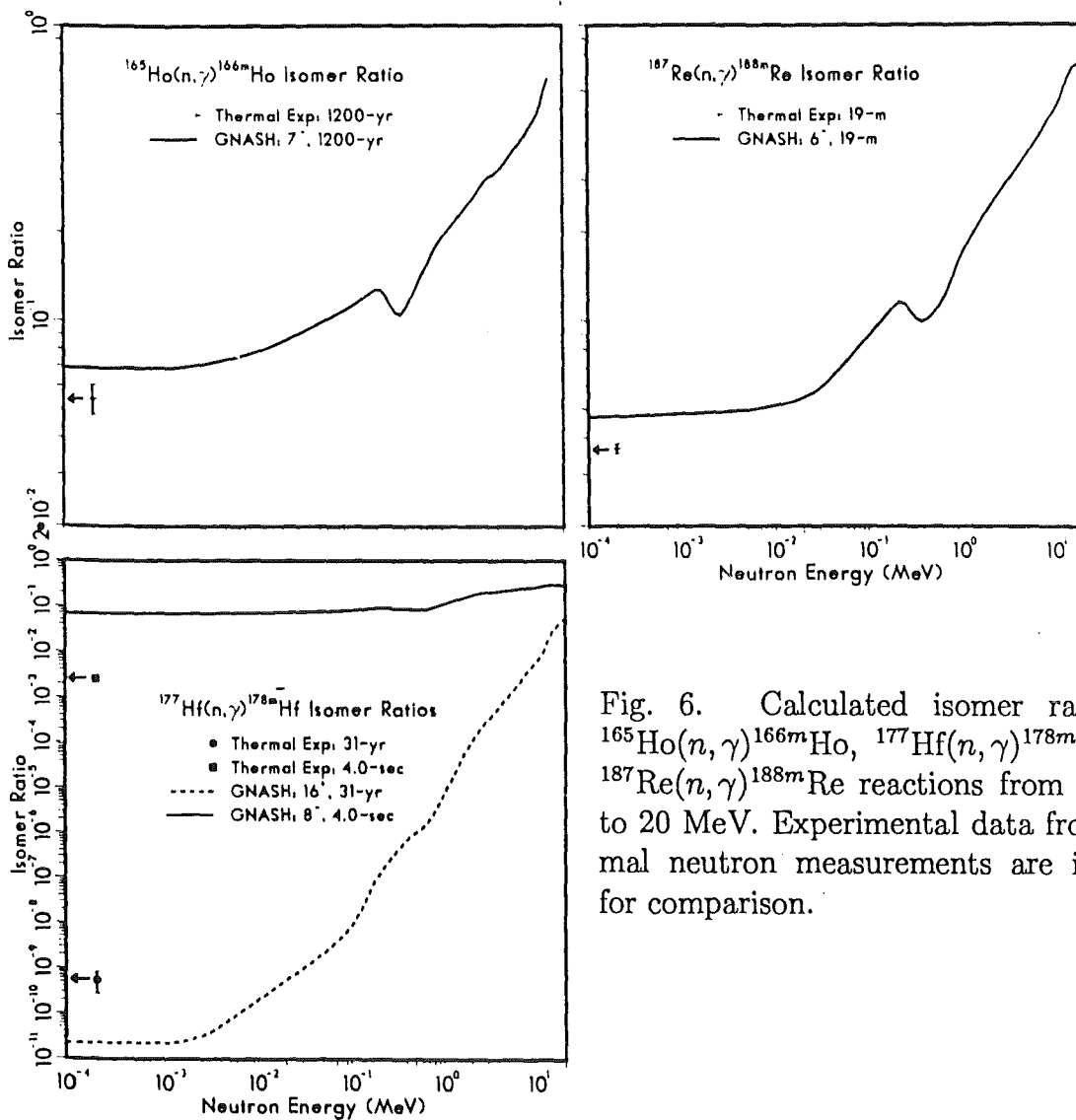
Fig. 6. Calculated isomer ratios for $^{165}\text{Ho}(n, \gamma)^{166m}\text{Ho}$, $^{177}\text{Hf}(n, \gamma)^{178m}\text{Hf}$, and $^{187}\text{Re}(n, \gamma)^{188m}\text{Re}$ reactions from 0.1 keV to 20 MeV. Experimental data from thermal neutron measurements are included for comparison.
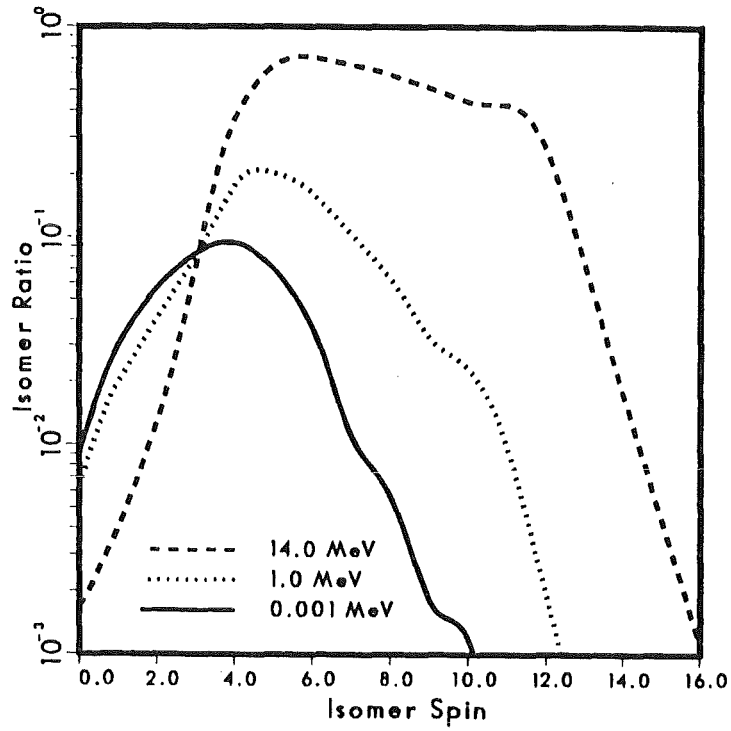
Fig. 7. Calculated isomer ratios as functions of incident neutron energy and isomer spin for the ^{187}Re$(n,\gamma)^{188m}$Re reaction. The calculations were performed by replacing the spin of the actual isomer in ^{188}Re($J^\pi = 6^-$, $E_x = 172$ keV) by values from 0 to 20.
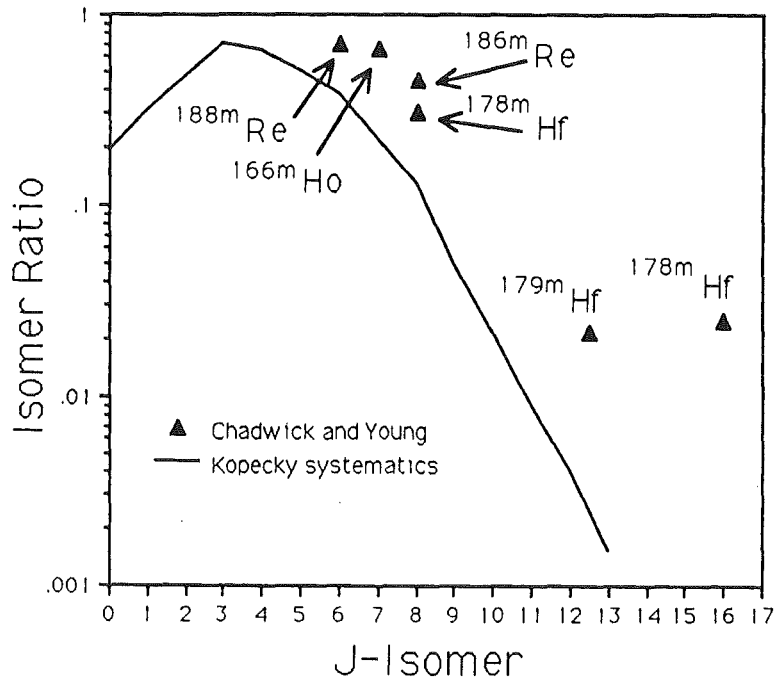
Fig. 8. The (n,γ) isomeric cross-section ratio as a function of isomer spin for 14-MeV incident neutrons. The Kopecky systematics for one-step reactions are compared with GNASH calculations.

Production of New Nuclear Data Libraries for Low-Activation Materials Development from Statistical/Preequilibrium Model Calculations

P. Obložinský[1], S. Cierjacks,S. Kelzenberg and B. Rzehorz

Kernforschungszentrum Karlsruhe, Association KfK-Euratom

Institut für Materialforschung

Postfach 3640, 7500 Karlsruhe

Federal Republic of Germany

Abstract

New major nuclear data libraries were developed for the kinematically complete treatment of sequential (x,n) reactions in fusion materials activation calculations. These libraries include data for virtually all isotopes with $Z \leq 84$ ($A \leq 210$) and half-lifes exceeding 1 day, primary neutron energies $E_n < 20$ MeV and secondary charged particles x = p, d, t, ^3He and α with energies $E_x < 24$ MeV. While production cross sections of charged particles for primary (n,x) reactions can be deduced from the European activation file EAF-1, we created for the corresponding normalized charged particle spectra the data file KFKSPEC. Our second file, KFKXN, contains cross sections for secondary (x,n) reactions. The third file is KFKSTOP with a complete set of differential ranges for all five light charged particles mentioned above and for all elements from hydrogen to uranium.

The libraries KFKSPEC as well as KFKXN are essentially based on nuclear model calculations using the statistical evaporation model superimposed with the preequilibrium contribution as implemented in the code ALICE. The library KFK-SPEC includes 633 isotopes of which 55 are in their isomeric states and contains 63 300 spectra of the type (n,x) with almost 1.5 million data points. The library KFKXN also includes 633 isotopes, contains all (x,n) and partly also (x,2n) cross sections for 4 431 reactions with about 106 000 data points. The KFKSTOP library is considered to be complete and has 11 040 data points.

1. Introduction

This paper reports on the development of the nuclear data base needed for the treatment of sequential (x,n) reactions in activation calculations, x being the charged particle created by primary neutron interactions. Such calculations are of importance in

---

[1] On leave from the Institute of Physics, SAS, 842 28 Bratislava, Czechoslovakia

the development of low activation materials (LAM) for fusion reactor applications [1]. It has been shown on several selected examples that sequential (x,n) reactions can contribute substantially to the total radioactive inventory [2, 3, 4, 5]. Due to that a major task has been undertaken to develop necessary nuclear data libraries that allow for a kinematically complete treatment of these reactions. An early stage of this activity has been reported earlier this year [6], where we described the first versions of our new libraries limited to outgoing p, d and α particles and to isotopes with the mass number $A \leq 100$. Our current second versions include also tritons and ^3He and the range of isotopes has been extended to $A \leq 210$.

Below we briefly explain the concept of sequential (x,n) reactions together with the data required for the corresponding inventory calculations. We proceed by explaining the methods used to develop the nuclear data libraries under discussion and summarize their current status. We remind that the code PCROSS has been developed for handling these libraries in full size inventory calculations [7]. Such calculations involve the European reference code FISPACT [8, 9].

2. Sequential (x,n) Reactions and Nuclear Data Needs

A so-called sequential (x,n) reaction is a two-step process in which charged particles x are created in a first-step neutron induced reaction $A(n, *x)$ which is followed by the second-step reaction $\bar{A}(x, n)C$ with the target isotope $\bar{A}$ (note that $\bar{A}$ is not necessarily identical with A) producing the residual nucleus C. In the first step the neutron flux is converted into the flux of charged particles via reactions $A(n, *x)$, where star means anything and $x = p, d, t, {}^3He, \alpha$. The charged particle flux $\Phi_x(E_{x_k})$ can be obtained as

$$
\begin{aligned}
\Phi_x(E_{x_k}) = & \sum_A \sum_{i=1}^{175} \Phi_n(E_{n_i})\sigma_{n,x}(E_{n_i})N_A\Delta E_{n_i} \\
& \times \sum_{j=k}^{24} f_{n,x}(E_{n_i}, E_{x_j})\Delta E_{x_j}\Delta R_x(E_{x_k}),
\end{aligned}
\tag{1}
$$

where $\Phi_n(E_{n_i})$ is the incident neutron flux, N_A is the initial inventory of nuclei A, $\sigma_{n,x}(E_{n_i})$ is the charged particle production cross section, $f_{n,x}(E_{n_i}, E_{x_j})$ is the normalized charged particle spectrum and $\Delta R_x(E_{x_k})$ is the differential range of the charged particle x with the starting energy E_x. In the second step the charged particle x proceeds by inducing the reaction $\bar{A}(x, n)C$ and thus creating a new nuclide C. One is interested in the related inventory N_C per unit time and unit volume

$$N_C = N_{\bar{A}} \sum_{k=1}^{24} \Phi_x(E_{x_k}) \sigma_{x,C}(E_{x_k}), \tag{2}$$

where $N_{\bar{A}}$ is the inventory of intermediary nuclei $\bar{A}$ and $\sigma_{x,C}(E_{x_k})$ is the cross section to produce nuclide C.

From these equations it becomes clear that the total nuclear data requirements are as follows. Needed are four libraries for charged particles $x = p$, d, t, ^3He, α, namely

- charged particle production cross sections in $(n, *x)$ reactions, $\sigma_{n,x}$,

- normalized charged particle spectra in these reactions, $f(n, x)$,

- production cross sections of final nuclei in (x,n) reactions, $\sigma_{x,C}$

- and differential ranges of charged particles in the material, ΔR_x .

The energy range for neutrons is $E_n < 20 MeV$ and we accepted the requirement from the Culham meeting [10] to adopt the 175 group VITMAMIN-J structure for it. The point is that the European activation file EAF-1 file as well as the neutron flux given for fusion devices also follow this energy pattern. The energy range for charged particles was selected as $E_x < 24 MeV$ to cover all possible cases with positive Q-values. The list of isotopes is very extensive, it should include all isotopes with half-lives $T_{1/2} > 1$ day (more than 600 cases).

We now briefly examine the status of these data. Charged particle production cross sections $\sigma_{n,x}$ can be deduced from the European Activation File EAF-1 as developed at Petten [11]. However, there is practically no information on the corresponding charged particles spectra. Therefore, we have developed the charged particle library KFKSPEC practically from scratch. More information is available as regards the data on $\sigma_{x,C}$. However, the available charged particle libraries ECPL-86 [12] and GRAZ-87 [13] are for very low A only. The Soviet charged particle library [14] is very limited. The Münzel's charged particle library is partially lost, it is based on data available before 1972 and moreover it also is rather limited [15, 16, 17]. We have, therefore, developed the new library for (x,n) cross sections, KFKXN, also from scratch. Finally, there seems to be no problem with the data for ΔR_x. There is available, for example, the well established Ziegler's code for stopping powers [18, 19]. This allowed us, for reasons of convenience, to develope also the dedicated new library for differential ranges of charged particles, KFKSTOP.

3. New Libraries

It is well known that in the energy range of interest the dominant nuclear reaction mechanism is that of the compound nucleus. This should be superimposed with the

contribution from preequilibrium stages of the reaction that preceed creation of the fully equilibrated compound nucleus. A notable advantage of these statistical/preequilibrium models is that, although they have a sound quantum-mechanical basis, they still can be formulated in a fairly transparent manner. Furthermore, their applicability for nuclear data evaluation has been widely tested and they are presently used almost as standard tools in predicting unknown cross sections by nuclear data evaluators. Another important advantage is that there is continuing international effort to improve the underlying physics as well as to establish well tested sets of parameters, such as those needed for optical potential and nuclear level density assumptions.

The code used here is ALICE as developed at the Lawrence Livermore National Laboratory by M. Blann et al. [20, 21, 22] over more than two decades. It is based on the preequilibrium hybrid model and the evaporation statistical model. We used the latest version due to December 1990 [23]. It can handle whatever incident particle, but it is limited to n,p,d, α and γ in exit channels.

All parameters that we employed are provided as optional by ALICE. We used global sets of optical potential parameters and the corresponding parabolic approximation to calculate inverse cross sections. For level densities we used the standard set of parameters. The calculations were performed for 623 target isotopes from ^{10}B to ^{210}Po, and for outgoing charged particles x = p, d, α. Incident neutron energies were set to the middle of the respective VITAMIN-J bins so that the whole energy range is reasonably well covered by 20 steps; we used E_n = 18.5, 17.1, 16.1, 14.7, 14.0, 13.2, 12.4, 11.3, 10.2, 9.3, 8.4, 7.6, 6.9, 5.9, 5.1, 4.3, 3.3, 2.4, 1.5 and 0.6 MeV. Contributions from appropriate reaction channels are summed up so that full production spectra of particles x are obtained. The spectra are given in 1 MeV steps of charged particle energies E_x = 0.5, 1.5, ..., 23.5 MeV. Spectra are normalized to unity and stored together with the calculated energy-integrated absolute cross sections.

An extra treatment was adopted for charged particle spectra from (n, t) as well as $(n, {}^3He)$ reactions. It is well known that neither the statistical nor the preequilibrium reaction model can presently reasonably calculate these reactions and corresponding spectra we are interested in. The reason is that the dominating reactions mechanism is the pick-up process. The evaporation contribution is generally negligibly small and all preequilibrium models face the long standing unsolved problem of clusterization mechanism. Due to that we, as a preliminary solution, resorted to a simple kinematical upper limit estimates of these spectra. This should provide us a reasonable guidance about possible contributions from the respective sequential reactions. If some of these contributions will appear to be of importance one should as a next step concentrate on these cases individually.

Another extra treatment was adopted for very light isotopes (10 isotopes with $Z \leq$ 4). For (n, x) spectra we basically again resorted to simple kinematical limits. However, the (x, n) cross sections are taken from the fairly recent GRAZ-87 file [13].

Examples of data as included into our new libraries can be found in Tab.I, Tab.II and Tab.III. The current status of the libraries can be summarized as follows.

- **KFKSPEC library: Normalized (n,x) spectra**
  - Elements: $Z \leq 84$
  - No. of isotopes: 633 including 55 isomers (matched with EAF-1)
  - Incident neutrons: $E_n = 18.5, 17.1, 16.1, 14.7, 14.0, 13.2, 12.4, 11.3, 10.2,$ 9.3, 8.4, 7.6, 6.9, 5.9, 5.1, 4.3, 3.3, 2.4, 1.5, 0.6 MeV
  - Outgoing charged particles: $x = p, d, t, {}^3He, \alpha$
  - Charged particle energies: $E_x = 0.5, 1.5, ..., 23.5\,MeV$
  - No. of spectra: 63 300
  - No. of data points: more than 1.5 milion
  - Status: version **KFKSPEC-2**

- **KFKXN library: (x,n) production cross sections**
  - Elements: $Z \leq 84$
  - No. of isotopes: 633 including 55 isomers (as in EAF-1)
  - Reactions (x, n): for $x = p, d, t, {}^3He, \alpha$
  - Reactions $(x, 2n)$: for $x = d, t$ (c.s. are large towards (d, n) and (t, n))
  - Charged particle energies: $E_x = 0.5, 1.5, ..., 23.5\,MeV$
  - No. reactions: 4 431
  - No of data points: about 106 000
  - Status: version **KFKXN-2**

- **KFKSTOP library: Differential ranges of charged particles**
  - Based on Ziegler's stopping power code
  - No. of elements: 92
  - Charged particles: $x = p, d, t, {}^3He, \alpha$
  - Charged particle energies: $E_x = 0.5, 1.5, ..., 23.5\,MeV$
  - ΔR_x given in cm for 1 MeV energy loss
  - No. of data points: 11 040
  - Status: **KFKSTOP** final.

Acknowledgements

to M. Blann for many useful suggestions and his ongoing advice on the use of the code ALICE. They appreciate also useful suggestions by J. Kopecký and H. Gruppelaar concerning the EAF-1 file and preequilibrium emission of clusters. Helpful information was obtained from M.B. Chadwick, F.E. Chukreev, P.P. Dmitriev, M. Drosg, H. Münzel, A. Pashchenko as well as R. White.

References

[1] K. Anderko, *unveröffentlichter Bericht* (KfK, Karlsruhe, 1990).

[2] S. Cierjacks and Y. Hino: *The role of sequential (x,n) reactions on element activation of fusion reactor materials and related nuclear data needs*, Proc. Specialists' Meeting on Neutron Activation Cross Sections for Fission and Fusion Energy Applications, Argonne, 13th - 15th September 1989, see Report NEANDC-259 'U', eds. M. Wagner and H. Vonach (OECD, Paris, 1989) pp. 19-28.

[3] S. Cierjacks and Y. Hino: *The importance of sequential (x,n) reactions on element activation of fusion reactor materials*, J. Nucl. Mater. **170** (1990) 134-139.

[4] S. Cierjacks and Y. Hino: *Study of element activities in fusion reactor materials*, Report KfK-4523 (KfK, Karlsruhe) in preparation.

[5] S. Cierjacks : *Nuclear data needs for "low-activation" fusion materials development*, Fusion Eng. and Design **13** (1990) 229-238.

[6] S. Cierjacks, P. Obložinský and B. Rzehorz: *Nuclear Data Libraries for the Treatment of Sequential (x,n) Reactions in Fusion Materials Activation Calculations*, Report KfK-4867 (KfK, Karlsruhe, July 1991).

[7] S. Ravndal, P. Obložinský, S. Kelzenberg and S. Cierjacks: *PCROSS - User Manual*, Report KfK-4873 (KfK, Karlsruhe, August 1991).

[8] R. A. Forrest, D. A. J. Endacott and A. Khursheed: *FISPACT - Program Manual*, Report AERE-M3655 (AERE, Harwell, 1988).

[9] R. A. Forrest and D. A. J. Endacott: *FISPACT - User Manual*, Report AERE-M3654 (AERE, Harwell, 1988).

[10] Recommendation of the Culham Workshop on Low-Activation Materials, Culham, April 1991.

[11] H. Gruppelaar, H. A. J. Van der Kamp, J. Kopecký and D. Nierop: *The REAC-ECN-3 Data Library with Neutron Activation and Transmutation Cross-Sections for Use in Fusion Reactor Technology*, Report ECN-207 (ECN, Petten, 1988). We use version No.5, due to December 1990, which is identical with the European Activation File EAF-1.

[12] *ECPL-86, The LLNL evaluated charged-particle data library, summary of contents by O. Schwerer*, Report IAEA-NDS-56, Rev. 1 (IAEA, Vienna, 1987).

[13] R. Feldbacher: *The AEP Barnbook DATLIB. Nuclear reaction cross sections and reactivity parameter, library and files*, Report INDC(AUS)-12/G (IAEA, Vienna, 1987). We use the name GRAZ-87 for the library throughout the present paper.

[14] P. P. Dmitriev: *Radionuclide yield in reactions with protons, deuterons, alpha particles and helium-3 (Handbook)*, Report INDC(CCP)-263/G (IAEA, Vienna, 1986).

[15] J. Lange and H. Münzel: *Abschätzung unbekannter Anregungsfunktionen für $(\alpha, xn)-$, $(\alpha, pxn)-$, $(d, xn)-$ und $(p, xn)-$ Reaktionen*, Report KfK-767 (KfK, Karlsruhe, 1968).

[16] K. A. Keller, J. Lange and H. Münzel: *Q-values and excitation functions of nuclear reactions. Part c: Estimation of unknown excitation functions and thick target yields from p, d, ^3He and α reactions*. In Landolt - Börnstein New Series in Physics (Springer-Verlag, Berlin, 1974) Vol. I5c.

[17] S. Pearlstein: *NNDC evaluated charged particle reaction data library*, Report IAEA-NDS-59, Rev. 1 (IAEA, Vienna, 1985).

[18] J.F.Ziegler, J.P. Biersack and U. Littmark: *The stopping and range of ions in solids* (Pergamon Press, New York,1985).

[19] A. Möslang, *unveröffentlichter Bericht* (KfK, Karlsruhe, 1990).

[20] M. Blann and J. Bisplinghoff: *Code ALICE/Livermore 82*, Report UCID-19614 (LLNL, Livermore, 1982).

[21] M. Blann and H. K. Vonach: *Global test of modified precompound decay models*, Phys. Rev. C 28 (1983) 1475-1492.

[22] M. Blann: *Code ALICE/85/300*, Report UCID-20169 (LLNL, Livermore, 1984).

[23] M. Blann (LLNL Livermore): *Code ALICE, version 1990*, private communication, January 1991.

Tab.I. Sample printout from the **KFKSPEC** library. Shown are normalized charged particle spectra from $^{23}Na(n, *x)$ reactions. A heading line and a comment line is followed by an identification line and 3 data lines. The identification line contains full specification of a particular (n, x) reaction (ENDF identifiers 1030, 1040, 1050, 1060, 1070 stand for $x = p, d, t, {}^{3}He, \alpha$, respectively); this is followed by 2 sequence numbers of VITAMIN-J groups and related neutron energy used by us, and by calculated production cross section in barns. Subsequent 3 lines keep 24 values of the normalized spectrum.

```
110230              ********* NA 23(N,*X) ***********         KFKSPEC-2
          ALICE OUTPUT: EN=18.5MEV; T AND H: KINEMATICAL LIMIT  KFKSPEC-2
110230 1030   1   1 18.5 0.382E+00 0.382E+00                   KFKSPEC-2
0.000000 0.228371 0.274213 0.185579 0.098549 0.061950 0.042209 0.029272
0.021716 0.017039 0.014078 0.011388 0.008960 0.006679 0.000000 0.000000
0.000000 0.000000 0.000000 0.000000 0.000000 0.000000 0.000000 0.000000
110230 1040   1   1 18.5 0.163E-01 0.163E-01                   KFKSPEC-2
0.000000 0.037683 0.148466 0.190795 0.172632 0.143579 0.109656 0.078796
0.054698 0.038109 0.025588 0.000000 0.000000 0.000000 0.000000 0.000000
0.000000 0.000000 0.000000 0.000000 0.000000 0.000000 0.000000 0.000000
110230 1050   1   1 18.5 0.000E+00 0.000E+00                   KFKSPEC-2
0.000000 0.000000 0.000000 0.000000 0.000000 1.000000 0.000000 0.000000
0.000000 0.000000 0.000000 0.000000 0.000000 0.000000 0.000000 0.000000
0.000000 0.000000 0.000000 0.000000 0.000000 0.000000 0.000000 0.000000
110230 1060   1   1 18.5 0.000E+00 0.000E+00                   KFKSPEC-2
0.000000 0.000000 0.000000 0.000000 0.000000 0.000000 0.000000 0.000000
0.000000 0.000000 0.000000 0.000000 0.000000 0.000000 0.000000 0.000000
0.000000 0.000000 0.000000 0.000000 0.000000 0.000000 0.000000 0.000000
110230 1070   1   1 18.5 0.126E+00 0.126E+00                   KFKSPEC-2
0.000000 0.000000 0.023083 0.127107 0.166862 0.155137 0.128963 0.108408
0.092009 0.071835 0.050581 0.035397 0.024140 0.016478 0.000000 0.000000
0.000000 0.000000 0.000000 0.000000 0.000000 0.000000 0.000000 0.000000
```

Tab. II. Sample printout from the library **KFKXN**. Shown are (p,n) cross sections on $^{44m,45,46}Sc$. A heading line and a comment line are followed by cross sections in barns for incident energies $E_p = 0.5, 1.5, ..., 23.5$ MeV. Identification of reactions follows the ECPL-86 style (2=incident proton, 11=outgoing neutron).

```
210441 2 11        SC 44M(P,N)                           KFKXN-2
                   ALICE OUTPUT                          KFKXN-2
0.0000E+00  0.0000E+00  0.9964E-01  0.1117E+00  0.1867E+00  0.2177E+00
0.2504E+00  0.2540E+00  0.2649E+00  0.2644E+00  0.2700E+00  0.2673E+00
0.2323E+00  0.1872E+00  0.1474E+00  0.1141E+00  0.8743E-01  0.7113E-01
0.5852E-01  0.4959E-01  0.4316E-01  0.3673E-01  0.3361E-01  0.3050E-01
210450 2 11        SC 45(P,N)                            KFKXN-2
                   ALICE OUTPUT                          KFKXN-2
0.0000E+00  0.0000E+00  0.0000E+00  0.1329E+00  0.2243E+00  0.2926E+00
0.3678E+00  0.3884E+00  0.4099E+00  0.4063E+00  0.4117E+00  0.4406E+00
0.4538E+00  0.4732E+00  0.4023E+00  0.3139E+00  0.2382E+00  0.1728E+00
0.1247E+00  0.9410E-01  0.7742E-01  0.6073E-01  0.5301E-01  0.4529E-01
210460 2 11        SC 46(P,N)                            KFKXN-2
                   ALICE OUTPUT                          KFKXN-2
0.0000E+00  0.0000E+00  0.1116E+00  0.1583E+00  0.3109E+00  0.4234E+00
0.5235E+00  0.5755E+00  0.5938E+00  0.5896E+00  0.5894E+00  0.5236E+00
0.4054E+00  0.2985E+00  0.2209E+00  0.1654E+00  0.1286E+00  0.1007E+00
0.8054E-01  0.6649E-01  0.5814E-01  0.4980E-01  0.4566E-01  0.4152E-01
```

Tab.III. Sample printout from the library **KFKSTOP**. Given are differential ranges of α particles for Ge (Z=32) through Br (Z=35). Data are given in cm and refer to 1 MeV energy steps from 0 to 24 MeV.

```
320740  20040  ALPHA      0-24MeV ;    1MeV-steps                KFKSTOP
  0.3633E-03  0.2907E-03  0.3402E-03  0.3920E-03  0.4418E-03  0.4897E-03
  0.5357E-03  0.5804E-03  0.6238E-03  0.6663E-03  0.7078E-03  0.7486E-03
  0.7887E-03  0.8281E-03  0.8670E-03  0.9053E-03  0.9431E-03  0.9805E-03
  0.1018E-02  0.1054E-02  0.1090E-02  0.1126E-02  0.1162E-02  0.1209E-02
330750  20040  ALPHA      0-24MeV ;    1MeV-steps                KFKSTOP
  0.3069E-03  0.2713E-03  0.3286E-03  0.3839E-03  0.4356E-03  0.4842E-03
  0.5307E-03  0.5753E-03  0.6186E-03  0.6606E-03  0.7017E-03  0.7419E-03
  0.7812E-03  0.8199E-03  0.8580E-03  0.8955E-03  0.9325E-03  0.9690E-03
  0.1005E-02  0.1041E-02  0.1076E-02  0.1111E-02  0.1145E-02  0.1191E-02
340800  20040  ALPHA      0-24MeV ;    1MeV-steps                KFKSTOP
  0.4218E-03  0.3433E-03  0.4089E-03  0.4731E-03  0.5344E-03  0.5929E-03
  0.6492E-03  0.7036E-03  0.7564E-03  0.8078E-03  0.8580E-03  0.9071E-03
  0.9554E-03  0.1003E-02  0.1049E-02  0.1095E-02  0.1140E-02  0.1185E-02
  0.1229E-02  0.1272E-02  0.1315E-02  0.1358E-02  0.1400E-02  0.1456E-02
350790  20040  ALPHA      0-24MeV ;    1MeV-steps                KFKSTOP
  0.6058E-03  0.4595E-03  0.5549E-03  0.6383E-03  0.7165E-03  0.7916E-03
  0.8644E-03  0.9353E-03  0.1005E-02  0.1073E-02  0.1140E-02  0.1205E-02
  0.1270E-02  0.1334E-02  0.1397E-02  0.1460E-02  0.1521E-02  0.1582E-02
  0.1643E-02  0.1703E-02  0.1762E-02  0.1821E-02  0.1879E-02  0.1956E-02
```

A Novel Algorithm for the Treatment of Sequential (x,n) Reactions in Standard Activation Calculations

P. Obložinský[1], S. Cierjacks, S. Ravndal and S. Kelzenberg

Kernforschungszentrum Karlsruhe, Association KfK-Euratom

Institut für Materialforschung

Postfach 3640, 7500 Karlsruhe

Federal Republic of Germany

Abstract

A new algorithm was developed that allows to handle sequential (x,n) reactions in standard activation calculations with the European reference code FISPACT. This possibility was achieved by introducing so-called "pseudo" cross sections for the treatment of two-step sequential (x,n) reactions. The new algorithm avoids any change in the intrinsic structure of the inventory code FISPACT. For suitable updating of the extended input data base, a new computer program, PCROSS, was produced at KfK. Using both the new processing code and the new data libraries KFKSPEC, KFKXN and KFKSTOP, a complete coverage of all sequential (x,n) reactions can now be achieved for single elements as well as for complex alloys. The KfK code PCROSS prepares a common input data file of collapsed "effective" neutron and (x,n) "pseudo" cross sections for FISPACT to run kinematically complete inventory calculations.

1. The Novel Algorithm

We summarize the concept of sequential (x, n) reactions together with the corresponding formalism for inventory calculations [1, 2]. A so-called sequential (x, n) reaction is a two-step process, in which charged particles x are created in a first-step neutron-induced reaction $A(n, x)$ which is followed by the second-step reaction $\bar{A}(x, n)C$ with the target isotope $\bar{A}$ producing the residual nucleus C. Note that $\bar{A}$ is not necessarily identical with A. The charged particle is of the type x, where x is $p, d, t, {}^3He$ and ${}^4He$. We are interested in the number of atoms of the nuclide C that are created via sequential (x, n) reacions. The inventory N_C $(atoms/sec\,cm^3)$ of nuclei C in the two-step process $A(n, x)B \rightarrow \bar{A}(x, n)C$ can be determined by the master equation [3]

---

[1]On leave from the Institute of Physics, SAS, 842 28 Bratislava, Czechoslovakia

$$N_C \quad = \sum_A \sum_{i=1}^{175} \Phi_n(E_{n_i})\sigma_{n,x}(E_{n_i})N_A \Delta E_{n_i}$$

$$\times \sum_{j=1}^{24} f_{n,x}(E_{n_i}, E_{x_j})\Delta E_{x_j} \sum_{k=j}^{1} \sigma_{x,C}(E_{x_k})N_{\bar{A}}\Delta R_x(E_{x_k}) \tag{1}$$

Here, $\Phi_n(E_{n_i})$ $(cm^{-2}s^{-1}u^{-1})$ is the neutron flux in the i-th energy interval of the fusion spectrum, ΔE_{n_i} (u) refers to the neutron lethargy energy bin as also used in the European Activation File, EAF-1 (its other name is REAC-ECN-5) [7], $\sigma_{n,x}(E_{n_i})$ (cm^2) is the production cross section of charged particle x in the neutron energy group E_{n_i}, and N_A (cm^{-3}) is the number of atoms of the initial nuclide A. Next, $f_{n,x}(E_{n_i}, E_{x_j})$ (MeV^{-1}) represents the normalized charged particle spectrum from the reaction $A(n, x)$ given in uniform energy steps of $\Delta E_{x_j} = 1 MeV$ and referring to the i-th incident neutron energy group, the charged particle energy being $E_{x_j} = 0.5, 1.5, \ldots , 23.5$ MeV. Furthermore, $\sigma_{x,C}(E_{x_k})$ (cm^2) stands for the production cross section of the nucleus C via the sequential reaction $\bar{A}(x, n)C$, and $N_{\bar{A}}$ (cm^{-3}) is the number of atoms of the intermediate nuclide $\bar{A}$. Finally, $\Delta R_x(E_{x_k})$ (cm) is the differential thickness of the surrounding material corresponding to 1 MeV of energy loss of charged particles with the starting energy E_{x_k}. A detailed description of the data needed to compute such an inventory N_C is given in [3].

The neutron flux Φ_n together with the initial inventory of stable nuclides A can be considered as a source of a charged particle flux, Φ_x. We assume that this charged particle flux Φ_x does not change considerably during irradiation time what seems to be a very reasonable approximation, except possibly of a few special cases. The charged particle flux $\Phi_x(cm^{-2}s-1)$ can be calculated by using the same physical quantities as in master equation (1)

$$\Phi_x(E_{x_k}) \quad = \sum_A \sum_{i=1}^{175} \Phi_n(E_{n_i})\sigma_{n,x}(E_{n_i})N_A \Delta E_{n_i}$$

$$\times \sum_{j=k}^{24} f_{n,x}(E_{n_i}, E_{x_j})\Delta E_{x_j}\Delta R_x(E_{x_k}) \tag{2}$$

The "pseudo" cross section $\sigma_{x,C}^{pseudo}(cm^2)$ for the sequential reaction $\bar{A}(x, n)C$ is the average cross section for the charged particle reaction per one incident neutron. The "pseudo" cross section can be calculated for any isotope $\bar{A}$ we are interested in and is defined as

$$\sigma_{x,C}^{pseudo} = \frac{1}{\Phi_n^{total}} \sum_{k=1}^{24} \Phi_x(E_{x_k})\sigma_{x,C}(E_{x_k}) \tag{3}$$

By introducing the "pseudo" cross section we can rearrange the master equation (1) as follows

$$N_C = N_{\bar{A}} \Phi_n^{total} \sigma_{x,C}^{pseudo},$$ (4)

which is valid for a projectile x, an initial nucleus $\bar{A}$ and final nucleus C.

An important feature of equation (3) is the formal similarity with 1-step neutron induced reactions (projectile n, initial nucleus A, final nucleus B. Such reactions are treated by the Euroepan reference inventory code FISPACT by using the so called "effective" cross sections, and these are defined as

$$N_B = N_A \Phi_n^{total} \sigma_{n,B}^{eff}$$ (5)

Full inventory calculations should include both the two-step sequential (x, n) reactions as well as one-step neutron induced reactions and requires the knowledge of "pseudo" as well as "effective" cross sections.

2. The KfK Processing Code PCROSS

The basic purpose of the code PROSS [4] is to calculate so-called "pseudo" cross sections for sequential (x, n) reactions. The code is merging these cross sections together with "effective" cross sections for primary neutron-induced reactions into a single file of "collapsed" cross sections which then serves as an input file for the well established FISPACT inventory code [5, 6]. FISPACT calculates activation of material irradiated in a given neutron flux spectrum. The calculation chain using PCROSS is sketched out in Fig.1. It is also described at which level of FISPACT calculations the code PCROSS is intercepting the usual calculation chain.

One of the basic features of the code is that is uses the libraries EAF-1, KFKSPEC, KFKXN, KFKSTOP [3]. It can furthermore handle a variety of tasks: from a simple single element case up to a complicated alloy with all sequential reactions and all intermediary isotopes considered. Finally it should be mentioned that the usage of PCROSS is, at present, reaching a certain limit: FISPACT reaction index is still limited to about 8000 reactions and the PCROSS output file is matched to it although the number of "pseudo" cross sections is considerably larger. In addition, decay data for about 200 radionuclides produced by kinematically allowed sequential (x,n) reactions are still lacking, so that treatment of the corresponding processes is suppressed. A suitable updating of FISPACT to amend for these shortcomings is planned. The full description of the code PCROSS can be found in two KfK Laboratory Reports [4, 8].

Input files
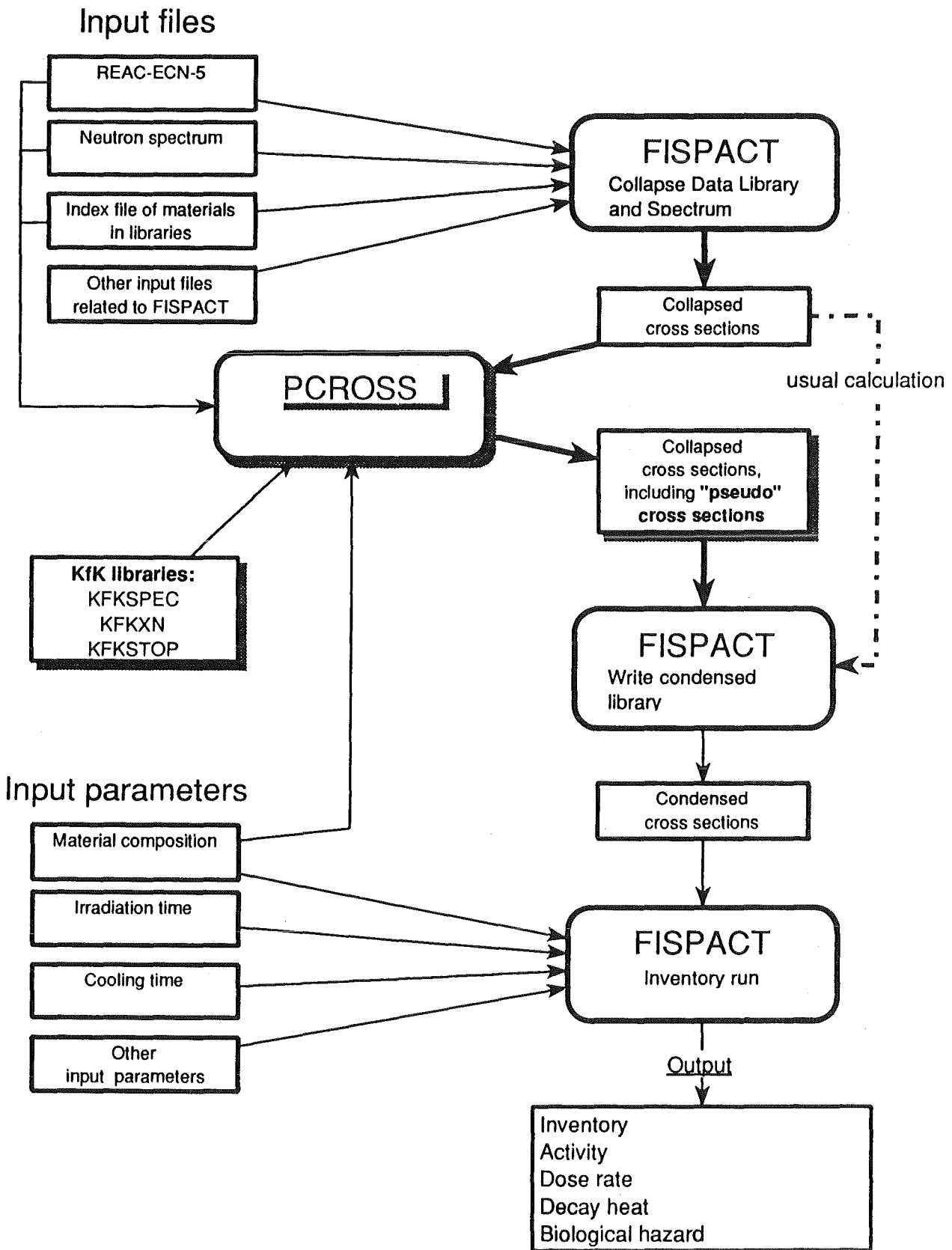
Fig. 1: Flow chart of inventory calculations with PCROSS and FISPACT.

Acknowledgements

The authors would like to thank Prof. K. Ehrlich and Prof. K.-H. Zum Gahr for stimulating discussions and their ongoing support of this work.

This work has been performed in the framework of the Nuclear Fusion Project of the Kernforschungszentrum Karlsruhe and is supported by the European Fusion Technology Program.

References

[1] S. Cierjacks and Y. Hino: *The role of sequential (x,n) reactions on element activation of fusion reactor materials and related nuclear data needs*, Proc. Specialists' Meeting on Neutron Activation Cross Sections for Fission and Fusion Energy Applications, Argonne, 13th - 15th September 1989, see Report NEANDC-259 'U', eds. M. Wagner and H. Vonach (OECD, Paris, 1989) pp. 19-28.

[2] S. Cierjacks and Y. Hino: *The importance of sequential (x,n) reactions on element activation of fusion reactor materials*, J. Nucl. Mater. 170 (1990) 134-139.

[3] S. Cierjacks, P. Obložinský and B. Rzehorz: *Nuclear Data Libraries for the Treatment of Sequential (x,n) Reactions in Fusion Materials Activation Calculations*, Report KfK 4867 (KfK, Karlsruhe, July 1991).

[4] S. Ravndal, P. Obložinský, S. Kelzenberg, S. Cierjacks: *User Manual for the KfK code PCROSS*, Report KfK 4873 (KfK, Karlsruhe, August 1991).

[5] R. A. Forrest, D. A. J. Endacott and A. Khursheed: *FISPACT - Program Manual*, Report AERE-M3655 (AERE, Harwell, 1988).

[6] R. A. Forrest and D. A. J. Endacott: *FISPACT - User Manual*, Report AERE-M3654 (AERE, Harwell, 1988).

[7] H. Gruppelaar, H.A.J. Van der Kamp, J. Kopecký and D. Nierop: *The REAC-ECN-3 data library with neutron activation and transmutation cross-sections for use in fusion reactor technology*, Report ECN-207 (ECN, Petten, 1988).
We use the updated version No.5 due to December 1990 which is identical with the European Activation File EAF-1.

[8] S. Ravndal, P. Obložinský, S. Kelzenberg, S. Cierjacks: *Reference Manual for the KfK code PCROSS*, Report KfK 4956 (KfK, Karlsruhe, December 1991).

Evaluation of 14-MeV Cross Sections for the
Main Isotopes of the Structural Materials Cr, Fe and Ni

by

A. Pavlik, S. Tagesen, H. Vonach and M. Wagner
Institut für Radiumforschung und Kernphysik
der Universität Wien, Austria

Extended Abstract

Cross sections for all important neutron induced reactions and Legendre coefficients describing the elastic scattering angular distributions were evaluated for the interaction of 14 MeV neutrons with ^{52}Cr, ^{56}Fe, ^{58}Ni and ^{60}Ni. For the purpose of this evaluation all measurements and their uncertainties were critically reviewed and the evaluation results derived as weighted average of the accepted - and if necessary - renormalized data.

In a first step, evaluations were performed from the respective experimental results independently for the following cross section types: total, total elastic, non-elastic, total inelastic, total neutron emission, total proton emission, total alpha-particle emission, total deuteron emission, (n,2n), (n,p), (n,np) and (n,α).

In a second step the results were further improved by least-squares adjustment taking into account the constraints that all partial cross sections must add up to total, and all reaction cross sections have to add up to the non-elastic cross section.

The resulting internally consistent cross section sets and their covariance matrices are given as the final evaluation results.

In addition the reduced Legendre coefficients of the P_1, P_2 and P_3 components of the elastic scattering distributions were also evaluated from the measured differential elastic scattering cross sections, as these are the relevant quantities needed in neutron transport calculations.

The results of this evaluation (with few exceptions) lie within the range of predictions of the new evaluated cross section files BROND, EFF-2, ENDF/B-VI and JENDL-3. The uncertainties of the results of these "experimental" evaluati-

ons, however, are on average considerably smaller than the spread of values of the mentioned cross section libraries indicating that considerable improvement of these libraries is possible by the use of the results of this work.

A detailed description of this work has been published as A. Pavlik, S. Tagesen, H. Vonach and M. Wagner, Physics Data Nr. 13-6 (1991), Fachinformationszentrum Karlsruhe.

A short version of this paper will appear in the proceedings of the International Conference on Nuclear Data for Science and Technology, Jülich, FRG, 13-17 May 1991.

Evaluation of the JENDL-3 Fusion File

Satoshi Chiba, Baosheng YU* and Tokio Fukahori

Japan Atomic Energy Research Institute
Tokai-mura, Naka-gun, Ibaraki-ken 319-11, Japan

* China Institute of Atomic Energy
Beijing, People's Republic of China

A special purpose file, "JENDL-3 Fusion File", is being prepared in order to improve the neutron DDX (double differential particle emission cross section) data stored in JENDL-3. This file is compiled in the ENDF-6 format, and adopts the energy-angle correlation of emitted neutrons in MF=6. It also contains composite charged particle DDX for primary knock-on atom (PKA) and KERMA calculations. The DDXs are calculated from systematics. The multistep statistical model calculation was made to provide basic data needed in applying the systematics.

I. Introduction

The DDX data are important in fusion neutronics applications. Recent studies show that there is strong energy-angle correlation in neutron spectra produced by 10-20 MeV neutron induced reactions.

In JENDL-3, the DDX is stored as a product of cross sections, angular distributions and energy distributions given in MF=3, 4 and 5, respectively[1]. This representation, however, cannot take the energy-angle correlation, and has been clamed to be inadequate for fusion neutronics applications from both the differential and integral studies[2]. Furthermore, it has been also pointed out that the DDX of charged particles should be stored in the new version because these data are essential in material damage investigation such as PKA and KERMA calculations[3]. Therefore, it was decided by JENDL compilation group to prepare a special purpose file called JENDL-3 Fusion File to overcome these drawbacks. In the present work, the DDX was calculated by systematics[4,5,6].

II. Basic Strategies

The JENDL-3 Fusion File is being prepared under the following basic strategies. They were determined partly by JENDL compilation group following the recommendations made in Ref. 2, partly from a request of JNDC PKA group[3], and partly by a subjective judgement of the authors:

1. Cross section data should be basically taken from JENDL-3. The data should be modified only if problems are found.
2. DDX of neutron and charged particles should be stored as compactly as possible. Both should be calculated from the systematics.
3. Format should be the ENDF-6 format.
4. Basic quantities required in applying the systematics should be calculated by SINCROS-II code system[7] as descrived in Ref. 6.
5. The data should be given for Al, Si, Ca, Ti, Mn, Fe, Cu, Ni, Co, As, Ge, Zr, Sb, Sn, Nb, Mo, W, Pb and Bi, and their stable isotopes.

III. Method of Evaluation

A schematic diagram of the evaluation method of JENDL-3 Fusion File is shown in **Fig. 1**. The SINCROS-II code system[7] was used to calculate the partial reaction cross sections, particle spectra and their multistep direct fractions (f_{MSD}). The f_{MSD} depends on the incident and outgoing particle energy, and outgoing particle, but was assumed to be independent of reaction channels. The DDXs of neutron and charged particles were calculated and converted to ENDF-6 format in program F15TOB, by using the systematics[4,5]. In applying these systematics, the f_{MSD} and composite particle spectra calculated by EGNASH2 were combined with the data given in JENDL-3. In the present work, DDXs of charged particles are given only as composite forms. Cross sections and neutron spectra given in JENDL-3 were replaced by results of the EGNASH2 calculation when it was necessary to make the agreement between the evaluated and experimental data better. The code CRECTJ5 and CRECTJ6 were used to manupulate data in the ENDF-5 and ENDF-6 format, respectively. The calculated and evaluated DDX were plotted using programs KMDDX, PLDDX and SPLINT89 together with the experimental data. Finally, format and physical consistency of the presently evaluated data were checked by programs supplied from NNDC/BNL.

In the present work, Kumabe's systematics[4] was mainly used for neutron

DDX, while Kalbach's systematics[5] was adopted for DDX of charged particles. Kumabe's systematics is known to reprodeuce the measured neutron DDX very well in the angular range from 30 to 150-deg[6]. However, we found later that this systematics sometimes overestimates the cross sections in the very forward angles (θ < 30-deg.) though experimental data themselves are quite uncertain due to large background caused by source neutrons. Therefore, Kumabe's systematics was slightly modified by changing the A_l parameter as $A_l = 0.0561 + 0.0377 \cdot l(l+1)$, instead of Eq. (5a) of Ref. 4. The new formula gives slightly smaller cross section in the angular region less than 30 degrees, and bigger values at backward region (θ > 150 deg.). This made the agreement with the experimental data slightly better, although still not perfect. We refer this formula as "modified Kumabe's systematics". In the angular region between 40 and 140-degrees, cross sections calculated by Kumabe's and this modified version are almost indistinguishable.

At present, evaluation and compilation of the data for Al, Mn, Fe, Cu, Co and Nb have been finished.

IV. Results and Discussion

In Figs. 2, 3, 4 and 5, DDX of ^{27}Al, ^{59}Co, Fe and Cu at 14 MeV are displayed. The DDXs calculated from the present work, JENDL-3 and ENDF/B-VI are compared with the experimental data measured by Takahashi et al.[8] and Baba et al[9].

As illustrated in Fig. 2, JENDL-3 underestimates the DDX of ^{27}Al at forward angles, while an overestimation is seen at backward angles. "Shape" of the DDX reproduced from JENDL-3 is close to the experimental data at the backward angles. However, the DDX obtained from JENDL-3 understimates the higher energy portion of the (n,n') continuum spectra at forward angles. These trends are common to other JENDL-3 data. On the contrary, a pseudo-level representation was adopted for ^{27}Al in ENDF/B-VI. This representation seems to be better in reproducing the energy-angle correlation observed in measured data. However, the data reproduced from ENDF/B-VI overestimate the DDX at backward angles. The present result slightly overstimates the DDX in the secondary energy region from 7 to 9 MeV at 30-deg.; still, it can reproduce the overall change of the DDX with respect to secondary neutron energy and emission angle very well.

In Fig. 3 it is seen that some of the discrete inelastic scattering

cross sections of ^{59}Co given in JENDL-3 are obviously overestimated. In the present result, the overestimation disappeared because all of the inelastic scattering cross sections were replaced by a new calculation made with SINCROS-II. Furthermore, the data reproduced from JENDL-3 overestimte the higher energy part of (n,n') continuum spectra at middle and backward angles. On the other hand, those obtained from ENDF/B-VI underestimate the same part of DDX at forward angles. The present result can reproduce the measured trends of DDX farily well.

In the DDX of Fe and Cu shown in **Figs.** 4 and 5, difference among the present result, JENDL-3 and ENDF/B-VI is less than the previous two examples. The data of Fe measured by Baba et al. are generally higher than those of Takahashi et al. The present result follows the trend of the data of Takahashi et al. The DDX obtained from JENDL-3 obviously understimate the measured data at forward angles. At backward angles, it is consistent with the data of Baba et al. The same tendency is more or less true in the DDX of Cu shown in **Fig.** 5.

In **Fig.** 6, DDX of Cu at 18 MeV is shown. It was more difficult to reproduce the data at this energy than at 14 MeV by using the systematics. JENDL-3 data are not too bad except at backward angles. ENDF/B-VI generally overestimates the (n,n') spectra. The present result can reproduce the data modestly, in the whole region of secondary neutron energy and emission angle.

The energy spectra of proton and a-particle emitted from ^{93}Nb at 15.0 MeV are shown in **Fig.** 7 and 8, respectively. It is seen that agreement between the measured data[10,11,12] and the present result is remarkable. These charged particle (including photon) spectra are given in the present file as composite forms, i.e., MTs = 202 to 207, by adopting Kalbach's systematics.

V. Summary Remarks

The JENDL-3 Fusion File is being prepared placing an emphasis on the neutron and charged particle DDX. These DDX were calculated by Kumabe's (or modified Kumabe's) and Kalbach's systematics. The multistep direct fractions were calculated by a multistep statistical model. It was shown that JENDL-3 Fusion File can reproduce the measured neutron DDX fairly well.

Acknowledgements

The authors would like to thank Dr. N. Yamamuro for many useful and inevitable comments on the use of the SINCROS-II code system. They also wish to acknowledge valuable discussions with the members of JAERI Nuclear Data Center: Drs. Y. Kikuchi, T. Nakagawa and Y. Nakajima.

References

1) Shibata, K., Nakagawa, T., Asami, T., Fukahori, T., Narita, T., Chiba, S., Mizumoto, M., Hasegawa, A., Kikuchi, Y., Nakajima, Y. and Igarasi, S.: "Japanese Evaluated Nuclear Data Library, Version-3, – JENDL-3 –", JAERI 1319 (1990).

2) Nakajima, Y. and Maekawa, H. (ed.): Proceedings of the Second Specialists' Meeting on Nuclear Data for Fusion Reactors, JAERI-M 91-062 (1991).

3) Kawai, M. and Fukahori, T.: private communication.

4) Kumabe, I., Watanabe, Y., Nohtomi, Y. and Hanada, M.: Nucl. Sci. Eng. 104, 280(1990).

5) Kalbach, C.: Phys. Rev. C37, 2350(1988).

6) Yu, B., Chiba, S. and Fukahori, T.: submitted to J. Nucl. Sci. Technol.

7) Yamamuro, N.: "A NUCLEAR CROSS SECTION CALCULATION SYSTEM WITH SIMPLIFIED INPUT-FORMAT VERSEION II (SINCROS-II)", JAERI-M 90-006 (1990).

8) e.g., Takahashi, A., Ichimura, E., Sasaki, Y. and Sugimoto, H.: Jour. Nucl. Sci. Tech. , 25, 215(1988); Takahashi, A., Ichimura, E., Sasaki, Y. and Sugimoto, H.: "DOUBLE AND SINGLE DIFFERENTIAL NEUTRON EMISSION CROSS SECTIONS AT 14.1 MEV", OKTAVIAN Report A-87-03 (1987).

9) e.g., Baba, M., Ishikawa, M., Yabuta, N., Kikuchi, T., Wakabayashi, H. and Hirakawa, N.: "DOUBLE-DIFFERENTIAL NEUTRON EMISSION SPECTRA FOR Al, Ti, V, Cr, Mn, Fe, Ni, Cu and Zr", Proc. of Int. Conf. on Nucl. Data for Sci. and Tech., Mito, Japan, May 30–June 3, 1988, Igarasi, S. (Ed.), Saikon Pub. (1988).

10) Fischer, R., Uhl, M. and Vonach, H.: Phys. Rev. C37, 578(1988).

11) Traxler, G., Chalupka, A., Fischer, R., Strohmaier, B., Uhl, M. and Vonach, H.: Nucl. Sci. Eng. 90, 174(1985).

12) Grimes, S., Haight, R., and Anderson, J.: Phys. Rev. C17, 508(1978).
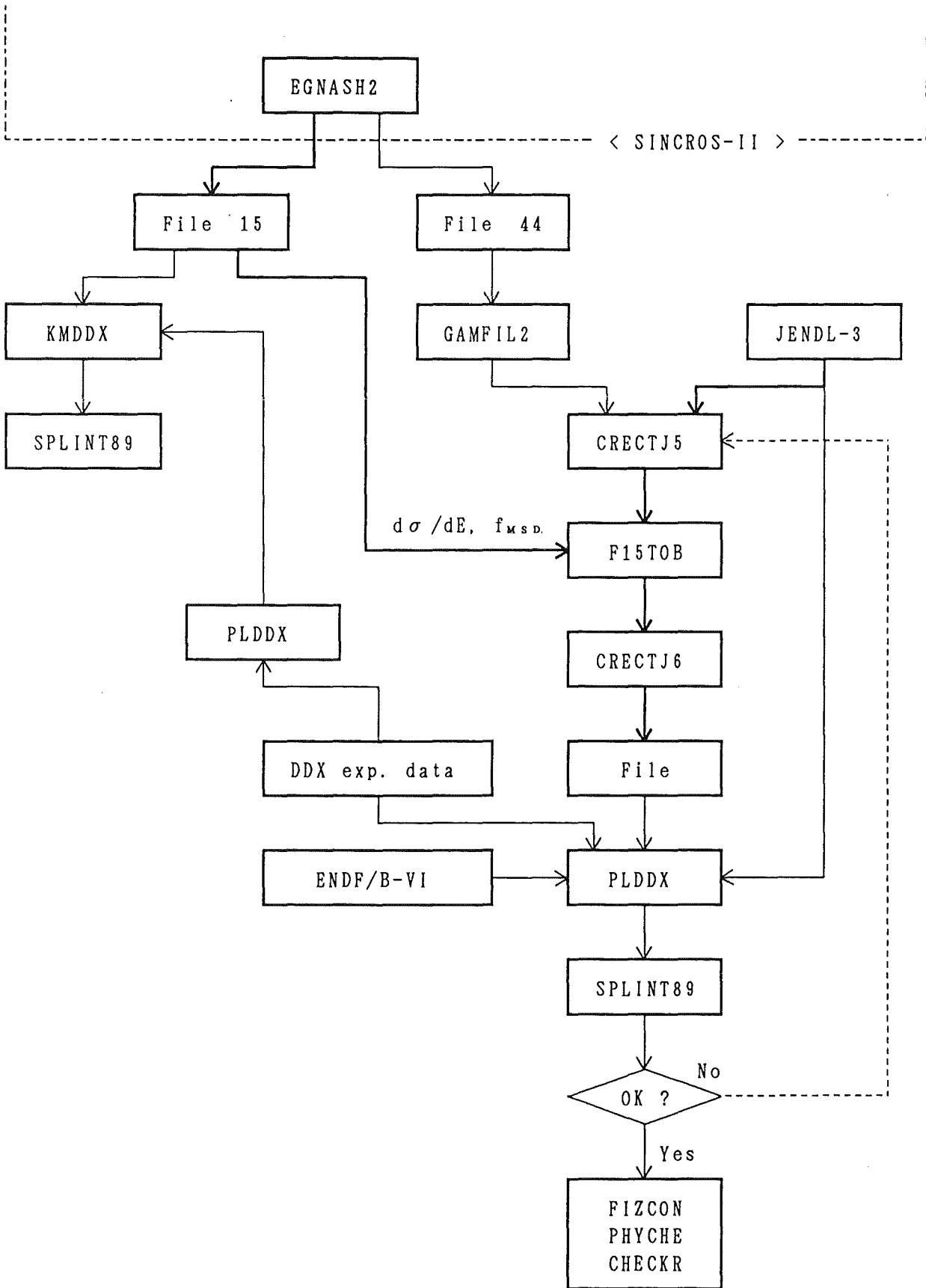
Fig. 1   Flowchart of compilation of JENDL-3 Fusion File

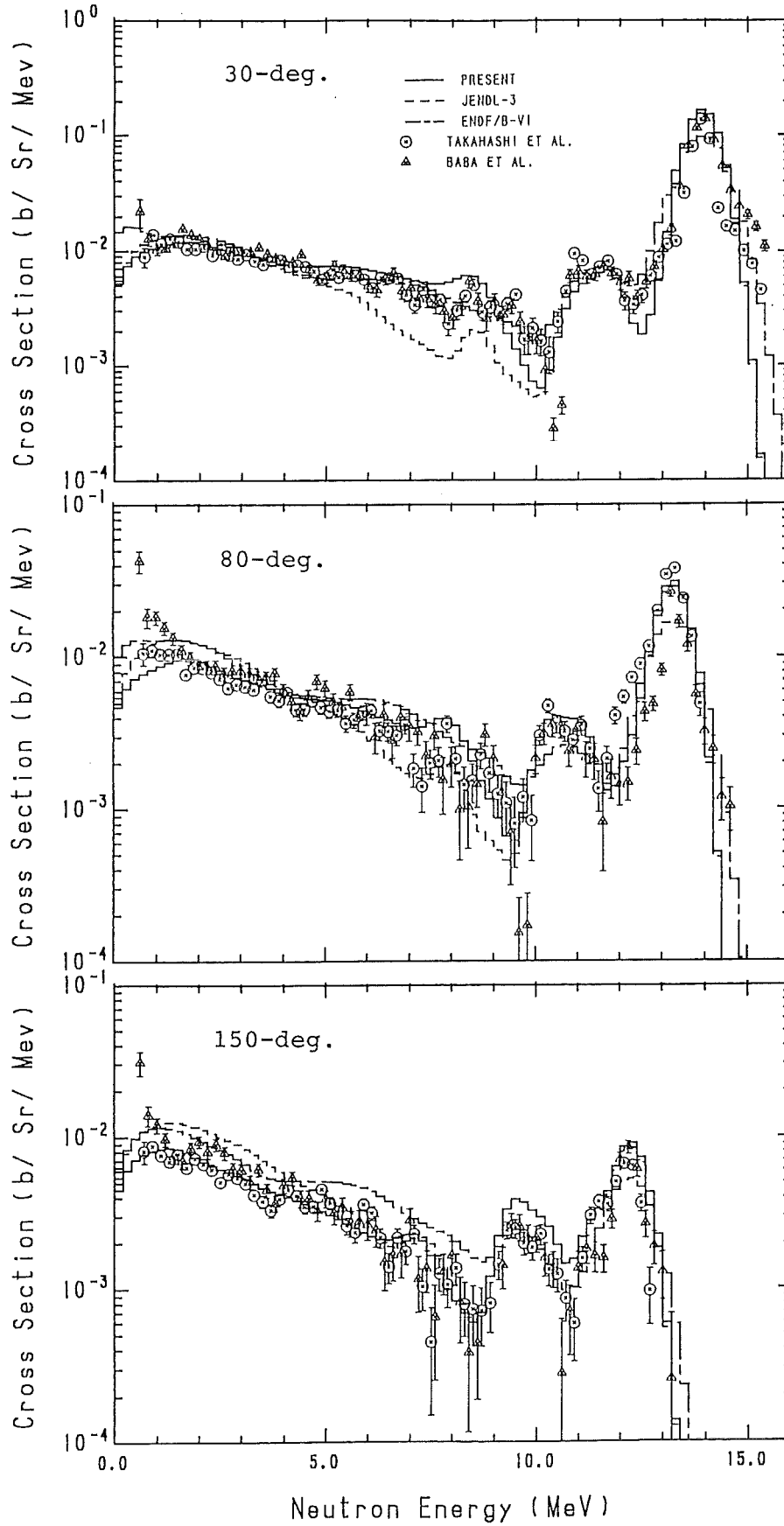Fig. 2   DDX of ^{27}Al at 14.1 MeV

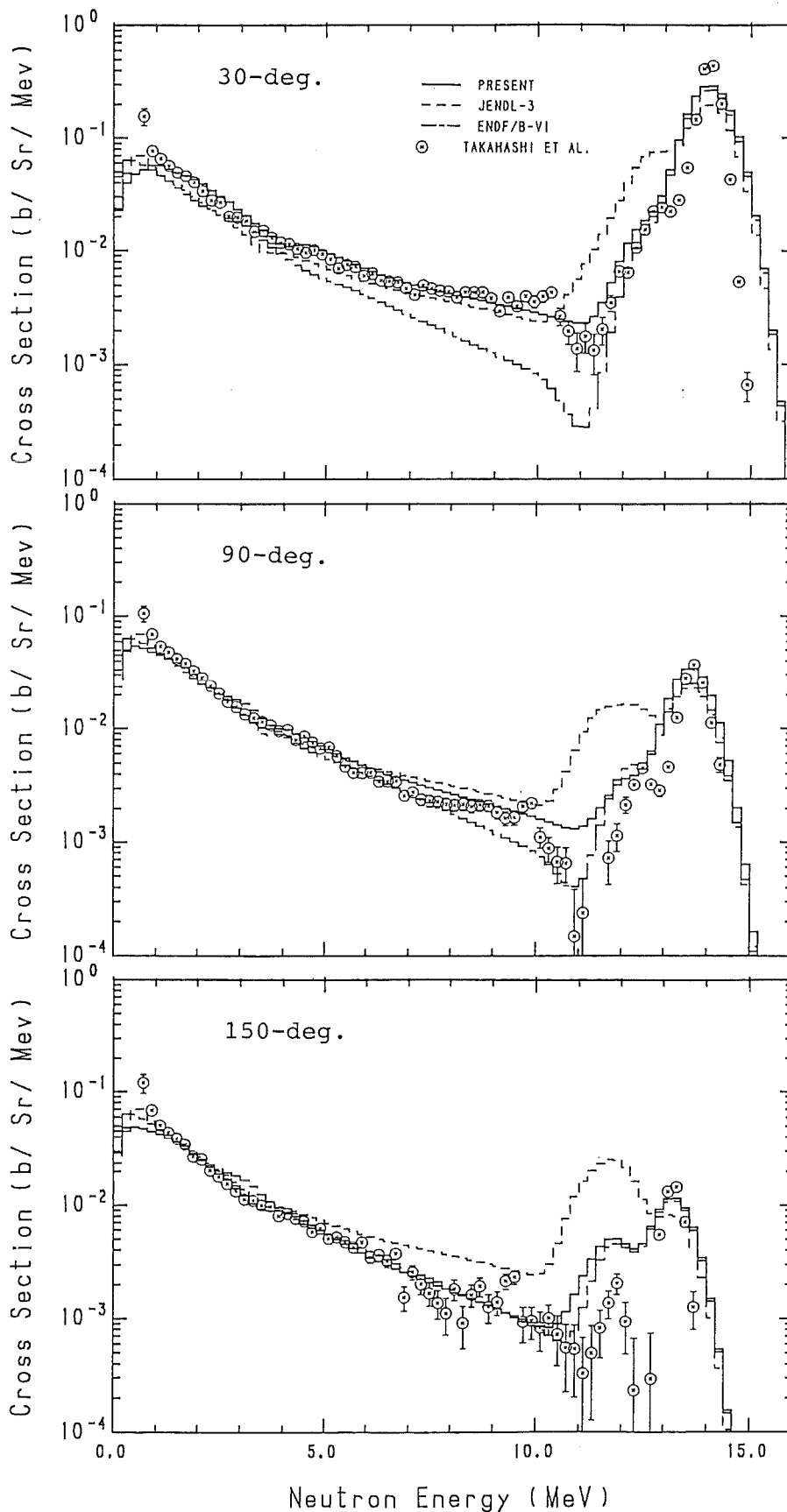Fig. 3 DDX of ^{59}Co at 14.1 MeV
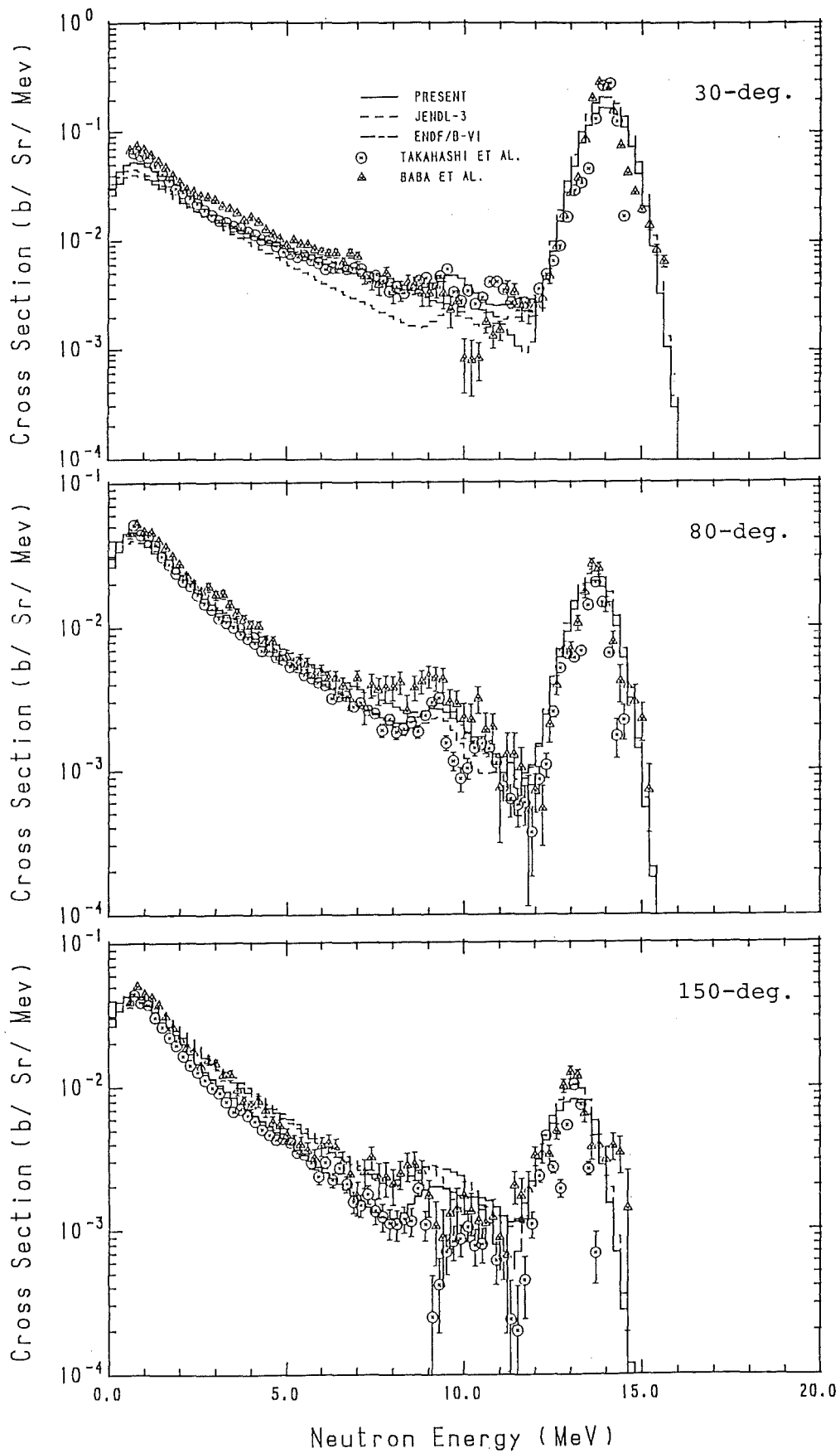
Fig. 4   DDX of Fe at 14.1 MeV
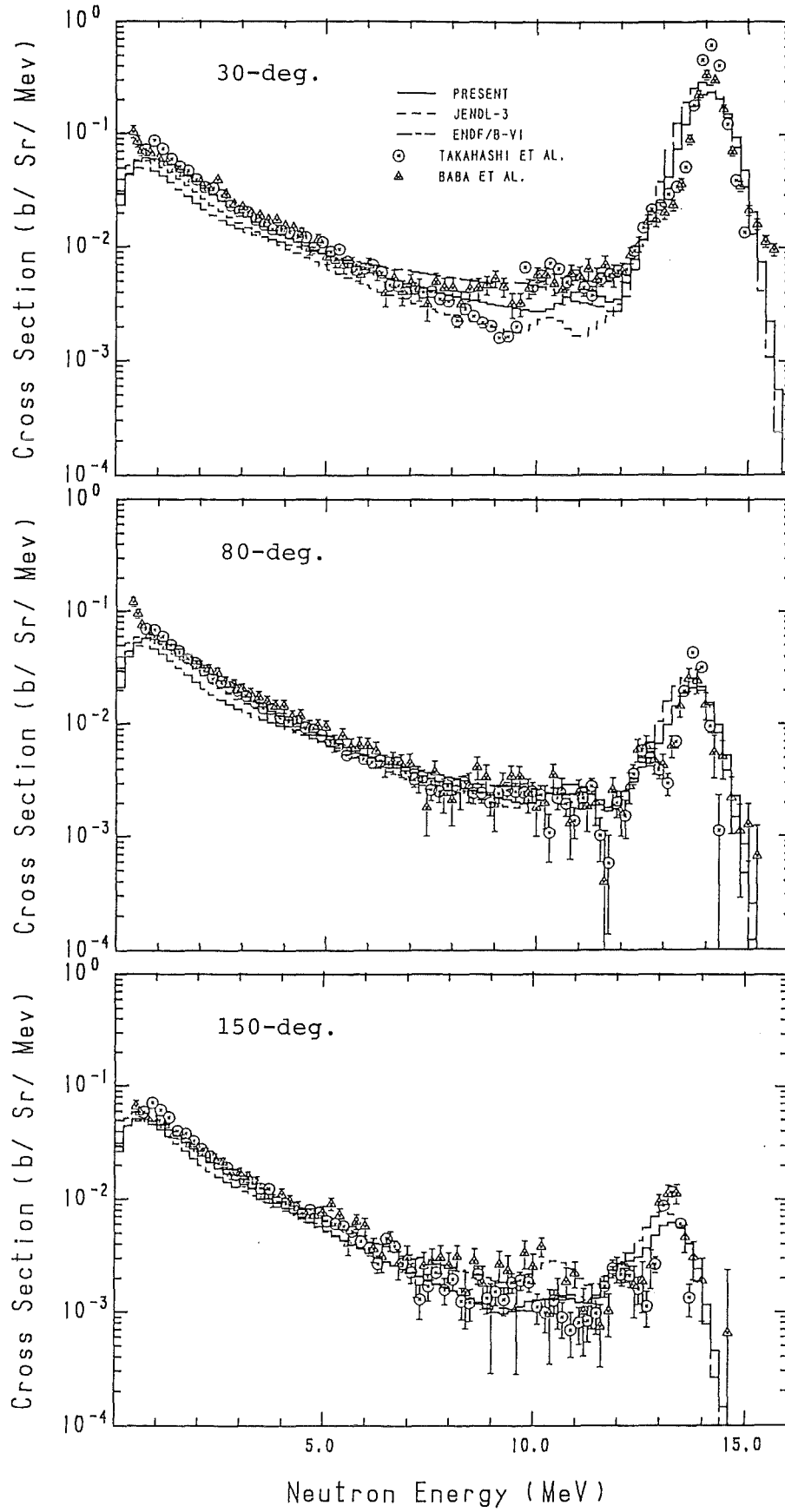
Fig. 5 DDX of Cu at 14.1 MeV
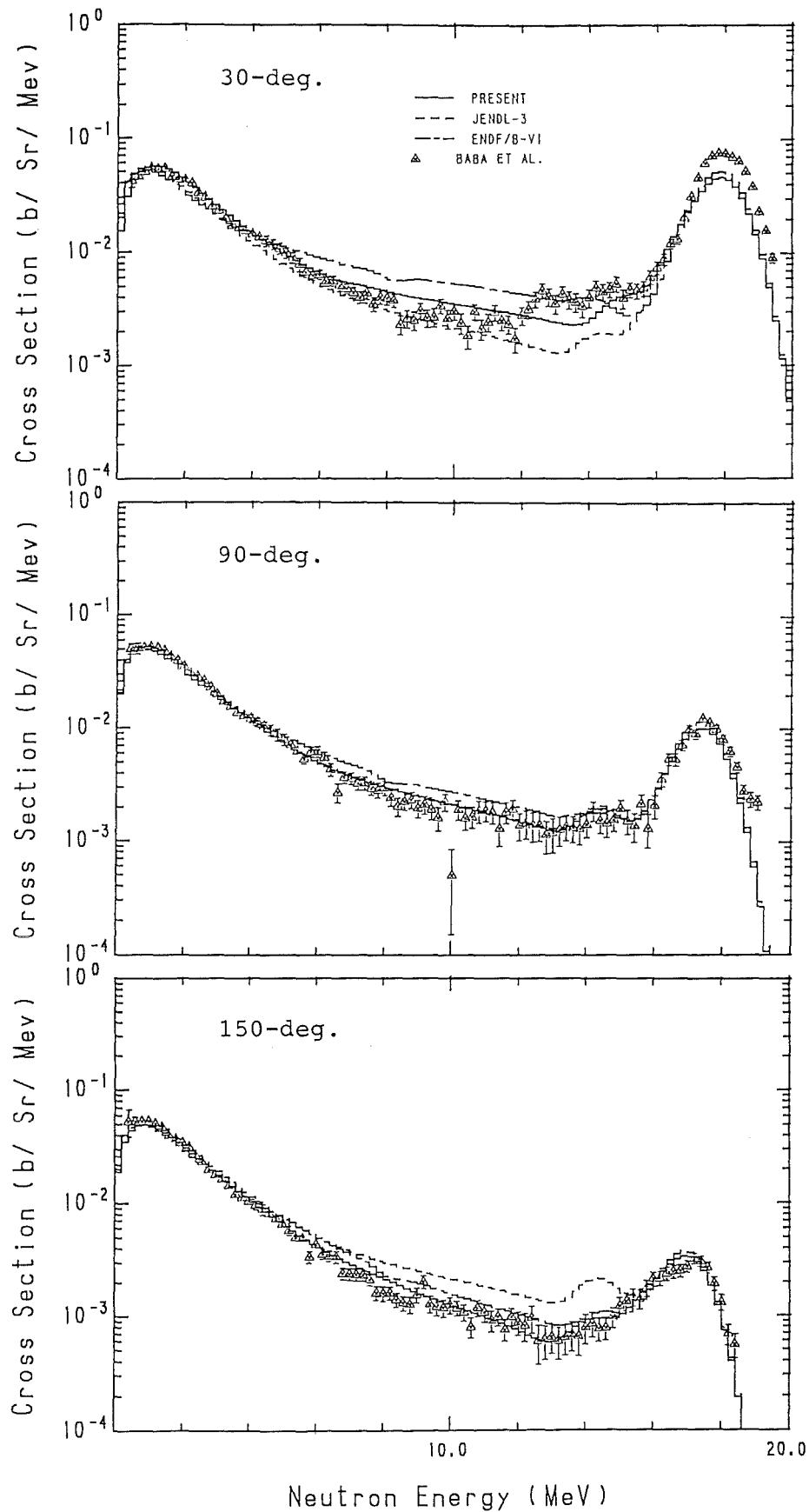
Fig. 6 DDX of Cu at 18.0 MeV
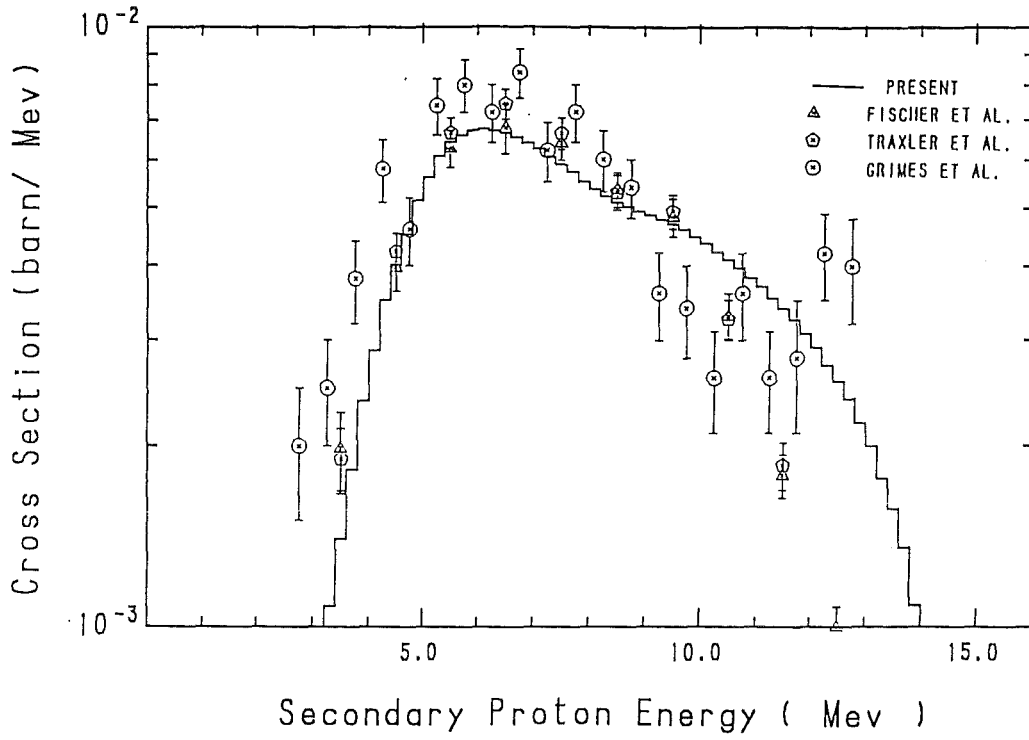
Fig. 7 EDX of ^{93}Nb(n,xp) reaction at 15.0 MeV
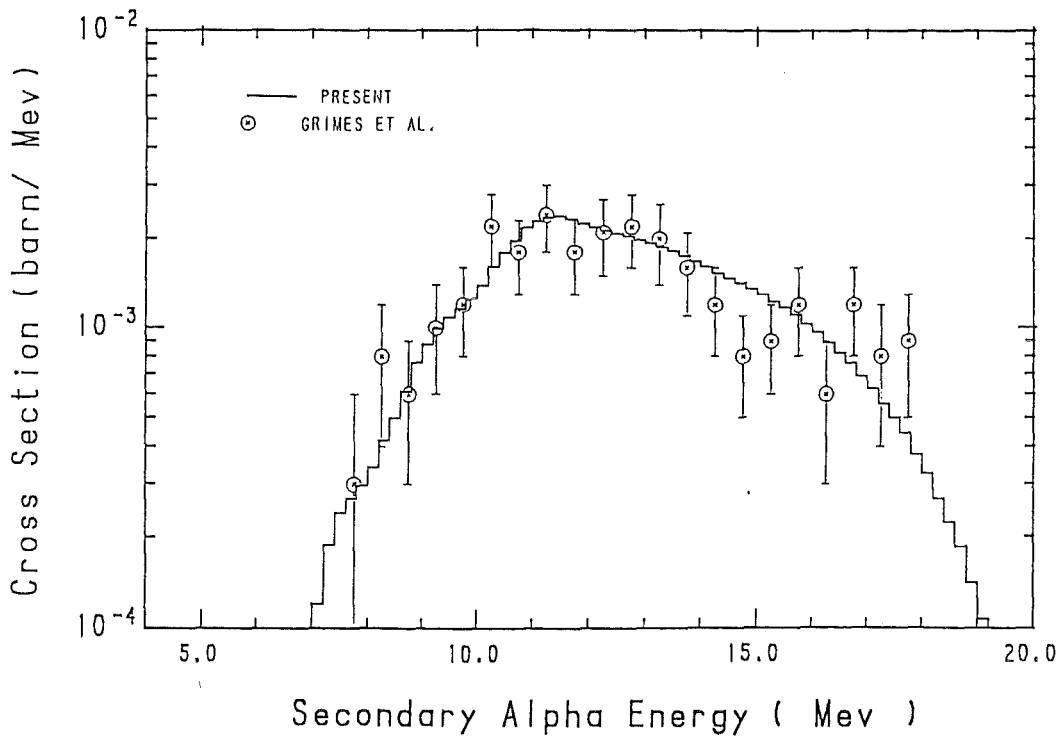
Fig. 8 EDX of ^{93}Nb(n,xα) reaction at 15.0 MeV

Status of the International Fusion Evaluated Nuclear Data Library (FENDL)

by
D. W. Muir, S. Ganesan and A. B. Pashchenko
(presented by J. J. Schmidt)
International Atomic Energy Agency
Nuclear Data Section,
Vienna, Austria

Extended Abstract

The IAEA Nuclear Data Section, in co-operation with several national nuclear data centres and research groups, is creating an internationally available Fusion Evaluated Nuclear Data Library (FENDL), which will serve as a comprehensive source of processed and tested nuclear data lailored to the requirements of the Engineering Development Activities (EDA) of the International Thermonuclear Experimental Reactor (ITER) Project and other fusion-reactor development projects. The first version of this library, FENDL-1, intended to be finalized and distributed around the middle of 1992, will consist of the following sublibraries:

- Coupled 175-group neutron - 42-group gamma cross section sets (VITAMIN-J structure) processed with the NJOY system for neutron and gamma-ray transport calculations for 62 elements and isotopes of primary fusion interest.

- 256 of the most important neutron activation cross sections for the estimation of radiation hazards.

- Charged particle nuclear reaction cross sections for the D-T plasma constituents p, d, T, ^{3}He and ^{4}He.

- Fusion-relevant neutron dosimetry cross sections.

For the multigroup cross section library, ENDF/B-VI files were selected by a series of IAEA advisory groups as major source of basic evaluated data, supplemented by JENDL-3 and BROND files. Pointwise cross section data have been re-

constructed from resolved resonance parameters and linearized with thinning tolerances of 0.1%. Self-shielded cross sections are being calculated for 300, 900 and 1500 Kelvin and dilution factors of 10^0, 10^1, 10^2, 10^3, 10^4 and 10^{10} barns. Thermal scattering-law data are being included for Be in B_1e metal, C in graphite and H in water. Following a request from ITER for neutron and gamma shielding calculations, the following specific elements were added: Na, Mg, P, S, Cl, K, Ca and Ta.

For the second version of FENDL, FENDL-2, extensive benchmark-testing of FENDL-1 data and intercomparisons with newly available data files are planned with the aim to improve the physical reliability of FENDL-1 data for neutron-gamma transport and activation studies. Also, in order to allow the users to carry out realistic activation calculations the activation cross section sublibrary will be extended by several thousand additional reactions in early 1992, so as to contain all targets with half lives greater than 10 days and all reactions energetically possible below 20 MeV.

For further details of the current FENDL project activities the reader is referred to references [1, 2].

References

[1]   D.W. Muir, S. Ganesan and A.B. Pashchenko; FENDL: a reference nuclear data library for fusion applications. Proceedings of the International Conference on Nuclear Data for Science and Technology, Jülich, Germany, 13-17 May 1991; to be published.

[2]   D. W. Muir, S. Ganesan and A.B. Pashchenko; Status, plans and international co-operation in the preparation of the International Fusion Evaluated Nuclear Data Library (FENDL), Proceedings of the International Workshop on Fusion Neutronics, Karlsruhe, Germany, 7 June 1991, JAERI-memo 03-305, September 1991, p-205f.].

Short Status Report on EFF and EAF Projects

H. Gruppelaar, Netherlands Energy Research Foundation
ECN, Petten, The Netherlands

Abstract

A short status report is given on the European Fusion File (EFF) and European Activation File (EAF) projects. The EFF-2 data file is nearly finished and processing and benchmarking is underway. There is also a second version (EAF-2) of the activation file which is a very extensive and complete data base. Recently follow-up programmes have been defined for the introduction of EFF-2 to the user community after benchmarking and for further improvement of the quality of the two data files. There is extensive international cooperation, which is becoming increasingly important to solve remaining difficult problems.

1. Introduction

The European Fusion File project (EFF) and the associated European Activation File Project (EAF) are sponsored by the European Community's Fusion Technology Programme, Tasks NSN1 and LAM-2, respectively. The first programme is directed to the short-term needs of the NET team which designs the Next European Torus, whereas the second programme is directed to long-term needs in the development of a Fusion Demonstration Reactor, in particular in connection with the study of low-activation materials. Many European laboratories participate in these projects. Further support is obtained from specific NET contracts on high-priority items. The file management is performed at ECN, Petten.

The programme of the EFF-project is at the end of its second phase, after the successful completion of the EFF-1 data file. The second phase programme ends this year and a third phase has been defined for the period 1992 to 1994. The emphasis of the first phase was on the improvement of the tritium breeding and neutron multiplication cross-sections, whereas the second phase emphasizes the improvement of a shielding data base. In practice the EFF-1 and EFF-2 projects aim to supplement the JEF-1 and JEF-2 data files, respectively, with high-energy data relevant for fusion applications. Therefore, the EFF and JEF projects are closely related (the Joint Evaluated File is a project of NEA Data Bank Member Countries and is primarily meant for fission reactor applications). The EAF programme started in 1989 and will continue for a second three-years period.

The present report is a short status report on the EFF and EAF projects. More extended reviews have recently been presented at a conference [1,2].

2. Status of the EFF-2 project

The EFF-2 project has been completed with respect to the development of the point-wise data file. The evaluation for the major structural materials has resulted in important new European evaluations for Li-7, Be-9, Al, Si, Fe, Cr, Ni and Pb [1,3-7]. For about 40 additional materials data have been selected from recent evaluations and the other materials should be supplemented from the JEF-2 data file. Efforts have been made to supply the structural materials with uncertainty and covariance estimates [7]] and to process the data in order to perform benchmark testing. Important applications have been studied (still with EFF-1 data) to implement the data for advanced applications, taking into account rigorous methods to deal with anisotropy in fusion neutronics calculations [8] and to predict uncertainties in quantities like the nuclear heating in the superconducting coils [9,10]. In this analysis also effects of uncertainties in angular distributions and in energy distributions were considered. Shielding benchmarks were analysed to further assess the validity of EFF-1 in NET reactor shielding calculations.

3. Follow-up programme EFF-2

During the past three years a very large effort was made to validate and test the EFF-1 data file and to introduce it to the users. Now this file is succesfully used by almost all European partners. The last phase of the project, defined from 1992 to 1994 will be mainly directed to test, validate and benchmark EFF-2 and to make some updates, revisions and extensions on: covariance data, double differential data at energies below 14 MeV, photon-production data and nuclear data for reliable heating and damage calculations. The highest priority of the follow-up programme is to allow for a fast introduction of EFF-2 as it is today by providing derived files: multigroup libraries, response libraries, covariance files and Monte Carlo libraries. Meanwhile, processing problems for the calculation of a multigroup transport library have been solved. Remaining problems still exists for kerma calculations [11], the calculation of covariance working libraries and the generation of data files for Monte Carlo calculations. Although the first priority is to solve these problems, there are also some remaining difficulties in the data, indicated by benchmarks or evident from inspection of the nuclear data. One of such problems is related to the description of self-shielding of Fe in the unresolved resonance range, at relatively high energies.

4. EAF project

The EAF project originated from earlier work at Petten, Harwell and Ispra to create a complete data file and a general inventory code for activation and transmutation calculations for fusion reactor studies in Europe [2,12]. The project was defined by three partners: Petten, Harwell and KfK, with as main tasks the development of a point-wise data file (EAF) [2], the improvement of an inventory code with associated working libraries (FISPACT) [12] and the study of "sequential" reactions [13], respectively. The last-mentioned topic was added, because charged particles emitted by neutron-induced reactions could lead to a second reaction. The present status of the point-wise data file is that there is an updated EAF-2 file which has been extended with all (n,γ) cross-sections necessary for all targets [14,15]. All stable and unstable targets (including isomers)

with half lifes larger than 0.5 days have been included. Isomer production
is included for all known isomers. Current research is aimed to further
improve the quality of the library, to add actinide targets and to create
an uncertainty data file. The complete system of codes and libraries is
known as the European Activation System EASY. Studies with EASY, that is
still further developed to include new features, are underway to better
identify the needs for high-quality re-evaluations and to assess un-
certainties in predictions of long-lived activations.

4. International aspects

In the past the EFF-1 and JEF-1 data files were restricted to the users in
Europe. However, already for EFF-1 some international collaboration was
established: (1) the exchange of Li-7 and Be-9 data files from Los Alamos
against cooperation in updating Li-7 (in the framework of EFF-2), (2) the
release of the Pb data file for an international benchmarking project by
IAEA and (3) cooperation with IAEA's FENDL project, e.g. by releasing 256
materials from EAF-1. At present there are no restrictions on the use of
the JEF, EFF and EAF libraries.

Recently, there is enhanced international collaboration organised by NEA
(OECD) on evaluation coordination, the so-called Evaluation Coordination
Working Group of the NEANDC/NEACRP Committee's [16]. This coordination
activity is directed to solve difficult evaluation problems by means of
task forces, rather than to create a new "super" file. The reasoning is
that the present "regional" data files are internaly consistent, which
makes it very difficult to compose a data file consisting of "selected"
data. However, it is expected that each data file will benefit from this
cooperation and that the various data files will converge to each other.
In this cooperation the EFF and JEF projects act closely together. It has
already been decided to release EFF-2 data files within the OECD area and
also the restrictions for further distributions have been removed, in
particular to serve the ITER project. The international (NEANDC/NEACRP)
collaboration on the covariance data for Fe, the one on intercomparison of
Fe, Cr and Ni data [17] and the one on processing problems are quite be-
neficial for the EFF-2 project. The EAF strategy is very much similar.
Both projects contribute to and benifit from IAEA's FENDL project.

There are also plans for a joint JEF/EFF data file (JEFF) for the near
future. In view of the close cooperation between the EFF and JEF projects
their half-yearly progress meetings have been combined.

References

[1] C. Nordborg and H. Gruppelaar, Status of the JEF and EFF
     projects, Invited poster Int. Conf. Nuclear Data for
     Science and Technology, Juelich, 13-17 May, 1991
[2] J. Kopecky, H. Gruppelaar, and R. Forrest, European
     Activation File for Fusion, Invited poster Int. Conf.
     Nuclear Data for Science and Technology, Juelich, 13-17
     May, 1991
[3] G.M. Field, T.D. Beynon and H. Gruppelaar, Modelling of
     double differential neutron emission cross-sections for
     Li-7, to be published in Progress in Nuclear Energy (1991).
[4] G.M. Field, T.D. Beynon and H. Gruppelaar, Modelling in-

elastic emission cross-sections for ^{9}Be(n,2n), Contr. Int.
Conf. Nuclear data for Science and Technology, Juelich,
13-17 May, 1991

[6] M. Uhl, H. Gruppelaar, H.A.J. van der Kamp, J. Kopecky
and D. Nierop, The EFF-2 evaluation for the reaction
systems n+52-Cr, 56-Fe, 58-Ni and 60-Ni, Contr. Int.
Conf. Nuclear Data for Science and Technology, Juelich,
13-17 May, 1991

[7] S. Tagesen and H. Vonach, Uncertainty estimates for the
EFF-files for ^{52}Cr, ^{56}Fe, ^{58}Ni and ^{60}Ni, Int. Conf.
on Nuclear Data for Science and Technology, Juelich,

[8] U. Fischer, A. Schwenk-Ferrero and E. Wiegner, Analysis of
14 MeV neutron transport in Beryllium, Contr. to the 2nd
ISFNT, Karlsruhe, June 3-7, 1991.

[9] A. Hogenbirk, Energy self-shielding and SED/SAD
effects in sensitivity calculations of a NET shielding
blanket, Paper contr. to 2nd ISFNT, Karlsruhe, June 3-7,
1991, ECN-RX-91-038.

[10] T. Parish and A. Santamarina, Sensitivity and uncertainty
analysis of the NET magnet neutronic design parameters
to uncertainties in cross section data, paper presented
at the Topical Conf. on Nuclear Data for Fusion Reactor
Technology, NEANDC meeting, Karlsruhe, October 22, 1991

[11] M. Konieczny, N.P. Taylor and T.D. Beynon, Methodology for
the generation of neutron kerma factors from EFF-2
Lithium-7 data, Contr. Int. Conf. on Nuclear Data for Scien-
ce and Technology, Juelich, 13-17 May 1991.

[12] R.A. Forrest and G.J. Butterworth, Objectives for low acti-
vation materials and the data implications, Invited paper
Int. Conf. on Nuclear Data for Science and Technology, Juelich,
13-17 May, 1991.

[13] S. Cierjaks, P. Oblozinsky and B. Rzehorz, Nuclear data libraries
for the treatment of sequential (x,n) reactions in fusion
materials activation calculations, KfK-4867 (1991).

[14] J. Kopecky, H.A.J. van der Kamp, H. Gruppelaar and D. Nierop,
European Activation File EAF-2 with neutron activation and
transmutation cross-sections, ECN-C--91-..., in press (1991)

[15] J. Kopecky and D. Nierop, Contents of EAF-2 - A supplement to
the EAF-2 data file, ECN-I--91-053 (1991).

[16] C.L. Dunford, Y. Kikuchi and M. Salvatores, Cooperation in
nuclear data evaluation among the OECD countries, Contr.
Int. Conf. on Nuclear Data for Science and Technology,
Juelich, 13-17 May, 1991.

[17] C.Y. Fu et al., International Evaluation Coordination Task
1: Intercomparison of evaluated files for Cr-52, Fe-56,
and Ni-58, Contr. Int. Conf. on Nuclear Data for Science
and Technology, Juelich, 13-17 May 1991.

Potential Improvements to ENDF/B-VI for Fusion Data

D. C. Larson and C. Y. Fu
Oak Ridge National Laboratory
Oak Ridge, TN 37831-6356

ABSTRACT

While ENDF/B-VI is a significant improvement over previous versions for fusion reactor design calculations, several areas have not received attention and may need improvement. In addition, broadening of the contents of the evaluations to contain information not easily derived at present should be considered.

INTRODUCTION

ENDF/B-VI, released in 1989, was aimed at providing significant improvements in nuclear data needed for fusion energy design studies. Much new experimental data was available since the release of ENDF/B-V in 1979, and developments in nuclear theory were incorporated in nuclear model codes used in the new evaluation work. Formats were improved, with the development of File 6 for energy-angle correlated data and the use of the Reich-Moore resonance parameter formalism for the structural materials. Energy balance was emphasized, which removed a general problem discovered after ENDF/B-V was released. For many of the structural materials, sufficient information is now given (for the first time) to allow direct calculation of KERMA from data given in the evaluation. Isotopic evaluations are given for most of the structural materials, thus eliminating average-Q-value problems (at the cost of increased processing time). Uncertainty files are provided for cross sections for most materials.

However, even with all these improvements, there are several general areas which remain weak. Some of them require new experimental data for improvement, while others relate to improved methods and techniques in model calculations and yet others may require format development. The rest of this paper outlines some of these general areas, but by no means is meant to be inclusive. Many of these concerns also exist for other evaluated libraries, such as JEF/EFF and JENDL, and may be viewed as suggestions for future NEACRP/NEANDC Evaluation Cooperation Working Group activities.

CAPTURE GAMMA-RAY SPECTRA

One of the results of the NEANDC Task Force on the ^{56}Fe 1.15 keV Resonance was the experimental observation of significant differences in the hardness of the capture gamma-ray spectrum from resonance to resonance [PE89]. There is no apparent correlation of spectrum hardness with the spin, parity, or energy of the capture resonance. This latter observation makes modeling

predictions of the spectra difficult and requires further work in this area. Thus, experimental data are required to meet this need.

At present, capture spectra data are generally available only from thermal energy neutrons and, occasionally, for a few low energy resonances. Typical evaluation procedures include using the thermal neutron capture spectrum for all energies up to 20 MeV, averaging the capture spectra from low energy resonances and using it, or even using the capture spectrum from a nearby material in the case of no measured data. Theory at present is inadequate to provide reliable results.

Experimentally, capture gamma-ray spectra can be measured efficiently in the resonance region with a white source. A germanium detector can be used where high gamma-ray energy-resolution is desired; however, the relatively low efficiency of these detectors is a drawback. Low-resolution detectors, such as C_6D_6 or barium fluoride, have good efficiency for detecting the high-energy primary gamma rays from capture, but the data must be unfolded and an appropriate response function must be generated. For many of the structural materials capture spectra for resonances with a large capture width would suffice, at least initially. It would also be useful to measure angular distribution effects in the capture spectra, particularly for model code improvements.

The impact of this improvement should be evident when calculating heating in the superconducting coils, since much of the heating comes from capture gamma rays.

GAMMA-RAY ANGULAR DISTRIBUTIONS

Much attention has been given to evaluating angular distributions for outgoing neutrons. Measured angular distributions are often used for elastic- and inelastic-scattering reactions. When model calculations are used, angular distributions for neutrons from compound, precompound, and direct processes are weighted according to their contribution to a given reaction, and the resulting angular distribution is often represented in terms of Legendre coefficients. File 6 was developed particularly for this capability. For some materials, such as silicon, where angular distributions of outgoing charged particles can be important, angular distribution information is included for reactions to discrete levels with the largest cross sections.

However, for most structural materials, gamma-ray angular distributions are given as isotropic, even though experimental information often exists to the contrary. This situation is probably related both to lack of demand by the users for such information, and the observation that cross-section information is often not given for discrete gamma rays but rather for binned groups of discrete gamma-ray energies. Thus, incorporation of such information would require a restructuring of the gamma-ray portion of the evaluation. Angular distribution information for the discrete gamma rays would be stored directly in File 14, but File 16 (corresponding to File 6 for particle emission) would be used to represent angular distributions for gamma rays emitted from the continuum. File 16 formats are not given in the ENDF/B-VI formats manual but should be a straightforward generalization of File 6 formats.

There have been recent requests in the U.S. to improve the information for gamma ray angular distributions for the 4.44-MeV gamma ray from the $^{12}C(n,n'\gamma)$ reaction. Since gamma rays can be penetrating radiation, overlooking such information for high-energy gamma rays produced with a large cross section may lead to incorrect conclusions by the users, particularly in shielding and heating calculations. A sensitivity analysis for some carefully chosen applied problem in fusion neutronics where at least rudimentary angular distribution information is available in the files should suggest if this area needs further work.

CROSS SECTIONS FOR THE (n,α) REACTION

One of the findings of Subgroup 1 of the NEACRP/NEANDC Evaluation Cooperation Working Group was a significant difference in the evaluated (n,α) cross section for the structural materials among ENDF/B-VI, JEF-II/EFF-II and JENDL-III [FU91]. The problem is particularly evident at energies where there were no experimental data and model codes were used for the results. Since this is an important cross section for radiation damage concerns, an effort is needed to better understand the source of these discrepancies. Initial indications are that the level densities used in the model calculations may be at fault, particularly in the (n,n') channel which is in direct competition with the (n,α) reaction at energies around 9 MeV, where the discrepancy is largest. Alpha-particle preformation factors may also contribute to the problem. Further testing will verify these hypotheses, but this example emphasizes the point that for energies where little or no data exist for any reaction on a nucleus, use of model calculations can lead to unexpected large uncertainties in the cross sections.

Results from this subgroup should be used to update the (n,α) cross sections for ^{58}Ni, and materials other than those reviewed by Subgroup 1 for which the (n,α) reaction is important should be reviewed.

NEUTRON EMISSION CROSS SECTIONS AT ENERGIES OTHER THAN 14 MEV

Several facilities, particularly those in Japan [TA83] and Eastern Europe [HE75], have provided a significant amount of neutron emission data for incident energies around 14 MeV. Often, angular distributions of the emitted neutrons are also measured, providing useful information for benchmarking of the precompound component of nuclear model codes. Such data are now available for most of the important structural materials.

During our evaluation of the Cu isotopes for ENDF/B-VI, available data for open reaction channels around 14 MeV, including neutron emission, were utilized in the TNG model calculations. A simultaneous reproduction of data for different reactions was achieved, including a good reproduction of the (n,xn) spectral data. When the TNG model calculations were done at 9 MeV, and compared with (n,xn) data from ORELA [MO79], differences were found. Small changes in level densities significantly improved the 9-MeV comparison, while retaining the quality of the 14-MeV calculation, by adjusting the precompound strength. With the precompound component rapidly rising below 14 MeV, the region from 8-15 MeV can be difficult to model correctly without experimental data guidance.

Neutron emission spectra for incident neutrons from 7-15 MeV at preferably more than one angle are needed to improve evaluations of the structural materials in ENDF/B-VI.

CHARGED-PARTICLE EMISSION CROSS SECTIONS FROM 7-15 MEV

Charged-particle (CP) emission spectra are important for radiation damage studies, as well as allowing direct calculations of KERMA. CP spectral data are less abundant than neutron emission data, with the bulk of the results measured near 14 MeV from the LLNL facility in the 1970s [GR79]. In general, integrating these spectral data provide good agreement with activation measurements, where such comparisons are possible.

Recently, (n,xp) and (n,xα) emission data for incident neutron energies of 8.0, 9.5 and 11.0 MeV have been published by Saraf et al. [SA91] from Ohio University for targets of ^{54,56}Fe. While

the published figures are in error, consultation with the authors provided the corrected results. The integrals of the data are not in consistent agreement with ENDF/B-VI (or other experimental data), but the spectral shapes are useful for benchmarking the TNG nuclear model code results used for the evaluations. A paper detailing these comparisons is in preparation.

CP emission spectra at energies from 7-15 MeV are useful for benchmarking nuclear model calculations. Angular distribution effects are not as important as for neutron emission spectra, so measurements at one or two angles should suffice to determine any anisotropic effects.

KERMA CALCULATIONS BELOW THE FEW-KEV ENERGY RANGE

KERMA factors can be obtained directly in the MeV region from the charged particle and recoil spectra data present in ENDF/B-VI for most of the structural material evaluations. However, for low energy incident neutrons where capture and elastic scattering are the only reactions, KERMA cannot be accurately obtained for the following reason. A large contribution to KERMA results from recoil due to emission of high-energy gamma rays from capture. This recoil is not accurately represented in ENDF/B, since sufficient information regarding correlations between primary and secondary gamma rays for decay from the capture state is not available. For example, if the decay is by a (high-energy) primary transition, the recoil due to this gamma ray can be calculated. However, if the decay is via two, equal-energy gamma rays which are emitted in opposite directions, there is no recoil and hence no KERMA. Thus, there is a distribution of recoil energies, which is dependent upon how the capture state decays. This correlation information is available only from nuclear model analysis for capture gamma-ray transitions, and the resulting multi-dimensional gamma-ray spectra output cannot currently be stored in ENDF/B formats.

The solution to this problem is obtained by coupling output from nuclear model codes to a code which calculates recoil spectra, displacement cross sections, and KERMA. New formats would be developed to store the resulting KERMA and displacement cross-section information directly for users. Work on this problem is underway at Oak Ridge.

IMPROVEMENTS IN UNCERTAINTY FILES

The fusion reactor design community has made use of the uncertainty file information included in earlier versions of ENDF/B. Unfortunately, uncertainty information for ENDF/B-VI is not much improved, either in content or coverage, from ENDF/B-V. Uncertainties are given for the cross sections, but not for angular or energy distribution files, nor for resonance parameters. Ad hoc (all-be-it consistent) methods have been used to derive uncertainty values and are documented for the structural materials evaluated at Oak Ridge [HE91]. Subgroup 2 of the NEACRP/NEANDC Evaluation Cooperation Working Group has compared uncertainties for ^{56}Fe cross sections from ENDF/B-VI and JEF-II/EFF-II and found some similarities and some significant differences [VO91]. There are some examples of carefully evaluated uncertainty files in ENDF/B-VI, particularly for the lighter breeding and fuel materials, and in cases of dosimetry reactions where Bayesian analyses provided uncertainties and correlation matrices.

Uncertainties are also generally inadequate for portions of the evaluations obtained from nuclear model calculations. The Japanese have been working in this area [KA91] and their work needs to be taken advantage of to improve this segment of the uncertainty files. Finally, although (untested) formats are available for File 34 (angular distributions) and File 35 (energy distributions), they have not been utilized in ENDF/B-VI evaluations. At present, no formats exist for File 36 (energy-angle correlated data uncertainties) and these formats need to be developed and utilized.

MODEL CALCULATION IMPROVEMENTS

Model codes have been significantly improved since ENDF/B-V. Precompound emission theories have been improved, fundamental work of Feshbach, Kerman and Koonin has been further developed and codes written for applied use, consistent level densities for both compound and precompound models have been developed, and the ability to compute particle emission from tertiary reactions has been improved.

Even with these improvements and additions, model code comparisons often lead to significantly different results, particularly where there are no experimental data to anchor the calculations. The recent activity of the NEANDC Working Group on Activation Cross Sections to calculate the $^{60}Co(n,p)^{60}Fe$ reaction is an example. Sixteen calculations of this reaction were performed, and they differ by a factor of two around 14 MeV. At least part of this scatter is caused by non-specification of level density and optical model parameters for the comparison. Each user was free to choose these parameters based on his experience. Other model code comparison efforts, in which the level density and optical model parameters are specified tend to have much less scatter in the results, particularly when there are experimental data available to fine-tune the results.

The concept of an "evaluated" set of level densities and optical model parameters for general use would reduce differences among model code calculations. However, there are difficulties with such a proposal which must be overcome. Nuclear model codes often use different representations for the level densities (e.g., Gilbert-Cameron, backshifted, empirical), as well as different treatment of level densities for compound and precompound emission modes. Thus, formalisms as well as parameters would need study. Optical model parameters should be easier to evaluate, but decisions on global versus regional parameter sets have to be made, as well as use of "best-fit" parameters from an individual analysis. The IAEA has a Consultant's Meeting arranged for November 1991 to initiate work on reference parameter libraries.

Progress continues to be made in on-line nuclear data structure libraries, but conversion of this information to a form usable in nuclear model codes needs further work. The largest problem with this compiled information is incompleteness. For example, if the spin/parity of a given level is not measured, it is not assigned a value. Nuclear data evaluation work requires a value, so the structure evaluations must be modified and "completed" via use of nuclear structure models, sum rules, etc. It would be very useful if the structure libraries could provide this information, appropriately labeled to indicate it not experimentally derived.

Use of dispersion relation results in optical model analyses has significantly improved these results, particularly at lower neutron energies. Nuclear model codes need to be adapted to take advantage of these advances, since correct calculation of the nonelastic cross section is very important in obtaining the correct split among the various partial cross sections.

LEVEL SPACINGS FROM RESONANCE REGION DATA

For ENDF/B-VI, results from very detailed resonance parameter analyses were available for ^{56}Fe [PE90] and $^{58,60}Ni$ [PE88]. Comparing the level spacings for $\ell = 0$ and $\ell > 0$ with the results from Mughabghab showed differences, with the recent analyses having smaller uncertainties and being well documented. When these results were used to update the Gilbert and Cameron level density parameters, refined parameter values were obtained. In addition, strength function values S_0 used in optical model calculations were obtained. Based on recent resonance parameter analyses,

Mughabghab's useful compendium of resonance parameters and average parameters should be updated.

SUMMARY

In this paper we have outlined areas of ENDF/B-VI which could be improved through the availability of new measurements and improved calculations. New nuclear data (with associated model interpretation) will be required for capture gamma-ray spectra, gamma-ray angular distributions, (n,α) cross sections, and neutron and charged particle emission cross sections at energies from 7-15 MeV. Model calculations and new formats will be required to obtain accurate KERMA calculations below 1 keV. Uncertainty file improvements require new formats, and development of consistent techniques for extracting uncertainties from experimental data and nuclear model calculations. Nuclear model calculations would benefit from development of a reference parameter library, and an easier-to-use nuclear structure library. Finally, Mughabghab's compilation of resonance parameters and associated, derived quantities should be updated to include the latest experimental information.

REFERENCES

FU91   C. Y. Fu et al, "International Evaluation Cooperation Task 1.1: Intercomparison of Evaluated Files for ^{52}Cr, ^{56}Fe, and ^{58}Ni", *International Conference on Nuclear Data, Julich, Germany, May 1991*, and private communication.

GR79   S. M. Grimes et al., *Phys. Rev.* **C19**, 2127 (1979).

HE75   D. Hermsdorf et al., Dresden Report ZfK-277 (U), 1975.

HE91   D. M. Hetrick, D. C. Larson and C. Y. Fu, *Generation of Covariance Files for the Isotopes of Cr, Fe, Ni, Cu, and Pb in ENDF/B-VI*, Report ORNL/TM-11763 (1991).

KA91   Y. Kanda, "New Perspective in Covariance Evaluation for Nuclear Data", *International Conference on Nuclear Data, Julich, Germany, May 1991*.

MO79   G. L. Morgan, *Cross Sections for the Cu(n,xn) and Cu(n,xγ) Reactions Between 1 and 20 MeV*, ORNL Report 5499, 1979

PE88   C. M. Perey, et al., ^{58}*Ni + n Transmission, Differential Elastic Scattering and Capture Measurements and Analysis from 5 to 813 keV*, Report ORNL/TM 10841 (1988), and C. M. Perey et al., *Phys. Rev.* **C27**, 2556 (1983).

PE89   F. G. Perey, private communication of data plots.

SA91   S. K. Saraf et al., *Nucl. Sci. Eng.* **107**, 365 (1991).

TA83   A. Takahashi et al., *Double Differential Neutron Emission Cross Sections, Numerical Tables and Figures (1983)*, Octavian Report A-83-01, 1983.

VO91   H. Vonach, Informal notes presented at the Evaluation Cooperation Working Group meeting, Petten, Netherlands, May 1991.

Local Organizing Committee

S. Cierjacks (chairman)	Institute for Materials Research,	KfK
K. Ehrlich	Institute for Materials Research,	KfK
S. Kelzenberg	Institute for Materials Research,	KfK
J. Kaneko [1]	Institute for Materials Research,	KfK
C. Nordborg	NEA Secretariate	NEA
P. Obložinský [2]	Institute for Materials Research,	KfK
E. Schröder	Public Relations Office,	KfK
E. Thun	Institute for Materials Research,	KfK

---

[1] On leave from the Institute of Physics, SAS, 842 28 Bratislava, Czechoslovakia
[2] On leave from the Department of Nuclear Engineering, Tokyo University, Japan